DRAINAGE GEOCHEMISTRY OF THE RECSK-LAHOCA MINING AREA, MATRA MOUNTAINS HUNGARY

Gift Rukezo

March, 2003

DRAINAGE GEOCHEMISTRY OF THE RECSK-LAHOCA MINING AREA, MATRA MOUNTAINS-HUNGARY

by

Gift Rukezo

Thesis submitted to the International Institute for Geo-information Science and Earth Observation in partial fulfillment of the requirements for the degree in Master of Science in Mineral Resources Exploration and Evaluation.

Degree Assessment Board

Thesis advisers

Drs. J. B. de Smeth
Dr. E. J. M. Carranza

Thesis examiners

Prof. Dr. M. Hale (ITC, TUD), Chairman
Dr. S. P. Vriend (Utrecht Univ.), External Examiner
Drs. J. B. de Smeth (ITC), Member
Dr. E. J. M. Carranza (ITC), Member

ITC

INTERNATIONAL INSTITUTE FOR GEO-INFORMATION SCIENCE AND EARTH OBSERVATION
ENSCHEDE, THE NETHERLANDS

Disclaimer

This document describes work undertaken as part of the study at the International Institute for Geo-information Science and Earth Observation (ITC). All views and opinion expressed herein do not necessarily represent those of the Institute and remain the sole responsibility of the author.

ABSTRACT

The mining of volcanogenic sulphide ore deposits in the Recsk-Lahoca mining area in the Matra Mountains of Hungary resulted in the exposure of sulphide bearing rocks to surface water and atmospheric oxygen, which accelerate oxidation, leaching and release of metals, a process called Acid Mine Drainage (AMD). Floatation tailings piles, which are a result of Cu, Au and Ag mining at the Recsk and Lahoca mines, are seen scattered along the streams in the area. A problem arises when heavy metals are leached into the drainage system, which result in pollution of the environments within the vicinity of the mine areas. Adits used to access ore in the ancient days are also still discharging acidic water, which is high in heavy metals, into the drainage system. In addition the quarrying operations in the floatation tailings for construction material continuously prevent stabilisation of the tailing leaching process. The streams in the Recsk-Lahoca mining area have been observed to contain high levels of base metals, giving rise to the need to understand the processes responsible for the loading of these metals in the streams, and effectively separate AMD processes from natural weathering processes of the different geologic environments in the area. The original aspects of the research survey were to determine parameters indicating pollution, which could be recognised in hyper-spectral remote sensing data. Unfortunately the hyper-spectral data, which was collected by DLR of Germany Remote Sensing Institute during the fieldwork period (August 2002), was not available in time for this research

An attempt was made to analyse the geochemistry of the stream drainages, mine tailings and waters oozing out of adits with the aim of determining element associations, which can explain the different processes responsible for heavy metal load in the waters and sediments in the Recsk-Lahoca area. The 79 waters and 64 sediments were analysed for major and trace elements by ICP-AES alongside with pH, which is very indicative in the hydrolysis of minerals and water metal constituents. The geochemical data on the 99 samples of the floatation tailing piles were studied to determine the relative abundances of the metals likely to leach out of the tailings material in the future. The presents of major elements and sulphate ions in water partly determines the chemical properties of water and may result in the mobility or precipitation of leached trace metals. For this reason water samples were also analysed for sulphate, major elements and electric conductivity (EC) Unfortunately heavy rainfall and access restriction prevented adequate and optimal sampling to a larger distance below the abandoned mine area.

Uni-variate geochemical data analysis methods were found to be effective in grouping element population into classes of similar spatial distributions, except for the hydro-geochemical data of base metals. This is partly due to the extremely low concentrations of these metals in the stream waters because of unforeseen excessive rainfall in the sampling period.

The scavenging effect of precipitating Fe in stream waters, which is revealed in the multivariate geochemical data analysis, is the main surface geo-fluvial process responsible for the depletion of most of the heavy metals from the waters draining the area and the loading of the same metals in the stream sediments. Element–pH relations effectively separated concentrations which are a result of the acid mine drainage process from those which are a result of the natural weathering processes of the geological units in the area. The stronger correlation of EC with base metals than with major elements in

the mine waters indicates the prevalence of leaching of sulphide minerals in these environments. In the streams the EC is more correlated with major elements than with the base metals indicating that the major elements, which have higher concentrations in the streams, control the properties of stream waters. Most of the geochemical data analysis results indicate that AMD is definitely taking place in the tailings and old adit excavations, and field observations revealed that the waters draining these mine areas are discharging into the streams. Comparing the concentrations of the metals in the waters with some standard parameters used as base lines for the quality of water for drinking has indicated the extent of pollution caused by the leached metals. The European Union (EU) standards for drinking water were used as thresholds for pollution due to metal load in the waters of the area.

Classifying element concentrations above the EU parametric standards according to their respective environments revealed that waters draining the tailings piles and waters oozing out of old adits are highly polluted with heavy metals. The main streams are also found to be polluted but to a lesser extent than the pollution in the mine waters. Concentration levels of metals in the streams are slightly above the EU threshold standards for drinking water. Pollution levels are relatively low in the part of the Bikk stream draining mine areas which leads to the conclusion that whilst AMD is taking place in the mine waters, the impact in the stream waters is not very extensive, mainly due to the chemical properties of stream waters, which favour precipitation of base metals, and partly due to the small quantities/volume of the mine waters discharging into the streams. However, chances are also high that the relatively low pollution levels, especially in Parad Bikk and the part of the stream after the confluence of the two main streams, are partly due to dilution due to the heavy rainfall during the fieldwork period for this research. In some of the stream sediments, pollution is observed to be relatively high when compared with the Dutch norms (NEN) for metal concentrations in soils.

The results of the study demonstrate the ability and usefulness of geochemical data analysis methods to qualify metal pollution problems to the respective environmental signatures causing them. The methods however fall short in effectively identifying the processes, like hydrolysis, which are responsible for dissolution or precipitation of metals. Mineral analysing methods like spectroscopy may be useful in this respect and can result in complete understating of the geochemical processes taking place. It is also necessary to analyse the bio-availability of base metals in the vegetation in the floodplains of the streams or to analyse vegetation stress using hyper-spectral methods in order to determine whether metals in the stream sediments are attenuated into plant life. Employing these analysis methods can effectively determine the processes attenuating metals in the different environments of the area.

ACKNOWLEDGEMENTS

I would like to thank the Government of The Netherlands, through its Netherlands Fellowships Program (NFP), to pursue a higher level of learning, and to thank ITC in particular for offering me the place to acquire this invaluable knowledge. The Government of The Republic of Zimbabwe is equally thanked for endorsing and facilitating my application for an NFP grant. Today, I find myself more knowledgeable and broad minded than before through this kind gesture. The help support and encouragement of many individuals during the tenure of my course is very much appreciated. I am forever indebted to you.

I am deeply thankful to my research supervisors, Drs Boudewijn de Smeth and Dr John Carranza for their guidance throughout the research without which the quality of the study would not have reached its present state. My sincere thanks go to Prof. Dr. Martin Hale for his guidance and Dr Paul van Dijk for his support throughout the tenure of this course. My brief encounter with Dr. Simon Vriend helped to shape my research into a more meaningful article and for this I thank him so much.

The fieldwork for this research was unique because of the friendly cooperation of the HySens 2002 Flight Campaign stakeholders, and for this I would like to thank them all. Special thanks go to the following people and their organisations for the special support they offered in making this research a reality: Dr. Zoltan Verkerdy (ITC team leader) for ensuring good welfare during my fieldwork in Hungary and for his professional and moral support; Dr. John Carranza (ITC) for his expert supervision in the collection of geochemical data in the field and for his companionship; Drs Boudewijn de Smeth (ITC) for his expert handling of geochemical samples throughout the analytical processing, which resulted in high quality geochemical data used in this research; Tibor Zelenka (Hungarian Geological Survey) for the guidance throughout the reconnaissance mapping in the field; Aniko Somody (Recsk Echbanya Company) for the field orientation: Gyozo Jordan (and the other members of The European Commission-Joint Research Centre for Environment and Sustainability) for his unwavering support in building up this research from the beginning to the end; Laszlo Roth (and the other members of the Geological Institute of Hungary(MAFI)) for the provision of the necessary map data and other technical support for the research.

My fellow course colleagues, Ariadna Suarez (Cuba), Ninik Suryiantini (Indonesia), Jerry Ahadjie (Ghana) and Todbileg Munkhjarghal (Mongolia), were special companions who gave me encouragement and support throughout the struggle to acquire more knowledge. I am very grateful. You are a special people whom I will always live to remember.

I am greatly indebted to my parents and parents in law for their support in making my family life a success. Your wisdom has landed me where I am today. To Sandra the mother of my daughter Anesu, you are a special friend and life companion and I owe everything to you for your special care and support.

Last and most of all I thank God for making me a signature on this planet.
Thank you; Dank u wel; Tatenda.
Gift Rukezo
March 2003

CONTENTS

CONTENTS vi
List of Figures viii
List of Tables ix
1. INTRODUCTION 1
1.1. The Research Problem 1
1.2. Background to Acid Mine Drainge 2
1.2.1. The Chemistry 2
1.2.2. Chemical processes 2
1.2.3. Physical processes 3
1.2.4. Biological processes 3
1.3. Previous Research Elsewhere 3
1.4. The Present Research 5
1.4.1. Hypothesis 6
1.4.2. Objectives 6
1.4.3. Methodology 6
1.4.4. Problems encountered 7
2. THE PROJECT AREA 8
2.1. Location 8
2.2. Climate and vegetation 8
2.3. Geomorphology 8
2.3.1. Topography and relief 8
2.3.2. Drainage 10
2.3.3. Weathering and erosion 11
2.4. Geology and Mineralisation 11
2.4.1. Geo-tectonic setting 11
2.4.2. Lithologies 11
2.4.3. Mineralization of the Recsk-Lahoca Mining area 12
2.5. Mining in the area 15
2.5.1. Mining of non-metallic deposits 15
2.5.2. Mining of Base metals, gold and silver. 15
2.6. Environmental Signatures and Effects of the Oxidation of Sulphide Deposits 16
2.6.1. Natural environmental signatures and effects 16
2.6.2. Mining-induced environmental signatures and effects 18
2.7. Conclusions 24
3. GEOCHEMICAL DATA: COLLECTION AND QUALITY ASSESSMENT 25
3.1. Base Map construction 25
3.1.1. Base map for drainage geochemical data 25
3.1.2. Base map for Tailings geochemical data 27
3.2. Collection and chemical analysis of geochemical samples. 27
3.2.1. Water samples 27
3.2.2. Stream sediment samples 28
3.2.3. Tailings Samples 29

3.3. Geochemical data quality 29
3.3.1. Data comparisons for water samples 30
3.3.2. Scatter plots 31
3.3.3. Analysis of Variance 35
3.4. Remarks 39
3.5. Conclusions 40
4. DRAINAGE HYDROGEOCHEMICAL DATA ANALYSIS 41
4.1. Univariate data analysis 41
4.1.1. Element data structure 41
4.1.2. Element distributions 42
4.1.3. Summary of the univariate data analysis 63
4.2. Metal concentrations along stream profiles 63
4.3. Multivariate data anlysis 68
4.3.1. Correlation analysis 68
4.4. Conclusions 72
5. STREAM SEDIMENTS GEOCHEMICAL DATA ANALYSIS. 73
5.1. Univariate Data Analysis 73
5.1.1. Element data structure 73
5.1.2. Element distributions 73
5.1.3. Summary of element Data 88
5.2. Metal concentrations along stream profiles 90
5.3. Multivariate Data Analysis 95
5.3.1. Correlation Coefficient Analysis 95
5.3.2. Principal Components Analysis (PCA). 95
5.4. Conclusions 101
6. GEOCHEMICAL DATA FROM MINE AREAS AND WATER DRAINING THROUGH THE (OLD) ABANDONED WORKINGS. 102
6.1. Descriptive statistics for tailings data. 102
6.2. Mine waters geochemistry 105
6.3. Conclusions 107
7. GEOCHEMICAL DATA RELATIONS AND ENVIRONMENTAL IMPLICATIONS. 108
7.1. Comparison of water, stream sediments and tailings geochemical data 108
7.1.1. Summary of geochemical data comparisons 111
7.2. Environmental implications of the geochemical data. 111
7.2.1. Environmental implications of hydrogeochemical data. 111
7.2.2. Environmental implications of Stream sediments geochemical data. 113
7.3. Conclusions 115
8. CONCLUSIONS AND RECOMMENTATIONS 116
8.1. CONCLUSIONS 116
8.2. Final remarks and Recommendations 117
References 119
Appendices 121

List of Figures

Figure 2.1. Location of Recsk in Hungary (insert-Hungary in Europe)…… 9
Figure 2.2. Topography and vegetation of Recsk area……... 9
Figure 2.3. Recsk drainage system…… 10
Figure 2.4. Geology around Recsk area (from Foldessy. 1996)…… 12
Figure 2.5. Schematic section of Recsk- Lahoca and "Recsk Deeps" ore complex (from Foldessy, 1996)….. 13
Figure 2.6. Sulphidised andesite breccia showing the grey colour of the breccia due to high prite content and the yellow tint in fractures due to pyrite oxidation……... 14
Figure 2.7. Clay pit…… 14
Figure 2.8. A collapsed adit entrance characterised by ground subsidence and acidic water discharges…….. 14
Figure 2.9. Pyritic and argillic alteration in a geochemical anomaly along Tarna creek……... 17
Figure 2.10. Vegetation poisoned by toxic acidic water from an ancient adit. Inset shows typical colour of acidic water, pH~2……... 17
Figure 2.11. Gully erosion on lahoca floatation tailings…….. 20
Figure 2.12. Vertical profile of floatation tailings (Recsk)…….. 20
Figure 2.13. Iron (III) precipitates (yellow boy) along Parad Tarna drainage channel……... 21
Figure 2.14. Metal drainage pipe draining acidic water from east Recsk floatation tailings piles…….. 22
Figure 2.15. Parad Bikk tributary passing through the east and west Lahoca tailings piles…..……... 22
Figure 2.16. Recsk tailings near a modified channel of Parad Bikk…… 23
Figure 2.17. Gully erosion and diggings of mine tailings…… 23
Figure 3.1. Base map showing water and stream sediment sample locations and the associated environmental features……. 26
Figure 3.2. Map showing sampling grid on the Lahoca east and west floatation tailings piles……. 27
Figure 3.3. Scatter graphs showing plots of 1st and 2nd sample analysis of field duplicate water samples in the drainages of the area…….. 32
Figure 3.4. Scatter graphs showing 1st and 2nd analysis for laboratory repeat samples on some of the metal and sulphate concentrations in waters draining the area…….. 33
Figure 3.5. Scatter graphs showing plots of 1st and 2nd sample analysis of field duplicate stream sediments samples in the drainages of the area…… 34
Figure 3.6. Scatter graphs showing plots of 1st and 2nd analysis of laboratory repeat samples for metal concentrations in the stream sediments and floatation tailings of the area. ……..…… 35
Figure 4.1. Spatial distributions of observed pH of the stream-waters draining the area…….. 44
Figure 4.2. Spatial distributions of observed EC of the waters draining the area…….. 45
Figure 4.3. Spatial distributions of observed sulphate concentrations in waters draining the area …….. 47
Figure 4.4. Spatial distributions of observed Fe concentrations in waters draining the area……. 49
Figure 4.5. Spatial distributions of observed Mn concentrations in waters draining the area…….…... 50
Figure 4.6. Spatial distributions of observed Zn concentrations in waters draining the area…… 52
Figure 4.7. Spatial distributions of observed Ca concentrations in drainage waters of the area…….…... 54
Figure 4.8. Spatial distributions of observed Mg concentrations in drainage waters of the area…….. 56
Figure 4.9. Spatial distributions of observed Al concentrations in drainage waters of the area…… 57
Figure 4.10. Spatial distributions of observed K concentrations in drainage waters of the area……. 59
Figure 4.11. Spatial distributions of observed Na concentrations in drainage waters of the area…….…... 60
Figure 4.12. Spatial distributions of observed total major cation concentrations in drainage waters of the area 62
Figure 4.13. Graphs of element concentrations in streams as functions of distance along stream profiles. Row A = Cu; B = Fe; C = Mn; D = Zn; E = Al; F = K; G = Ca; H = Mg; I = H = hydrothermal alteration zone; TC = tributary confluence with P. Tarna; H/A = hydrothermal alteration/ancient adits area; C = confluence of P. Tarna and P. Bikk; L = Lahoca tailings area; W52 = sample location with extreme acidic waters; R = Recsk tailings piles area……. 65, 66, 67,

Figure 4.14. Scatter graph showing the relationship between sulphate and the total concentrations of major element cations……. 70
Figure 4.15. Scatter graph showing the relationship between EC and the total concentrations of major element cations……. 71
Figure 4.16. Scatter graph showing the relationship between EC and sulphate concentrations…….. 72
Figure 5.1. Spatial distributions of observed As concentrations in sediments of streams draining the area…. 75
Figure 5.2. Spatial distributions of observed Cd concentrations in sediments of streams draining the area…. 78
Figure 5.3. Spatial distributions of observed Cu concentrations in sediments of streams draining the area…. 79
Figure 5.4. Spatial distributions of observed Fe concentrations in sediments of streams draining the area….. 80
Figure 5.5. Spatial distributions of observed Mn concentrations in sediments of streams draining the area… 82
Figure 5.6. Spatial distributions of observed Ni concentrations in sediments of streams draining the area….. 84
Figure 5.7. Spatial distributions of observed Pb concentrations in sediments of streams draining the area…. 85
Figure 5.8. Spatial distributions of observed Sb concentrations in sediments of streams draining the area….. 87
Figure 5.9. Spatial distributions of observed Zn concentrations in sediments of streams draining the area…. 89
Figure 5.10. Graphs of element concentrations in sediments against distance along stream profiles. Row A = As; B = Cd; C = Cu; D = Fe; E = Mn; F = Ni; G = Pb; H = Sb; I = Zn; H = hydrothermal alteration zone; TC = tributary confluence with P. Tarna/P. Bikk; H/A = hydrothermal alteration/ancient adit area; C = confluence of P. Tarna and P. Bikk; L = Lahoca tailings area; W52 = sample location with extreme acidic waters; R = Recsk tailings piles area…….. 92, 93, 94
Figure 5.11. Spatial distributions of the calculated scores from PC1 showing the antipathetic relationship between Fe (and the scavenged elements) and Mn…….. 99
Figure 5.12 Spatial distributions of the element associations explained by PC2 scores……. 100
Figure 6.1. Recsk area showing sampled tailings and old adits……. 104
Figure 6.2. Graphs showing the relationships between metal concentrations with pH and EC: A. EC vs pH; B. Sulphate vs pH; C. Fe vs pH; D. Major cations vs pH; E.EC vs Sulphate; F. EC vs Fe…… 106
Figure 7.1. Ficklin diagram showing the classification scheme for mine and natural drainage waters (from Plumlee, 1995; named after the late Walter Ficklin, an environmental geochemist)…….. 109
Figure 7.2. Plots of dissolved base metal concentrations as a function of pH of the waters draining the area.. 110
Figure 7.3. Plots of dissolved major element cation concentrations as a function of pH of the waters draining the area……... 111
Figure 7.4. Map of the Recsk-Lahoca area showing drainages with base metal concentrations above the maximum permissible limits for EU drinking water standards…… 114
Figure 7.5. Map of the Recsk-Lahoca area showing drainage segments with base metal concentrations in sediments requiring additional investigations and cleaning up according to the NEN standards for soils……. 114

List of Tables

Table 2.1. Recsk mine production summary from 1931 to 1979……... 16
Table 2.2. Amount of waste material around Recsk mine……. 16
Table 2.3. Residual amounts of Cu, Au & Ag in Recsk floatation tailings generated in 1931-1979…… 19
Table 3.1. Comparison of 1st and 2nd sample results of field duplicate data for water samples. Concentrations are given in mg/l. …… 30
Table 3.2. Comparison of 1st and 2nd analysis results of laboratory repeat samples for element concentrations that fell below/within detection limits. Concentrations are given in mg/l……..….. 31
Table 3.3. Summary of quality assessment for water sample data using simple nested one-way ANOVA….. 37
Table 3.4. Summary of quality assessment for stream sediment sample data by simple nested one-way ANOVA…… 38

Table 3.5. Summary of quality assessment for tailings sample data by simple nested one-way ANOVA…… 39
Table 4.1. Summary of descriptive statistics for water sample measurements (n=63). Concentrations are given in mg/l for the metals and sulphate ions while EC is given in µs/cm…….. 42
Table 4.2. Summary of observed spatial distribution of pH in the waters draining the area……. 43
Table 4.3. Summary of observed spatial distribution of EC in the waters draining the area……. 46
Table 4.4. Summary of observed spatial distribution of SO_4^{-2} concentrations in waters draining the area….. 46
Table 4.5. Summary of observed spatial distribution of Mn concentrations in waters draining the area…….. 48
Table 4.6. Summary of observed spatial distribution of Zn concentrations in waters draining the area…….. 51
Table 4.7. Summary of observed spatial distribution of Ca concentrations in waters draining the area…….... 53
Table 4.8. Summary of observed spatial distribution of Mg concentrations in waters draining the area…….. 55
Table 4.9. Summary of observed spatial distribution of Al concentrations in waters draining the area…….... 58
Table 4.10. Summary of observed spatial distribution of K concentrations in waters draining the area……. 58
Table 4.11. Summary of observed spatial distribution of Na concentrations in waters draining the area…….... 61
Table 4.12. Summary of observed spatial distribution of total major cation concentrations in waters draining the area…….. 63
Table 4.13. Correlation coefficient matrix for the stream water geochemical data……. 68
Table 5.1. Summary of descriptive statistics for stream sediments geochemical data (n=53). Concentrations are given in ppm except for Fe which is in percentage……. 73
Table 5.2. As sub-population groups and their environmental associations…….. 74
Table 5.3. Cd sub-population groups and their environmental associations…….. 76
Table 5.4. Cu sub-population groups and their environmental associations…….. 77
Table 5.5. Fe sub-population groups and their environmental associations…….. 77
Table 5.6. Mn sub-population groups and their environmental associations……. 81
Table 5.7. Ni sub-population groups and their environmental associations…….. 83
Table 5.8. Pb sub-population groups and their environmental associations…….. 83
Table 5.9. Sb sub-population groups and their environmental associations…….. 86
Table 5.10. Zn sub-population groups and their environmental associations…….. 88
Table 5.11. Correlation coefficient(r) matrix for stream sediments data……. 95
Table 5.12. Principal Component Loadings for stream sediments geochemical data…….. 96
Table 6.1. Summary of descriptive statistics for Lahoca east geochemical data. Element measurements are given in ppm except for Fe which is in percentage (n = 53)…… 102
Table 6.2. Summary of descriptive statistics for Lahoca west geochemical data. Element measurements are given in ppm except for Fe which is in percentage (n = 44)…… 103
Table 6.3. Average element concentrations in the four sampled tailings piles. Element measurements are given in ppm except for Fe which is in percentage. LE. Lahoca East; LW. Lahoca West; RE. Recsk East; RW. Recsk West…….. 103
Table 6.4. pH, EC, SO_4^{2-} and base metal concentrations in waters draining the tailings and waters oozing out of old adits. Sample numbers M10 to M13 are from waters oozing out of old adits while the other samples are from tailings waters…….. 105
Table 7.1. Base metals, sulphate, EC and pH measurements above the European Union standards for drinking water. Base metal and sulphate concentrations are given in mg/l and EC is given in µs/cm…… 112
Table 7.2. Distributions of trace element concentrations classified according to the NEN standards in the four main drainage environments of the area…… 113

1. INTRODUCTION

1.1. The Research Problem

Mining of sulphur-bearing ore deposits exposes sulphidic rocks to surface water and oxygen, which accelerate oxidation, leaching and release of metals and generation of acid - a process called **Acid Mine Drainage (AMD)**. Any modern mining project involved with sulphur-bearing ore deposits is faced with the greatest challenge of controlling (if not preventing) the environmental impact of mine waste, which can contain large amounts of sulphur-bearing gangue (or uneconomical) minerals. Degradation of the quality of surface and ground waters that come in contact with acid producing mine tailings piles is the major environmental problem associated with acid mine drainage. Depending on the composition of the ore deposits, the heavy metals released into surface and ground waters can typically include arsenic, cadmium, cobalt, copper, iron, manganese, nickel, lead, antimony, zinc, aluminium, selenium, or many others. In areas where the environment (including fauna and flora) is threatened by acid mine drainage, information on spatial distribution of mine wastes and contaminants becomes important in taking remedial measures.

In Hungary, volcanic-hosted sulphide ore deposits in the Matra Mountains have been mined for their base and precious metals since the 19th century (Cox and Singer, 1986) The mining activities, especially in the last half of the 20th century, have resulted in large volumes of waste rock dumps and fine grained floatation tailings, which contain high amounts of sulphide-bearing gangue minerals. Oxidation of the sulphide minerals in the mine wastes has been taking place over the years resulting in acidic waters, which corrode heavy metals into solution. Attenuation of heavy metals in aquatic, soil and plant life threatens the ecosystem and endangers human life. Events of flooding in the past resulted in increased erosion and deposition of the mine wastes into floodplains, thus accelerating processes of environmental pollution (Odor et al, 1999). The understanding of the geochemistry of these pollution processes, field and remote sensing studies can be useful in mapping sources of contamination and contaminated areas and in finding remedial solutions to the problem. The Anthracite Region of Pennsylvania in the United States of America is a good example of an area where mine drainage pH has been assessed from the geochemistry, colour and spectral reflectance of chemical precipitates (Williams et al, 2001)

Two major sulphide ore mining areas affected by acid mine drainage in the Matra mountains are in the Recsk-Lahoca and in the Gyongyosoroszi districts. The geoenvironmental problems in the mining area in the later district are well understood (Odor et al, 1998), whilst those of the mining area in the former district are less studied. This research thus focuses on geoenvironmental problems in the Recsk-Lahoca mining area.

The sulphide mineral deposits in the Recsk and Lahoca areas have been mined for copper, gold and silver that were hosted in volcanogenic sulphide ore deposits (Odor et al, 1998). Huge dumps of rock waste and mill tailings are scattered around the mines. Oxidation of gangue sulphide minerals in the dumps and subsequent leaching of heavy minerals and sulphate ions into drainage systems are observably taking place. Gully and sheet erosion that accelerate acid mine drainage are observable on

the mine dumps. Adits that were developed in the ancient mining times are also observed to discharge acidic water with high heavy metal content. These are among the mining-related processes that can adversely affect the Recsk-Lahoca area and its environment**.** Studying these processes can lead an understanding useful for mitigation (if not prevention) of environmental impact of mineral development such as in the Recsk-Lahoca area and elsewhere.

1.2. Background to Acid Mine Drainge

1.2.1. The Chemistry

Sulphide minerals form under reducing conditions within the Earth's crust. These minerals are not stable when brought near or on the Earth's surface. They react with oxygen (O_2), which makes up about 20% (by volume) of the atmosphere, and water through hydrolysis resulting in the release of heavy metals, sulphate and hydrogen ions. Pyrite (FeS_2), being the most common and abundant sulphide, can be used as a model sulphide mineral and its oxidation reaction can be represented by the chemical equation:

$$FeS_2 + 7/2O_2 + H_2O = Fe^{2+} + 2SO_4^{2-} + 2H^+ \quad (1)$$

The generated hydrogen ions are responsible for making water acidic. The acidic water further reacts with rock minerals, resulting in more heavy metals being brought into solution either as complex or simple ions (Durkin and Hermann, 1994). The Fe^{2+} dissolved in water easily looses an electron giving rise to Fe^{3+}. As pH rises downstream, Fe^{3+} easily hydrolyses to form solid $Fe(OH)_3$ and liberate H+ ions. Below are the stoichiometries of the reactions:

$$Fe^{2+} = Fe^{3+} + e \quad (2)$$

$$Fe^{3+} + 3H_2O = Fe(OH)_3 + 3H^+ \quad (3)$$

The liberated H^+ in equation 3 is capable of producing more acidic waters than that of equation 1. The dissolved Fe^{2+} and Fe^{3+} can be transported several kilometres from the sulphide (pyrite) source (where reaction 1 took place) before reactions 2 and 3 occur. As a result, the problems of metal contamination caused by AMD can persist for more than tens of kilometres downstream of the sulphide source.

1.2.2. Chemical processes

At the onset of acid mine drainage, natural drainage water has near neutral to neutral pH and is characterized by low total dissolved solids (TDS) in the range of 0 to 100mg/l. With sulphide oxidation, pH decreases to less than 4. As pH decreases, element mobility increases as minerals dissolve in acidic water resulting in increased total dissolved solids in the range of hundreds to tens of thousands milligrams per litre. This results in high heavy metal load in water drainage systems emanating from or influenced by mining activities. Water containing high levels of heavy metal concentration is toxic and harmful to nearby ecosystems.

Once the metals are in solution, more chemical processes take place in the drainage systems. Metals precipitate at certain pH levels. Iron and manganese precipitate at relatively low pH. The other metals require higher pH to precipitate. However, due to the scavenging effects of precipitating Fe-Mn oxides/hydroxides, other metals are sorbed onto and co-precipitated with Fe-Mn oxides/hydroxides. This is more so in areas where groundwater surfaces and comes into contact with contaminated drainage system. As a result, heavy metal precipitation can be expected in the sediments of floodplains of drainage systems with high metal load and this can have a deleterious impact on the ecosystems nearby.

1.2.3. Physical processes

The exposure of sulphide minerals by natural or human activities accelerates heavy metal contamination from mine deposits. Mining and milling results in a marked increase in surface area of mineralised rocks exposed to water and oxygen, which induces chemical reactions leading to acid mine drainage. Erosion exposes and transports mine wastes, thereby accelerating oxidation of sulphide wastes. Gully erosion channels in mine/mill tailings dumps can accelerate penetration of water and oxygen into the inner parts of the sulphide wastes.

1.2.4. Biological processes

Acid tolerant bacteria, like the Thiobacillus ferrooxidans, can survive and thrive in acidic and toxic conditions. They use ferric iron as electron receptors in substrate sulphate anaerobic conditions to obtain energy. The bacteria can also obtain energy from oxidizing copper and other heavy metal ions. These acidophillic bacteria, which survive by converting the energy found in inorganic chemical compounds into energy usable for their life processes, increase the rate of pyrite oxidation in mine tailings piles, which accelerates formation of acidic drainage and release of heavy metals into the environment (Horan, 1999).

1.3. Previous Research Elsewhere

Many of the major mining regions of the world experience environmental problems associated with AMD. In a bid to understand the problems of heavy metal load in drainage basins, research has focused on trying to establish geochemical baselines of stream waters in areas affected by heavy metal contamination.

In the Summitville mining area in Colorado (USA), drainages are highly acidic and have high heavy metal load (Miller and McHugh, 1999). The area has been mined since 1870 for gold, silver and copper hosted in epithermal deposits that are characterized by advanced argillic alteration (Miller and McHugh, 1999). Mining progressed from the ancient adit mining in the 1870's through modern underground mining to large open pit mining that ended in 1992 (Miller and McHugh, 1999).

Remediation of environmental problems resulting from the open pit mining at Summitville raised questions of what the pre-mining geochemical baselines of stream waters may have been like in the vicinity of Summitville site. Because of lack of geochemical data before adit mining in 1870, a prediction of the heavy metal load and acidity of water prior to mining was based on geologic models, acid-base geochemical tests, mathematical models and geographical comparisons with similar ore bodies

that lie in similar climatic conditions (Miller and McHugh, 1999). The presence of fossil iron bogs in the vicinity of Summitville deposit confirmed the findings that prior to mining, natural acid drainage generated by oxidation of sulphides was common at Summitville. However, the exact heavy metal load and acidity prior to mining could not be determined.

With geochemical data before and after modern mining at Summitville, it was established that heavy metal load increased and pH decreased as the mining progressed from ancient adit mining period to underground mining and open pit mining period (Miller and McHugh, 1999). Whilst acid rock drainage increased over the years due to increased mining that exposed more sulphides to the surface, the Summitville research has shown that there is need to establish geochemical baselines in order to be able to quantify the contribution of mining to acid rock drainage.

Research has also focused on establishing the onset of acid mine drainage after exposure of the sulphides to the surface. The old school of thought believed that acid mine drainage only takes place after a long period from the time the sulphide minerals are exposed to the surface. The amount of acid mine drainage generated was also linked to the amount of sulphides exposed to the surface due to mining (Environmental Mining Council, 2001). Events at old Mt. Washington mine on Vancouver Island in Brittish Columbia, Canada, proved otherwise. A small, open-pit mine was operated for a mere 3 years, and the effects of acid mine drainage were noticed a few years after the closure of the mine (Reece, 1995). The mine left a legacy of acid mine drainage that persists today. The acid mine drainage contributes to the leaching of copper, which has been called "the dreaded enemy" of young salmon. The amount of copper that finds its way into the Tsolum River, 10 km from the mine, not only kills young salmon, but also deters adults from returning to the river to spawn. Largely as a result, the river, which used to support major salmon and steelhead runs, is essentially barren. The loss of fishery costs the local community approximately $2 million per year (Environmental Mining Council of Brittish Columbia, 2001).

Research into the devastating effects of acid mine drainage generated by Mt. Washington mine, which had so little sulphide waste from the three years of operation, indicated that acid mine drainage is more dependent on rock composition and climate coupled with milling and ore recovery processes and environmental measures taken during and after dumping of mine waste than the amount of waste exposed by mining. On the other hand, the high quantity of heavy metals in the Odiel and Rio Tinto that drain from the volcanic massive sulphides of the Iberian Pyrite Belt in the Huelva and Andalusia provinces of Spain has been linked to the magnitude of the sulphide waste that has been exposed to the surface due to the more than 3000 years of mining. The heavy metal load has had devastating effects in the Mediterranean Sea where the Rio Tinto and Odiel discharges. Acidophillic bacteria like *Thiobacillus ferrooxidans* have however been found to be influential in accelerating the oxidation of sulphides to produce acidic waters and heavy metal loads (Internet web references on Rio Tinto).

The Tinto Odiel River Ocean Study (TOROS) of University of Liege, Spain, initiated a project aimed at studying inputs of the two acidic and metal-rich rivers, draining one of the most important sulphide mineralisation in the world, to the Gulf of Cadiz, which provides a major source of water for the Mediterranean Sea (Beckers and Nomérange, 1998). The TOROS research showed that metal mobility can span up to hundreds of kilometres since heavy metal contamination could be identified in the Mediterranean sea that lies about 100 kilometres from the source of the contamination, the Iberian

Pyrite Belt. Dissolved trace metal concentrations in the surface waters of the western Mediterranean Sea have been reported to be higher than those measured in open oceans like the Atlantic. A hydrodynamical model of the area of the Gulf of Cadiz and the Strait of Gibraltar was set up in order to investigate the fate of the waters from the Tinto and Odiel rivers and from the Gulf through the Strait into the Mediterranean Sea. By introducing a passive tracer in the model at the river mouth in Huelva, the hypothesis of a riverine input of metals into the ocean can be tested and the dispersion of the metals originating there can be simulated. The Tinto and Odiel river water dispersion model results matched with the observations in the Gulf of Cadiz (Beckers and Nomérange, 1998). The metal concentration results in this study are however likely to be biased due to heavy pollution from the Huelva metallurgical industries.

Recent research on problems associated with acid rock drainage has also tried to establish secondary minerals that precipitate at various pH ranges. Mine drainage sediments collected from sites in the Anthracite Region of eastern Pennsylvania showed that sediments occurring in acidic waters contained jarosite, swertmannite and goethite while near neutral waters produced ferrrihydrite (Williams et al, 2001). The predominance of a particular mineral precipitate in a particular pH environment has enabled researchers to use the physical and chemical properties of those minerals to separate and determine mine drainage quality and acidic environments using remote sensing. This has been achieved through advances in the spatial and spectral resolution of airborne and satellite systems and improved understanding of the relationship between the aqueous geochemistry and mineralogy of ochreous precipitates from mine drainage (Robins et al., 2000). Among the remote sensing techniques used in the Anthracite region, and most popular the world over, was hyperspectral imaging spectroscopy (Williams et al, 2001).

Research on the impact of mining in the Matra Mountains has been carried out on a regional and mine scale. Most of the research has been focused on the Gyongyosoroszi mine and it resulted in measures being taken to remedied problems of heavy metal contamination. Waters draining from mine adits, which have been found to contain high heavy metals and pH of between 1 and 2, are treated with lime to precipitate the metals and neutralize the acidity before discharge into surface drainages.

The failure and subsequent erosion of Gyongyosoroszi floatation tailings piles resulted in the deposition of tailings materials in the floodplains of Toka creek. The tailings materials, which have been transported onto the flood plains, are easily distinguishable by a characteristic yellow colour due to the strong staining effects of iron (III) oxides, commonly referred to as ‘the yellow boy’ sand (Odor et al, 1998). The yellow colour of the deposited tailings materials is an indication of processes of oxidation taking place on the sulphide minerals of the deposited tailings materials. Sediment samples taken from the deposited tailings materials and water samples from Toka creek draining the floodplains have been found to contain high heavy metals, especially lead and arsenic. The high heavy metal contents are indications of acid mine drainage taking place in the deposited mine tailings materials.

1.4. The Present Research

A joint program, called HySens 2002 Flight Campaign**,** was initiated in August 2002 to undertake a survey of areas suspected of pollution due to mining in the Matra Mountains. Field surveys were carried out in mining areas and floodplains affected by floatation tailings. The main purpose was to ac-

quire field data to be used as a basis for analysing hyperspectral imaging data in environmental impact assessment. Field data included geochemical, hydrological and vegetation data. The focus is on the synergy of airborne hyperspectral data with existing vegetation, geochemical and hydrological information, and the determination of the possibilities and limitations of imaging spectrometry techniques to derive spatially distributed information about soil and water contamination due to impacts of mining. The fieldwork for this research was part of the joint research program.

Remarks
The focus of this research was to analyse stream water and stream sediments geochemical data and hyperspectral imaging data to determine and map areas affected by heavy metal contaminations due to mining. The hyperspectral imaging undertaken by DLR of Germany Remote Sensing Centre could not be available during the tenure of this research, and as a result, focus of the research shifted to mapping contamination due to mining using geochemical data.

1.4.1. Hypothesis

The MSc research will attempt to test the following hypotheses:

- There is metal contamination due to mining of sulphide ore deposits in the project area.
- Geochemical analysis can determine metal contamination in the project area.
- Spatial analysis can determine the sources of metal contamination in the project area.
- Hyperspectral imaging can map areas affected by acid mine drainage and heavy metal contamination in the project area.

1.4.2. Objectives

The research will attempt to identify and assess the impacts of mining on the environment through the following sub objectives:

- To identify metal contamination due to sulphide ore deposit mining in the project area.
- To map environmental signatures likely to cause metal contamination in stream waters.
- To use geochemistry to determine metal contamination in the area.
- To use spatial variability in determining sources of heavy metal contamination in the project area.
- To use hyperspectral imaging to map areas affected by acid mine drainage in the project area.

1.4.3. Methodology

Existing data and information were studied in formulating the research hypothesis. This was followed by a reconnaissance survey of the geology, structures and other features of importance in order to determine factors indicative of heavy metal contamination due to sulphide ore deposit mining in the project area. Water and stream sediment samples were collected from areas suspected of contamination from acid mine drainage and areas outside the contamination zones. The geochemical composition of the collected samples were analysed and the spatial distributions of the element contents were displayed on maps. Samples were also collected from tailings piles for mineralogical and geochemical analysis in order to determine any secondary minerals that are indicative of oxidation and leaching, hence acid mine drainage. A selection of stream sediments and tailings samples was analysed by spectrometry methods. All the field/ground data forms the basis

for the analysis of airborne hyperspectral imaging data. The details of procedures are given in the relevant sections.

1.4.4. Problems encountered

The Sampling of the stream suspected of metal contamination due to mining was done for only two kilometres downstream of the mine areas due to access limitations and restrictions by the Hungarian authorities. As a result, metal distribution trends could not be determined beyond the 2km distance to fully establish the extent of metal contamination in this drainage.

The fieldwork for this project (July/August 2001) was also constrained by the unexpected excessive rainfall, which was not normal in the climatic patterns of the area. The rains, which resulted in flooding, is most likely to have diluted the sampled stream waters giving rise to underestimations of the stream element concentrations which are present under normal climatic conditions.

Mapping of metal contamination due to mining using the hyperspectral imaging data collected by DLR of Germany Remote Sensing Centre could not be achieved due to the unavailability of the data during the tenure of this research. The hyperspectral data was only availed in mid February, which was too late to use it for the purposes of this research. Aster data of good quality for the area, which can be used in similar manner to the hyperspectral data, could not be obtained from the vendors of remotely sensed data.

The mineralogy of the stream sediments and other geological environmental signatures like tailings and lithologies could not be established due to lack of facilities to analyse the samples from those areas. The available spectrometry methods are not suitable to distinguish iron precipitates which are the main indicators of metal leaching from sulphide minerals. The available PIMA (Portable infrared mineral analyser) is not capable of detecting iron oxides, which have absorption bands in the visible range of the spectra. The GER3700, which is capable of detecting mineral absorption characteristics within the full range of the visible to the infrared wavelength, developed a technical problem in its visible range making it impossible to use it to determine iron precipitates in the collected samples. The analysis of precipitates using XRD method was not possible due to lack of funds in the research budget. About €50.00 per sample for at least 100 samples was required to analyse the samples using XRD methods.

As a result of these encountered problems, restrictions and limitations towards achieving the original objectives of this research were inevitable. Focus of the research was therefore put on those objectives which are achievable by using the available geochemical and map data.

2. THE PROJECT AREA

2.1. Location

The Recsk mining area is located in the Matra Mountains in the northern part of Hungary. It is about 110 km northeast of Budapest, the capital city of Hungary. The area is within latitudes 47°50'00"N and 48°00'00"N and within longitudes 20°00'00"E and 20°07'30"E (figure 2.1). The area is covered by a 1:200,000-scale geological map and by 1:25,000-scale topographic (Recsk and Kekesteto) map sheets. The topographic map sheets are georeferenced to the Hungarian National Uniform Projection (EOV), which is a metric easting–northing coordinate system. Due to lack of formula to convert the EOV projection to other international projections, 'EOV' has been used to georeference spatial data used in this research.

2.2. Climate and vegetation

The area experiences a temperate continental climate. The mean annual temperature ranges from 5^{o}C to 10^{o}C in the Matra Mountains. The average annual rainfall is about 700 mm. The wettest part of the year is at the end of fall and the beginning of winter. It is estimated that two thirds of the rainfall is lost to evapotranspiration. Exceptional climatic conditions occur in some periods of other seasons as evidenced by the heavy rainfall during the field work in August 2002, which caused flooding in the low-lying areas.

The Matra Mountains are characterized by thick vegetation of tall forest (figure 2.2). The forests consist of mixed beech and evergreen trees. Various oak forests interspaced with bushy grassy areas cover the low-lying regions. Pine trees are found only in plantations. In the floodplain areas, there are thick reed grasses, especially in areas around the mines. Dense vegetation in the area, especially in floodplains, results in high humus content in the soils and drainage waters in the area.

2.3. Geomorphology

2.3.1. Topography and relief

The rugged terrain is a direct result of the geology of the area. The relatively young volcanic rocks gave rise to mountain domes with very steep slopes of 40^{o} to 60^{o}. The slope is gentle at the foot of the mountain domes, giving rise to undulating plains. Flat areas are limited to floodplains where sediments have been deposited. An overview of the topography and relief is shown in figure 2.2.

Like the rest of the Matra Mountains, the relief of the Recsk area can be divided into two major groups. The first group includes primary volcanic features, whilst the second group includes landforms shaped by erosion. Mountain domes of mono and parasitic cones and elongate ridges reminiscent of fissure volcanic origin can be seen in the area. The highest mountain peak in Hungary, Mount Kekes (1 014m a.s.l.), lies in this area. It is a strato-volcano with a cone shape consistent with its origin.

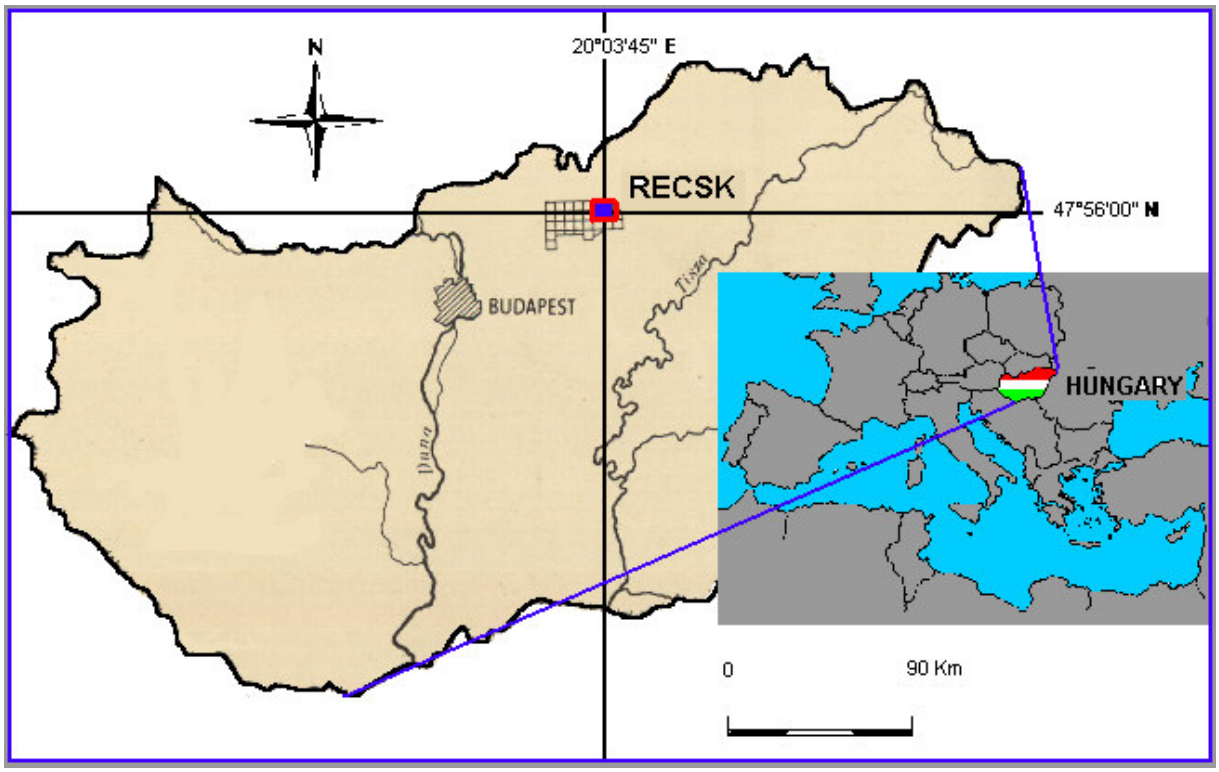

Figure 2.1. Location of Recsk in Hungary (insert-Hungary in Europe).

Figure 2.2. Topography and vegetation of Recsk area.

2.3.2. Drainage

The higher hills of the Matra Mountains form the watershed of the area. Small streams originate from the mountain slopes in a dentritic pattern. On the foot of mountain domes, where slope is gentler and the terrain is undulating, the streams show a meandering pattern. In some areas, the streams cut across heavily weathered and argillised rocks, giving rise to steep cliffs. In some areas, the streams follow tectonic lines like faults and tectonic lithological boundaries resulting in elongate drainage patterns.

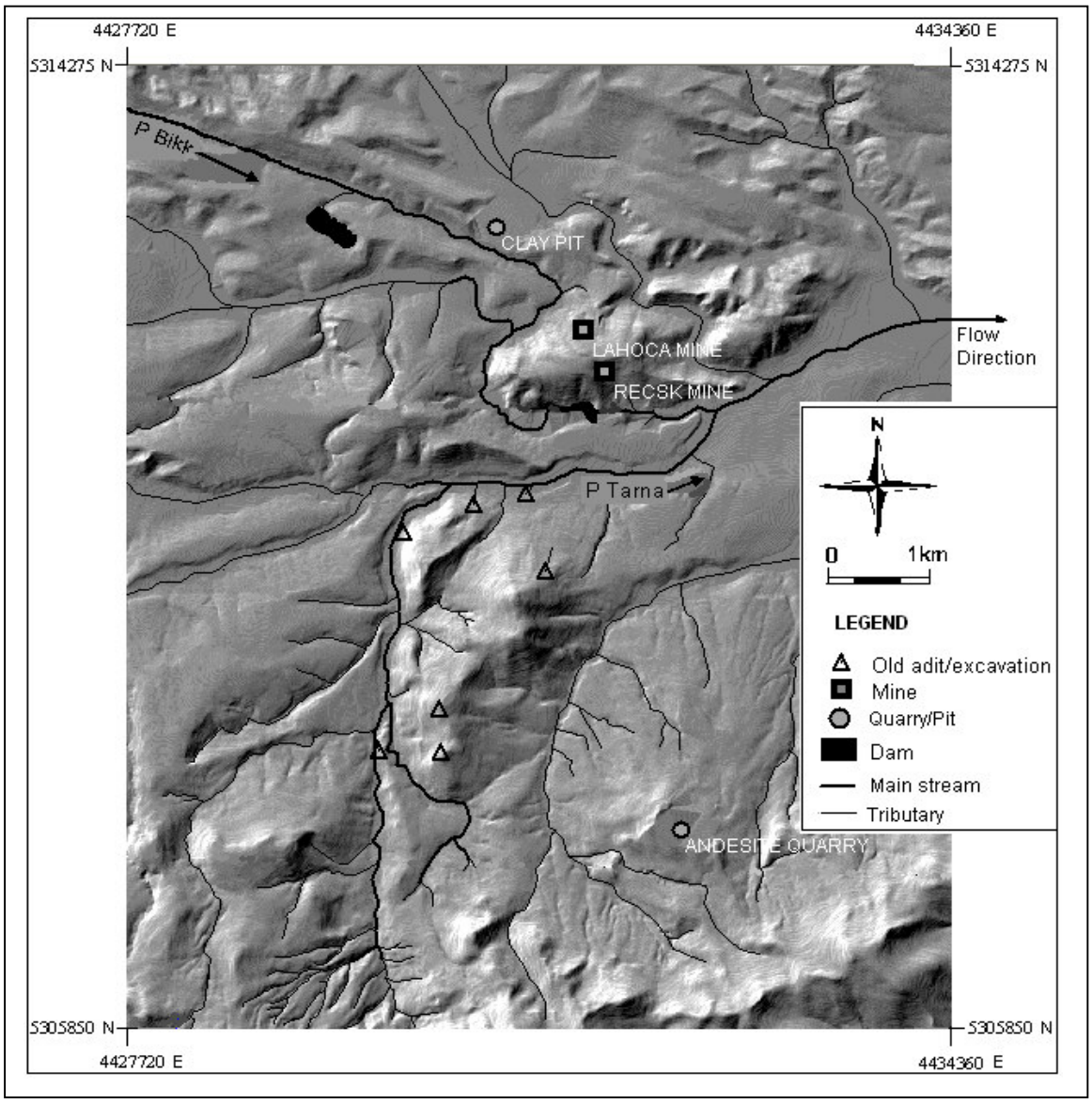

Figure 2.3.Recsk drainage system.

The small streams drain into the two major streams of the area, the Parad Tarna and the Parad Bikk, which are shown by thicker line presentation in figure 2.3. The Parad Tarna flows from south to north, through ancient mine workings areas up to the Recsk mine area, where the stream course changes to flow in an eastwards direction. The Parad Bikk flows in a south-easterly direction through the Lahoca and Recsk mine areas before it joins the Parad Tarna. After the confluence, the stream flows east-wards down into the low-lying flat areas. Figure 2.3 shows the drainage patterns of the area.

2.3.3. Weathering and erosion

The degree of weathering varies with the type of lithology. The andesitic rock formation in the research area is highly weathered and argillised in some areas, resulting in relatively thick soil profiles. Other areas are less weathered due to silicification of the andesite that has made the rocks resistant.

In areas where landform has been shaped by erosion, drainage valleys and small flat depositional surfaces can be seen. Erosion of mill tailings is also high giving rise to gullies and sheet erosion. This has accelerated the deposition of mine waste in the floodplains.

2.4. Geology and Mineralisation

2.4.1. Geo-tectonic setting

The Matra Mountains are among the largest units of the inner Carpathian volcanic arc (Czako and Zelenka, 1981) and comprise the largest Tertiary volcanic ranges of Hungary. They are a result of overthrusting and subduction due to convergent motions that took place between the European and African plates. The volcanic magmatism in the thrust-subduction zones produced andesitic and rhyolitic subvolcanic bodies, and subaerial and submarine stratovolcanos. Ore minerals are hosted in these volcanic rocks.

The tectonic activity gave rise to linear and curved faults. The curved faults are indicative of compressional conditions. The straight lineaments are of two types: (1) short lineaments, which are normal faults; (2) longer lineaments, which are strike slip faults. The straight lineaments are older than the Carpathian volcanic event since they off set older lithologies.

2.4.2. Lithologies

The geology of the Recsk-Lahoca mining area and the immediate surroundings is mainly comprised of volcanic rocks that range in age from the Eocene to Miocene (figure 2.4.). Underlying the volcanic rocks, but not exposed in the area, are the Triassic carbonate rocks that are intruded by a diorite (Akos, 1999).

The Eocene strato-volcanic sequence consists of sub-marine andesite flows, dacite flows and pyroclastics. The lithologies of this sequence are the main hosts of sulphide mineralisation. At Recsk mine, three major host lithologies have been identified. The lower most unit is a shallow seated subvolcanic body of hornblende diorite porphyry. The middle unit is a thick breccia, which is partially overlain by hornblende andesite. The andesite forms plugs and dykes that blankets over the breccia. The lithologies are frequently silicified and argillised. There are also marine sediments of Oligocene to early Miocene age, commonly known as Oligocene clay sediments. Overlying the Oligocene sediments are Miocene magmatics comprising of sub-volcanic bodies and strato-volcanic sequences. They are mainly pyroxene andesite lava flows and rhyolite tuffs with some agglomerates, and biotitic and dacitic tuffs.

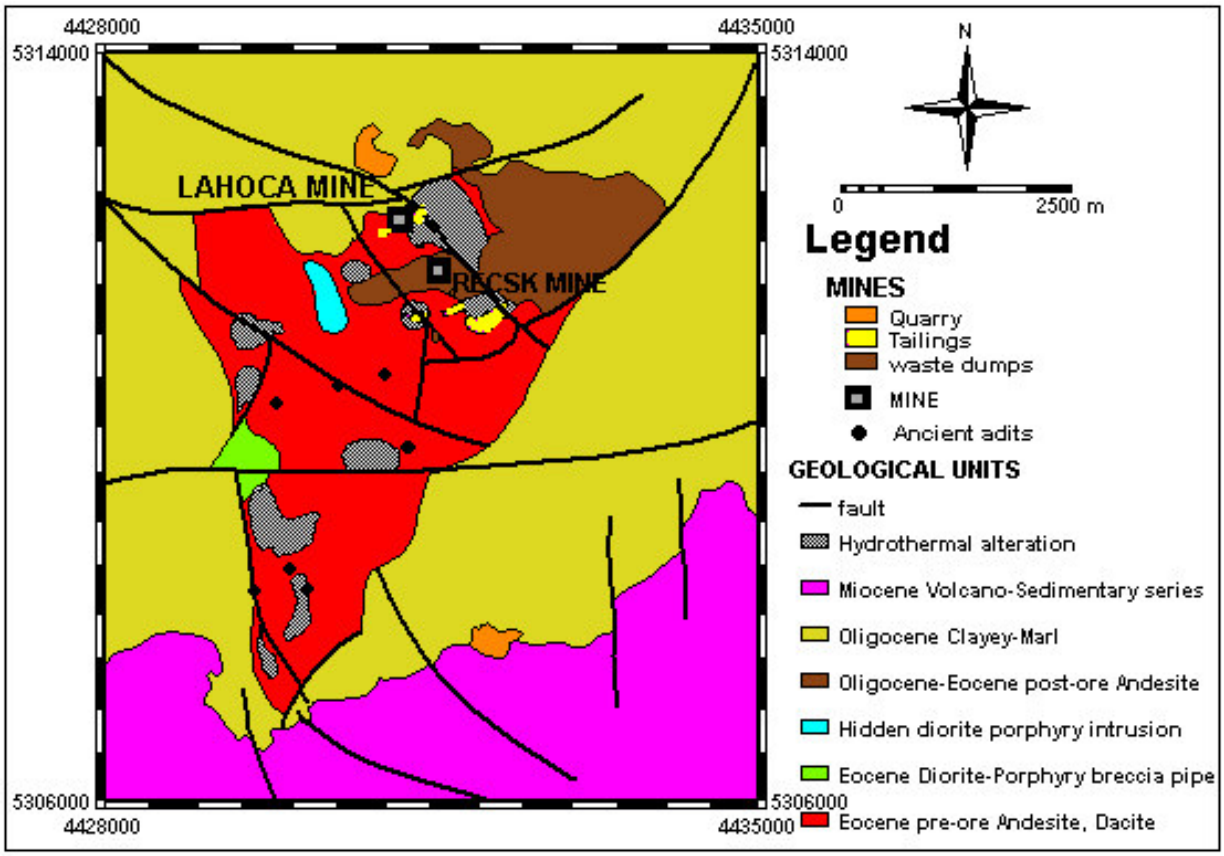

Figure 2.4. Geology around Recsk area (from Foldessy, 1996).

2.4.3. Mineralization of the Recsk-Lahoca Mining area

The strato-volcanoes and sub-volcanic intrusives of the Matra Mountains host gold, silver and base metal deposits of epithermal, porphyry, massive sulphide and skarn type of mineralisation. Vein type and disseminated sulphide deposits are of a younger age, and mainly associated with younger fault systems that are controlled by later subduction related geotectonic events (Akos, 1999).

The epithermal mineralisation is characterised by Au-Cu high sulphidation deposits found near surface. The porphyry copper, Cu-Zn skarn, vein and replacement mineralisation are found at deeper levels, and are commonly known as the 'Recsk Deeps' (Akos, 1999). A schematic section of the Recsk-Lahoca ore complex is shown in figure 2.5.

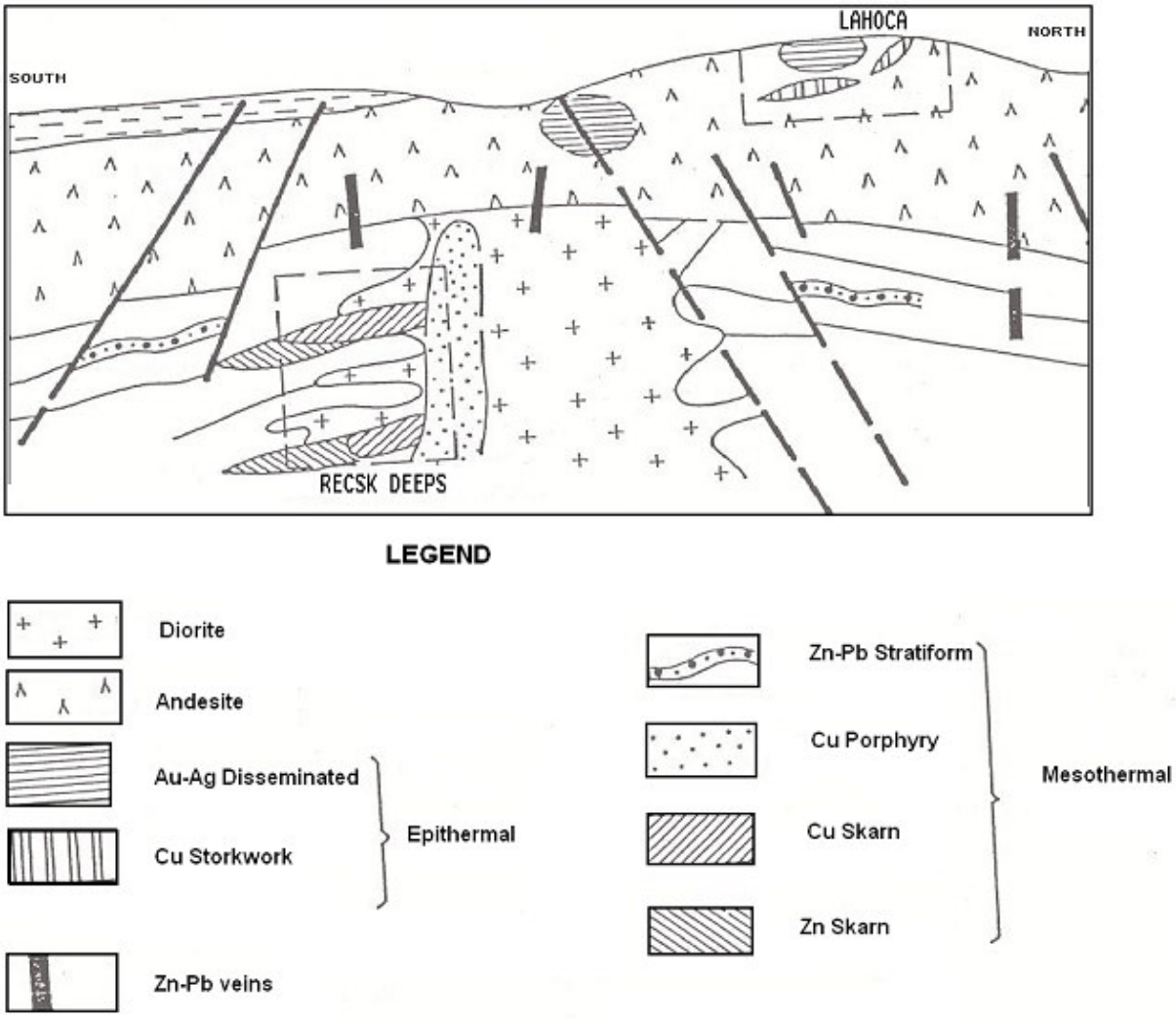

Figure 2.5. Schematic section of Recsk- Lahoca and "Recsk Deeps" ore complex (from Foldessy, 1996).

The near surface Au-Cu-epithermal deposits are hosted by the uppermost Eocene calc-alkaline andesitic stratovolcanic sequences, which are cut by mylonitized tectonic zones. The mylonite zones are composed of highly altered, argillised and brecciated andesite (figure 2.6). The angular texture of the mylonites indicates a tectonic origin. Pipe-like intrusions gave rise to hydrothermalized breccia zones at the contacts. These zones are characterized by the presents of vuggy silica and highest gold content. An advanced argillic zone containing kaolinite, smecktite, illite, dickite and quartz surrounds the silicified and pyritized zone. In the mineralised zones, the most common ore sulphides are pyrite, chalcopyrite, sphalerite, enargite, luzonite (Cu_3AsS_4) and tetrahydrite while the gangue minerals are calcite, quartz, barite and other sulphides.

Figure 2.6. Sulphidised andesite breccia. The grey colour of the breccia is due to high pyrite content whilst yellow tint in fractures is due to pyrite oxidation.

Fig. 2.7. Clay pit.

Figure 2.8. A collapsed adit entrance characterised by ground subsidence and acidic water discharges.

The Recsk Deeps are mainly composed of three ore mineralisation types. These are galena-sphalerite vein type deposit, porphyry copper deposit and Cu-Zn skarn. The porphyry copper deposit also has some gold mineralisation in zones where propylitic alteration is overprinted by skarn. The Cu-Zn skarn lies in the upper part of a diorite intrusion in a zone of strong propylitic alteration and andularia –sericite alteration. The Cu-Zn skarn and replacement deposits are developed along the contact between the diorite intrusion and the Triassic limestone and dolostone, and within the Triassic carbonates.

2.5. Mining in the area

2.5.1. Mining of non-metallic deposits

There are two major industrial non-metallic mineral resources in the area: (1) the Miocene andesite-rhyolite rock; (2) the Oligocene clay deposits. The unaltered pyroxene andesites of glassy matrix are quarried mainly for road construction purposes. The quarries have been opened in the youngest andesite sequences where post-volcanic alteration is minimal. The Oligocene clay deposits are mined for brick manufacturing. Figure 2.7 shows an open pit for clay mining.

2.5.2. Mining of Base metals, gold and silver.

Base and precious metal mining in the Recsk area started about 200 years ago. Several ancient adits exist in the area. These adits were used to access the ore bodies, which were mined for copper and silver from narrow veinlet zones. The portals of many of these adits have since collapsed but there locations can be traced by distinctive depressions (figure 2.8) due to ground subsidence and acidic water leaking out of these depressions.

The major mining activities took place mostly between the 1950s and 1998. The Lahoca hill has been mined for copper since 1852 up to 1979. The ore deposit was accessed by an adit. Fifty-five kilometres of drifts, large open stopes and 44 mine levels were developed during the period of its production.

A project to mine copper from the Recsk Deeps resulted in the development of an 8-m diameter shaft that was 1200 m deep. Drives and crosscuts were also developed at 700, 900 and 1100 m depths for ore production. The mine was meant to produce 3 to 5 million tonnes of ore per year but it never went into production since its construction in 1970. In 1991, an exploration survey led to the discovery of the Recsk-Lahoca near surface copper-gold epithermal deposit that was mined for copper, gold and silver up to 1998.

Mine production figures that were made available to this research are for the Recsk mine and are for the period 1931 to 1979 (table 2.1.).

Table 2.1. Recsk mine production summary from 1931 to 1979.

PERIOD (Years)	Amount of ore Processed (x1000t)	METALS RECOVERED								
		COPPER			GOLD			SILVER		
		Ore Grade (%Cu)	Metal Content (x1000t)	% Recovery	Ore Grade (g/t Au)	Metal Content (kg)	% Recovery	Ore Grade (g/t Ag)	Metal Content (tons)	% Recovery
1931-1935	133.3	0.99	1.32	78.0	3.92	522.8	64.0	18.80	2.50	70.8
1936-1944	529.0	0.88	4.67	61.0	3.98	2 107.5	64.0	27.82	14.74	73.0
1945-1979	1 804.7	0.66	11.86	86.0	2.12	3 820.7	68.0	19.66	35.48	90.0
TOTAL	2 467.8	0.72	17.86	80.8	2.61	6451.1	66.4	21.37	52.73	84.7

(Source-Recsk Ercbanya Company.)

The amount of material mined and dumped around the mine was also quantified. The material includes fine floatation waste, rock waste and ore rock that was never processed during the life of the mine. Table 2.2 summarises the quantity of the material and its aerial extend to date.

Table 2.2. Waste material around Recsk mine

MATERIAL	Floatation waste	Rock waste	Unprocessed mined ore	Total
Area covered (m^2)	52 000	33 000	54 660	139 660
Amount (Tonnes)	1 350 000	307 000	478 000	2 135 000

(Source-Recsk Ercbanya Company.)

2.6. Environmental Signatures and Effects of the Oxidation of Sulphide Deposits

The sulphide deposits in the area and the mining of these deposits have observable environmental signatures and effects. **Environmental signatures** of mineral deposits are suites, concentrations, residences, and availabilities of chemical elements in soil, sediment, airborne particulates and water at a site that result from the natural weathering of mineral deposits and from mining, mineral processing and smelting. **Environmental effects** of mineral deposits are spatially broader than environmental signatures in that they include the influence of a mineralised site or a mining site on the surrounding environment. An example is the environmental effects of mine drainage on a river into which the mine drainage flows (Plumlee et al, 1995).

2.6.1. Natural environmental signatures and effects

Sulphide mineral deposits have natural environmental signatures in the form of secondary geochemical anomalies due to natural weathering, which result in the natural formation of acid drainage and release of heavy metals into the nearby ecosystems

The natural environmental signatures of the sulphide mineral deposits in the area are concentrated in mineralised and altered zones and their environmental effects can be observed particularly along the

drainage systems in the area. Figure 2.9 shows the sidewall of a valley cut by Parad Tarna creek in a weathered zone, which is within a geochemical anomaly of base metals. The grey material is mineralised and altered pyrite-rich rock while the white material indicates argillised rock. Ground and surface waters in this geochemical anomalous area contain elevated metal content, unlike in the non-mineralised areas. Yellow iron precipitates can also be seen on the riverbed. Geochemical anomalous zones in the area given, as the one shown in figure 2.9, give rise to natural heavy metal load in the drainage system due to leaching of metal sulphides during weathering.

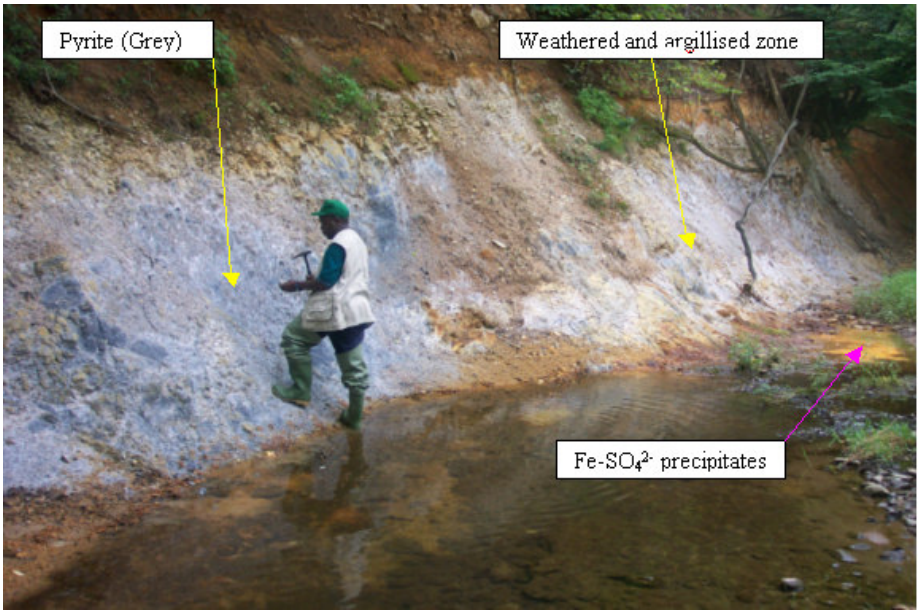

Figure 2.9. Pyritic and argillic alteration in a geochemical anomaly along Tarna creek.

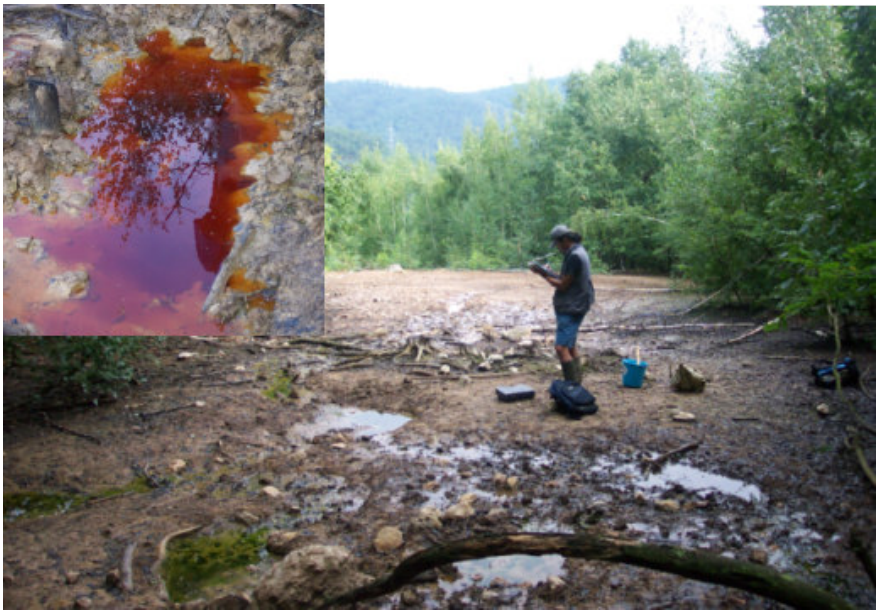
Figure 2.10. Vegetation poisoned by toxic acidic water from an ancient adit. Inset shows typical colour of acidic water, pH~2.

Faults and fractures are expected to play significant roles in the chemistry of water draining the area. They act as conduits for water and oxygen that oxidize and weather the minerals and liberate metals into solution, which is then discharged into the drainage systems. The area, being a zone of high tectonic activity, is intensely faulted and fractured. In many sections of the area, river channels follow fault lines, which is a phenomenon that can enhance the natural environmental signatures and natural environmental effects of the sulphide mineral deposits in the area particularly because the deposits are fault/fracture controlled.

2.6.2. Mining-induced environmental signatures and effects

Mining has significant influence on the environmental signatures of sulphide deposits in the area. Ancient mining resulted in underground openings, which accelerate oxidation of sulphide minerals. As a result, most of the old mine adits discharge highly acidic water (pH~2) with high sulphate and heavy metal content like the one shown in figure 2.8. In some areas, the water is so acidic and toxic that vegetation has been poisoned in discharge zones (figure 2.10.). The water is deep red and suspended sediments/colloids are orange yellow in colour due to iron hydroxide-sulphate precipitation. The amount of water draining from ancient adits is small and most of it evaporates or seeps back into the ground before reaching the main river channels. It is probable that environmental contamination from adits is minimal compared to that of waste dumps and tailings piles in the area.

Recent mining at Recsk and Lahoca mines gave rise to large volumes of waste dumps and mill tailings containing high amounts of sulphide minerals. The waste dumps and tailings piles are major point sources of heavy metal contamination in the area. A cadastral survey carried out in the area shows that there are about 2,135,000 tonnes of floatation tailings piles, waste dumps and unprocessed ore, which cover an area of about 139 660m^2 (table 2.2.). Most of the sulphide-rich waste materials are exposed to surface water and oxygen, which causes oxidation and subsequent leaching of heavy metals. The unprocessed ore piles constitute more than a third of the area covered by the exposed sulphide-rich waste material. It is therefore most likely to be the highest contributor to heavy metal contamination since it covers a large area and contains higher metal content than the floatation tailings and waste rock.

The production figures from Recsk Ercbanya Company can be used to estimate the amount of copper, gold and silver remaining in the flotation tailings generated in the period 1931 to 1979. Given the milled ore quantity, grade and recovery, the amount of residual metal quantity can be calculated. Let X be the total ore mined, G the ore grade, and R the percentage of metal recovered. The total ore metal content (M) is M = X*G. The total metal extracted (E) is E = X*G*R/100. The percentage of the residual metal = 100-R. Therefore, total residual metal (T) in the tailings = X*G*(100-R)/100. Table 2.3 summarises the estimated amount of copper, gold and silver remaining in the floatation tailings after milling and metallurgical processing for the period 1931 to 1979. The values in the summary table have been calculated from table 2.1.

Table 2.3. Residual amounts of Cu, Au & Ag in Recsk floatation tailings generated in the period 1931 to 1979.

METAL	**Copper**	**Gold**	**Silver**
Total ore metal content (M)	18,000tons	6,450kg	53tons
Recovery (R) in percentage	80	66	85
% Residual (100-R)	20	34	15
Total residual metal in tailings	3,600 tons	2,190kg	8tons

Thus about 3,600tons of copper, 2,190kg of gold and 8tons of silver remained in mill floatation residues from the production period 1931-1979. The residual metal contents in the mill tailings are highly vulnerable to oxidation and leaching since these materials are exposed to surface water and oxygen. Unlike in-situ rock, floatation tailings are composed of finely ground particles with increased surface area and pore space for oxygen and water penetration and contact with the residual metals. As a result, these remaining metal quantities are potential environmental contaminants that can have devastating effects over a long period of time.

Most of the waste dumps and floatation tailings piles were not properly disposed. As a result, the waste dumps easily yield to geomorphologic processes of weathering and erosion. Both sheet and gully erosion are so intense that most of the soils used to cover the tailings piles to mitigate environmental contamination have been washed away together with the tailings. Figure 2.11 shows gully erosion on the slopes of west Lahoca soil-covered mill tailings dump. With no preventive measures being taken, the gully widens as more materials are washed away. This result in more surface exposure of the sulphide mine wastes to oxygen and water that initiate and accelerate acid mine drainage. Oxidation and leaching is evident in the profiles of the Recsk mine tailings that are exposed by erosion. Distinct horizons indicate an upper oxidation zone and a lower leached zone (figure 2.12). The upper horizon is yellow due to the strong staining effect of iron oxides like limonite and jarosites, while the lower horizon is whitish-grey due to heavy leaching of iron and other heavy metal minerals. The boundary between the oxidized and leached zones marks the general lower limit of the tailings water table.

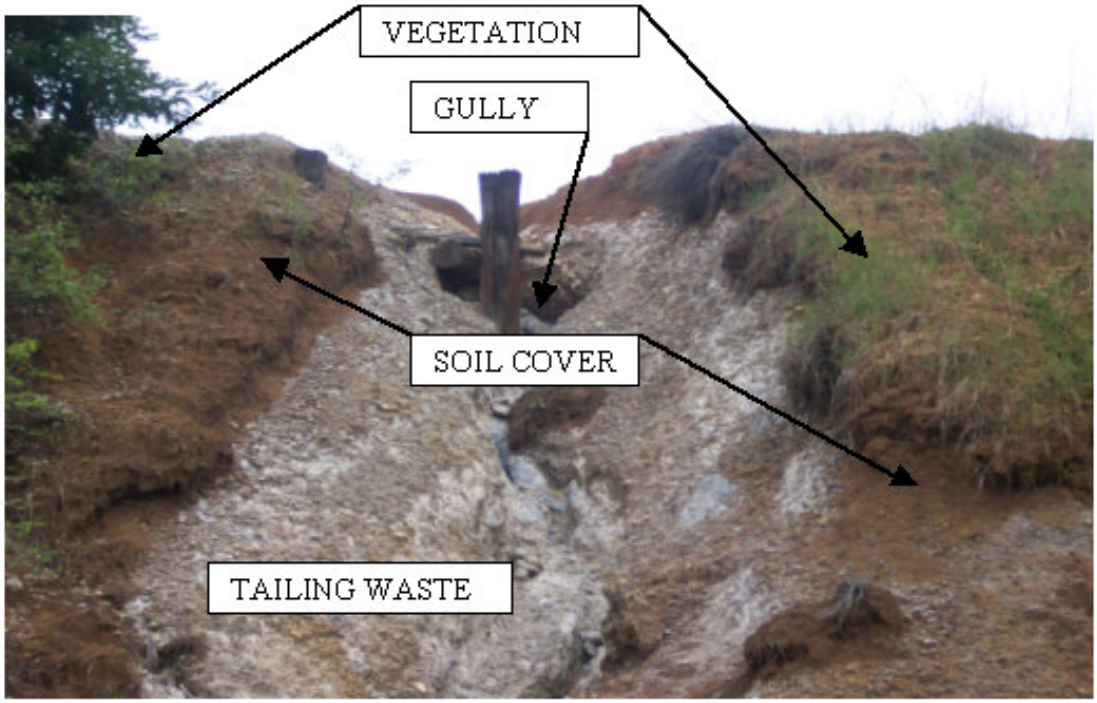

Figure 2.11. Gully erosion on lahoca floatation tailings piles.

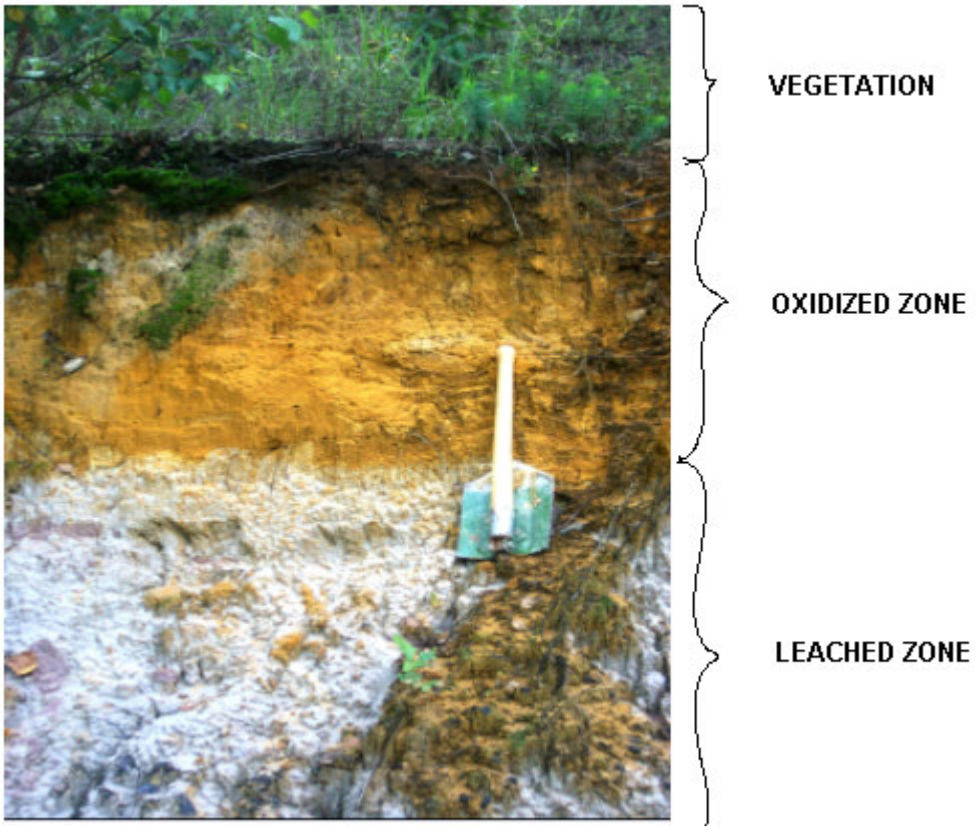

Figure 2.12. Vertical profile of floatation tailings (Recsk).

The erosion of mine wastes has observable environmental effects in the area. A lot of waste materials have been transported into rivers and later deposited into flood plains. “Yellow boy” is noticeable in some of the streambeds, banks and sediment deposits. The “yellow boy” is a result of iron (III) ions (Fe^{3+}) that are often released into surface waters as a result of weathering of pyrite in mine wastes (Horan J, 1999). This mine drainage is typically very acidic. The acid mine drainage is often diluted by fresh water as tributaries mix with the water draining from the mine tailings. The acid mine drainage may also become neutral when it comes into contact with acid consuming minerals (e.g. calcite). In either case, the pH rises. As the pH of the mine drainage increases, soluble Iron (III) ions will hydrolyse and precipitate out of solution as $Fe(OH)_3$ through reactions 2 and 3 explained in chapter 1. The precipitated iron (III) hydroxide ($Fe(OH)_{3(s)}$) is called "yellow boy". It is an unsightly, slimy, yellow or orange coloured solid that coats the streambed and discolours the water. "Yellow boy" also has a negative impact on all living organisms in the stream (Horan J, 1999). "Yellow boy" are observable along the Parad Bikk and Parad Tarna. Figure 2.13 shows “yellow boy” along a section of Parad Tarna. The iron (III) is from acidic water discharged from mine workings or in areas where the streams drain hydrothermal alteration and argillised areas.

Metal drainage pipes have been constructed into the tailings piles to drain water and regulate the amount of water and thus erosion in the tailings (figure 2.14.). The metal drainage pipe discharges water into a small canal that further empties into the Parad Bikk. The Recsk and Lahoca waste dumps and tailings piles are located very close to Parad Bikk, making it easy for water draining from tailings to discharge into the streams (figure 2.15). In sections where the stream passes through the Recsk tailings, a concrete drainage channel has been constructed to redirect the stream flow (figure 2.16). Because of the smooth bed of the concrete channel, sediment transportation is facilitated. This results in high quantity of mine derived sediments being deposited onto the floodplains downstream of the tailings. Surface run-off from Recsk

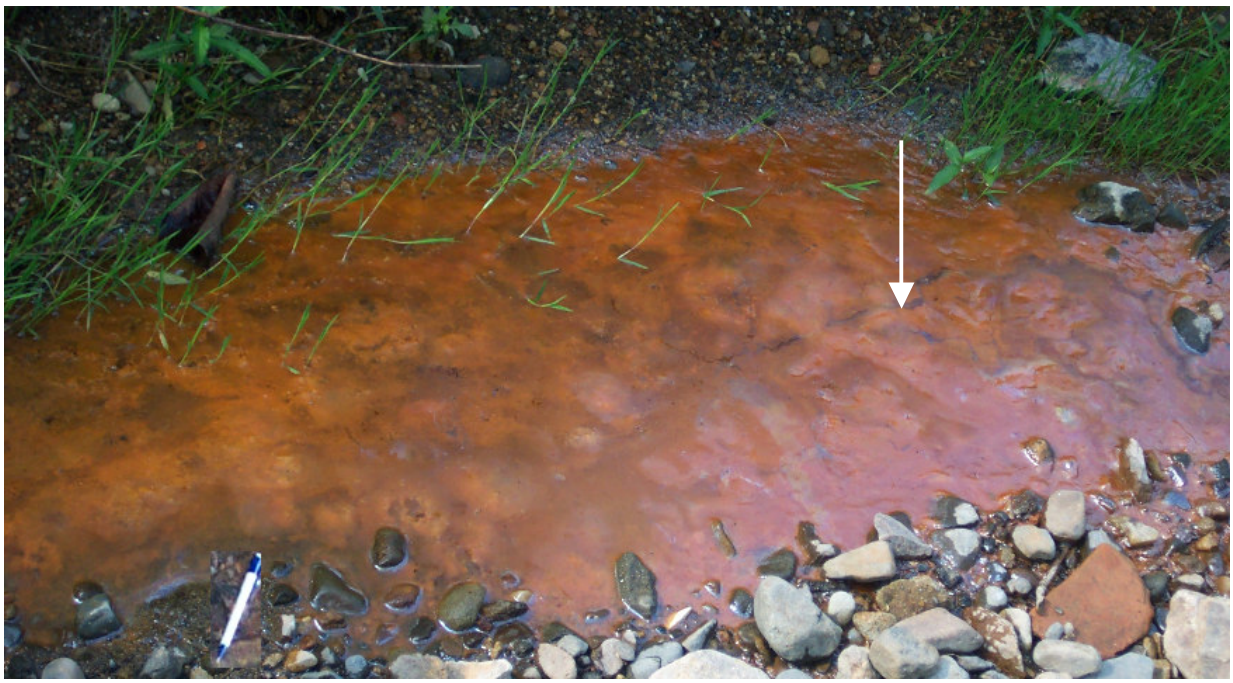

Figure 2.13. Iron (III) precipitates (yellow boy) observed at interface between Parad Tarna waters and waters oozing out of old mine adit.

floatation tailings was also found to be highly acidic and contain high heavy metals and sulphate ions.

Figure 2.14. Metal drainage pipe draining acidic water from east Recsk tailings pile.

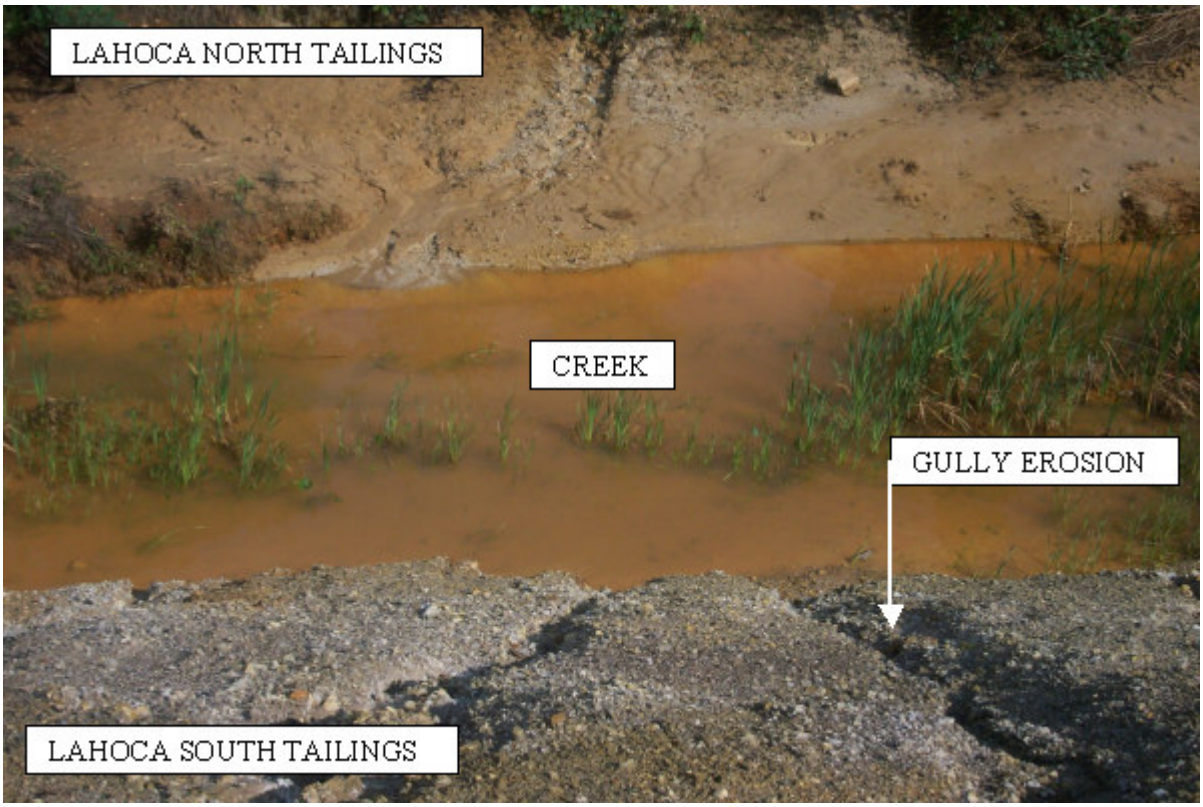

Figure 2.15. Parad Bikk tributary passing through Lahoca east and Lahoca west tailings piles.

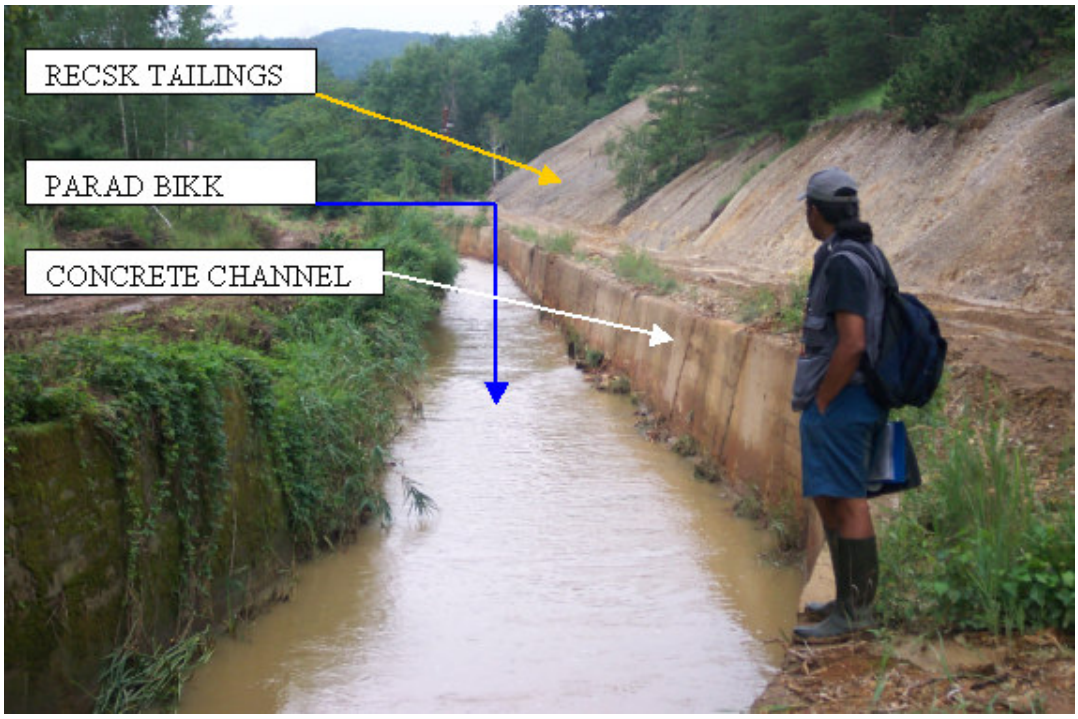

Figure 2.16. Recsk tailings near a modified channel of Parad Bikk

There are also human post mining activities that contribute to environmental effects in the area. The local people dig floatation tailings for use as building material. The resulting pits expose more sulphide waste to weathering. The pits also accelerate erosion of the tailings deposited in the floodplains. Figure 2.17 shows a portion of the tailings pile exposed to the surface by pits dug to extract materials for building purposes.

Figure 2.17. Gully erosion and diggings of mine floatation tailings.

2.7. Conclusions

The geology of the area is mainly comprised of hydrothermally-altered and sulphide mineralised andesitic rocks. Argillised and pyrite-impregnated rocks outcropping along streams form natural drainage geochemical anomalies. Yellow precipitates of iron oxides/hydroxides and sulphates have been observed along these drainage geochemical anomalies. Fault/fractures and breccias in argillised and mineralised rocks act as conduits for water and oxygen, which react with sulphide minerals and subsequently leach heavy metals and sulphates into the drainage system of the area. All these natural processes give rise to natural acid rock drainage in the area

The lack of vegetation in the vicinity of ancient adit portals where mine waters leak through to the surface indicates that the mine waters are toxic to plant life, which further indicates that waters coming out of the adits are most likely acidic and contaminated by heavy metals. Oxidation of mill tailings is evident on the Recsk dumps. The yellow colour of the tailings indicates precipitation of iron oxides, hence leaching of sulphates and heavy metals by the waters draining these tailings dumps. These are mining induced processes that give rise to acid mine drainage related problems in the downstream area.

Gully and sheet erosion processes are taking place on the tailings dumps on the mines. The erosion processes are facilitated by (a) their close proximity to the streams and (b) the local people digging the tailings material for construction purposes. These erosion processes facilitate transportation of mine waste into streams and subsequent deposition of mine waste in floodplains. Thus heavy metal load is expected along the streams and in the flood plains.

The natural and mining induced environmental signatures cause natural rock drainage and acid mine drainage respectively. Geochemical analysis of waters draining the mine area can be helpful in confirming the environmental effects that result from the environmental signatures and processes taking place in the area. An understanding of the geochemistry of stream sediments can be useful in determining precipitates that result from the elements leached out of rocks exposed by mining. Geochemical analysis of the tailings can also be used in determining those areas prone to cause acid mine drainage. Analysis of the spatial distribution of geochemical data in relation to environmental signatures and physical processes taking place in the area can lead to the mapping and classification of natural and mining-induced environmental effects of the geology and mineralization of the area.

3. GEOCHEMICAL DATA: COLLECTION AND QUALITY ASSESSMENT

In areas of mine-induced heavy metal contamination, understanding geology and mineral deposits and mineral extraction processes is necessary to determine the contribution of these factors to the heavy metal load and the attenuation of heavy metals in the drainage system. Geochemical data can be used to qualify environmental signatures, and to quantify environmental effects of geogenic and anthropogenic factors of mine-induced heavy metal contamination (Plumlee and Nash, 1995). In order that results of geochemical data analysis adequately characterise these processes, it is imperative to understand the quality of data used and to present the data in a manner that adequately portrays the spatial geochemical variations due to the geogenic and anthropogenic factors.

3.1. Base Map construction

3.1.1. Base map for drainage geochemical data

After a ground reconnaissance survey of the Recsk-Lahoca mining area, a base map was prepared for the sampling of stream waters and sediments. The spatial data used in preparing the base map include 1:25,000-scale Recsk and Kekesteto topographic map sheets, 1:200,000-scale geological map of the Matra Mountains, a DEM, aerial photographs and other unpublished maps from the Recsk Ecbanya Company. The analogue spatial data were digitally scanned and imported to a GIS. Using a georeference created from the EOV metric coordinate system of the topographic maps, topographic features such as roads, drainage courses, existing mine workings and mine sites, tailings/waste dumps etc were digitized. The outlines of known geochemical anomaly zones were digitized from the geological map. Six DEMs, which cover the research area, were imported to the GIS, glued together and then georeferenced. An overlay of the spatial features resulted in a map used as basis for presenting the geochemical data and displaying the results of geochemical data analysis. Displayed in figure 3.1 is the generated base map showing drainage sample locations and spatial features likely to affect the drainage geochemistry of the area.

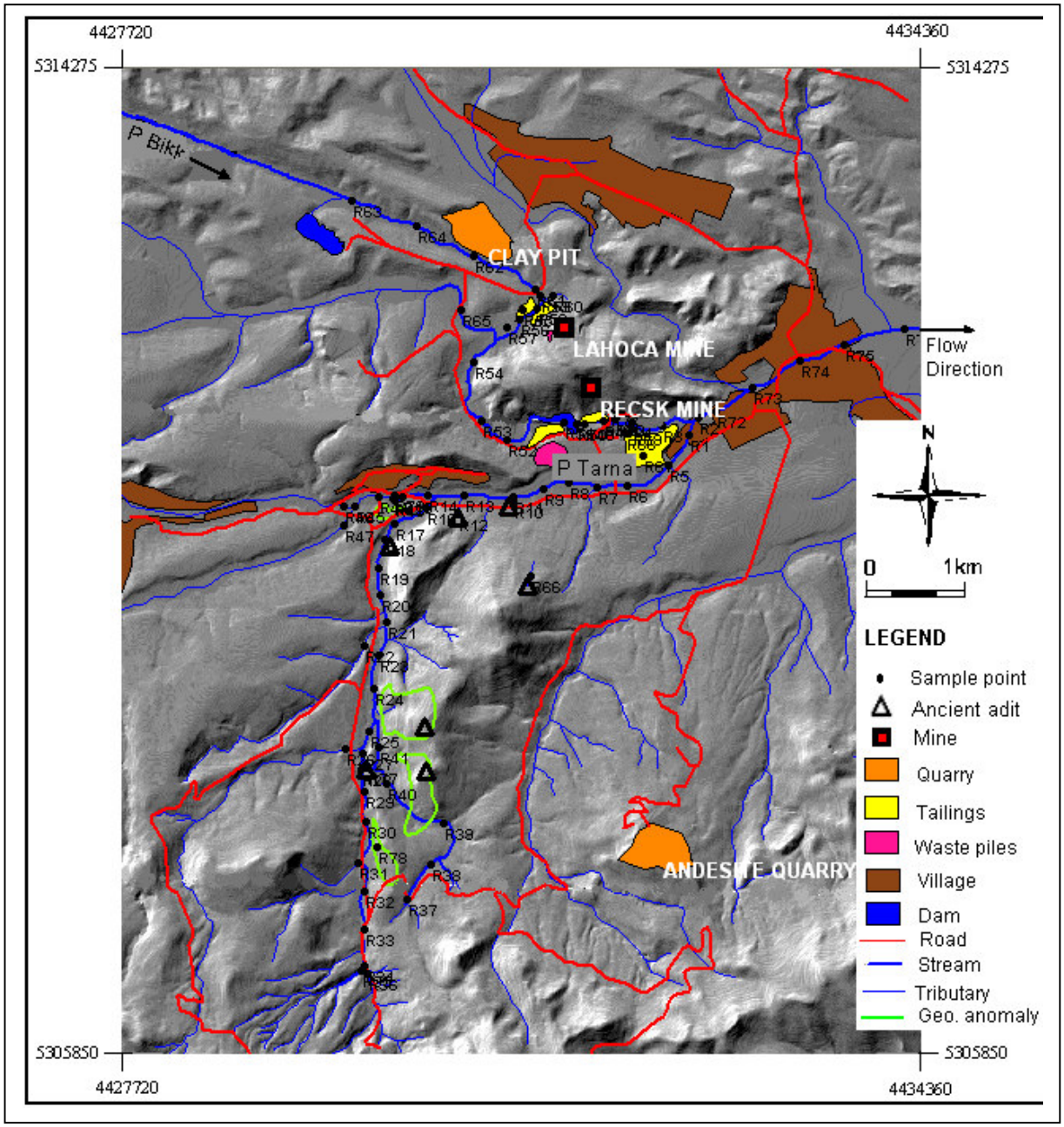

Figure 3.1. Base map showing water and stream sediment sample locations and the associated environmental features.

3.1.2. Base map for Tailings geochemical data

A base map was prepared for plotting the tailings grid geochemical data collected from the detailed sampling carried out on the Lahoca tailings piles. The EOV coordinate system was used to georeference the map. The 99 sample sites established for the collection of tailings samples are displayed in figure 3.2.

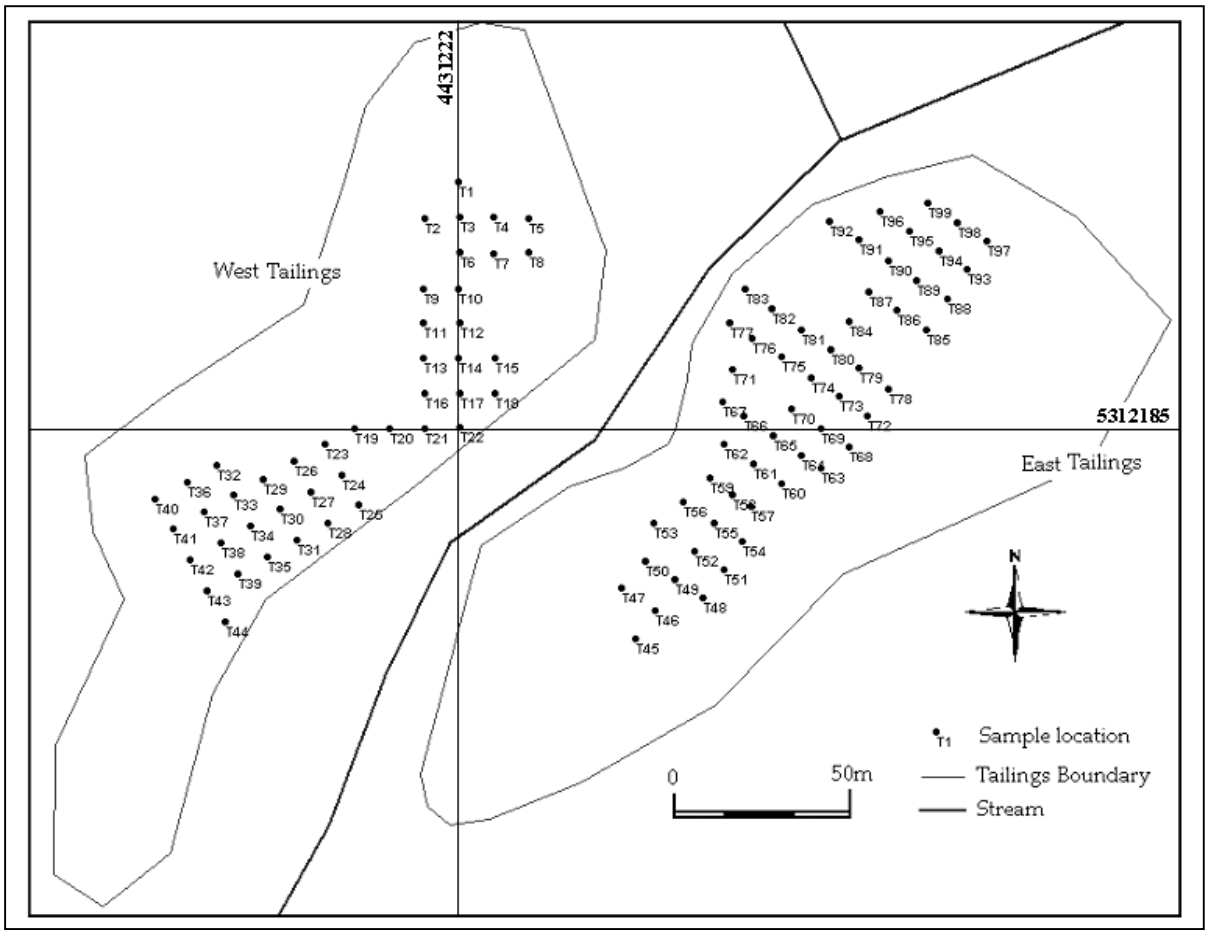

Figure 3.2. Map showing sampling grid on the Lahoca east and west floatation tailings piles.

3.2. Collection and chemical analysis of geochemical samples.

3.2.1. Water samples

Water samples were collected from Parad Tarna and Parad Bikk, and their tributaries. Samples were also collected from waters draining ancient adits, tailings piles, gas seepage area and a groundwater well in the area. A total of 79 stream water samples were collected at about 250 m intervals along the stream courses in the study area (figure 3.1). Two water samples were collected into 60ml bottles at each sample point and duplicate samples were collected after every 10 sampling points. One sample was filtered and acidified with nitric acid while the other was neither filtered nor acidified. The samples were acidified to keep metal ions from precipitating and were filtered to leave out any suspended

solids that can possibly dissolve and change the concentrations of the dissolved metals. Filtering was achieved by the use of a 45μm filter mounted on a syringe from which water is injected past the filter into a sample bottle. To minimise contamination of the samples, a filter was used only once per sample and discarded.

Field measurements that were taken on sample sites were temperature, pH, electrical conductivity, and site locations using GPS. The pH of water was measured using a portable field pH-meter. Indicator paper was also used to measure pH. Because the interpretation of pH indicator paper is subjective, it was only used to check the performance of the pH meter, which was expected to give measurement readings within the range of pH indicator paper. Electrical conductivity and temperature of water were measured using a portable field EC meter, which has an inbuilt thermometer. Arsenic and sulphate measurements were taken intermittently on some selected locations.

Samples were carefully marked and the sample sites plotted on a base map (figure 3.1.).The letter W is prefixed to the sample location number for water samples and the letter S is prefixed to the sample number for stream sediments. At the field camp, the samples were then kept in a refrigerator until the day of dispatch to the laboratory where they were further kept in a refrigerator until the day of analysis. Keeping samples refrigerated minimises chances of chemical reactions, which can result in the precipitation of dissolved elements.

In the laboratory, 20 ml measures of acidified and filtered water samples were analysed for heavy metals and major cations. Element concentrations of As, Cd, Cu, Fe, Mn, Ni, Pb, Sb, Zn, Al, Ca, k, Mg, and Na were determined using the ICP-AES analyser. The unacidified and unfiltered water samples were analysed for sulphate concentration using the portable data logging spectrophotometer. Repeat samples were analysed after every 10 samples. Results of the chemical analysis are shown in appendix D.

3.2.2. Stream sediment samples

A total of 59 stream sediment samples were collected on the same sample sites as stream water samples (figure 3.1), except on sites where collection of stream sediments was not possible. A sample was composed of several grabs of fine sediments collected on the active part of the stream around the water sample site. A 2-mm mesh sieve was used to homogenise the sample particle sizes before being packed into standard stream sediments sample bags. Details of sample sites were recorded on the FOREGS sampling sheets for stream water and stream sediments, which were also used for recording water sample details (Appendix A). The samples were air dried at the field camp and packed for dispatch to ITC laboratory.

In the laboratory, the samples were further dried in an oven at 40^{o}c. Sample fractions of minus-80 mesh (< 180 μm) were then collected for subsequent chemical analysis. Measurements of 500 mg of the sieved sample fractions were placed in clearly labelled test tubes for decomposition. Repeat samples were randomly measured, and some standards included for assessment of precision and accuracy of laboratory procedures. Each sample measurement was decomposed by adding 2 ml of concentrated 63% hot nitric acid followed by shaking on a vortex shaker and shaking in a water bath at 90^{o}C for 2 hours. The samples were further shaken on a vortex shaker at intervals of 30 minutes within the 2-

hour water bath period. After digestion, the samples were diluted to 20 ml with distilled water. A correction for evaporation during water bath period was determined by measuring the volume of some of the sample test tubes before and after decomposition. The average difference of the measured volumes was taken to be equivalent to the overall loss due to evaporation and therefore compensated for by an equivalent addition of distilled water. The sample batches were left overnight (~20 hours) to allow residues to settle. The liquid portions of the decomposed samples were then decanted into test tubes for metal determinations on the ICP-AES. Elements determinations of As, Cd, Cu, Fe, Mn, Ni, Pb, Sb and Zn are shown in Appendix E.

3.2.3. Tailings Samples

Ninety-nine tailings samples were collected from portions of the Lahoca tailings piles without vegetation cover. Systematic sampling grids of 10m x 10m were prepared on the Lahoca east and west tailings piles (figure 3.2). Samples were collected from the top surface tailings material. A total of 12 grab samples were collected from the Recsk tailings piles. Sampling information and field observations for tailings were recorded in the FOREGS sampling sheets for soils (Appendix B). All samples were treated in the same manner as stream sediment samples and analysed for the same element determinations. Shown in appendix F are concentrations of the element determinations.

3.3. Geochemical data quality

The Forum of European Geological Surveys (FOREGS) procedures were used for sampling and chemical analysis of the samples in order to ensure maximum quality of geochemical data. The FOREGS observation sheets allowed recording of detailed field observations, which are useful in the analysis of water sample data. Sampling information, field measurements and field observations were therefore recorded in the FOREGS sampling sheets for stream water and stream sediments (Appendix A) and for soils (Appendix B). Shown in Appendix C are details of sample coordinates, measured physical properties, bed-rock geology, stream channel characteristics and possible sources of contamination. For the purposes of consistency, all samples were processed and analysed at ITC geochemical laboratory.

In any data analysis, confidence is required on the quality of the data. It is necessary to ensure that data of sufficient quality is capable of producing the required result for the hypothesis test. Data quality methods enable testing of significance levels in data interpretation, and can be used to test whether data randomness is due to natural geological settings or due to failure or bias of measurement procedures. Precision and accuracy are the main parameters used in determining the quality of data. A measurement is **precise** if repeated measurements of the same geological entity are similar, and is **accurate** if it is close to the "true" established value (Swan and Sandilands., 1995). Scatter plots and analysis of variance are important tools in data precision analysis. The methods employed in this analysis of geochemical data quality objectively determined data precision unlike accuracy which was subjectively analysed due to lack of duplicate standard samples geochemical data, which are used to determine data accuracy. Methods employed in the analysis of the quality of geochemical data were comparisons of data, scatter plots and analysis of variance. Geochemical data obtained from a second sample collected from the same site in the field is referred to as duplicate data whereas data obtained from a repeat of laboratory procedures on the same sample is referred to as repeat data.

3.3.1. Data comparisons for water samples

Due to the extremely low concentrations of As, Cd, Cu, Ni, Pb and Sb in the analysed water samples, most of the original-duplicate and original-repeat concentration results fell below the lower detection limits of the analysed elements. As a result, only those element pairs with significant results were compared in tabular form for those elements, while the other analysed elements were compared using scatter graphs. Table 3.1 shows the comparisons for 1st and 2nd sample results of field duplicate data.

Table 3.1. Comparison of 1st and 2nd sample results of field duplicate data for water samples. Concentrations are given in mg/l.

Element	Detection limit	First sample	Second sample	Difference	Percent difference	Remarks
	0.05	0.10	0.16	0.07	70.53	Close to lower detection limit
As	0.05	0.10	0.16	0.07	70.53	Close to lower detection limit
	0.05	1.40	1.45	0.05	3.57	Very low variation
Cd	0.01	0.70	0.60	0.10	14.29	Low variation
Cu	0.01	53.29	54.54	1.25	2.35	Very low variation
	0.01	229.51	191.02	38.49	16.77	Low variation
Ni	0.05	6.62	5.66	0.96	14.50	Low variation
Pb	0.05	4.25	2.75	1.50	35.29	High variation
	0.02	0.11	0.11	0.00	0.00	Very low variation
Sb	0.02	0.02	0.03	0.01	50.00	Close to lower detection limit
	0.01	0.18	0.16	0.02	11.11	Low variation
	0.01	0.04	0.05	0.01	25.00	Close to lower detection limit
Zn	0.01	0.02	0.04	0.02	100.00	Close to lower detection limit
	0.01	0.03	0.02	0.01	33.33	Close to lower detection limit
	0.01	44.33	46.51	2.18	4.92	Very low variation

Extremely low element concentrations are not very representative of the geo-fluvial processes taking place in the area due to high variability between the 1st and 2nd sample results of field duplicate data observed in table 3.1. Most of the duplicate pairs with high variability were from samples with metal concentrations that fell below/within their detection limits.

High variability is also observed in the data of 1st and 2nd analysis of laboratory repeat samples for element concentrations that fell below/within detection limits. Table 3.2 shows the observed variations in the comparison of 1st and 2nd analysis of laboratory repeat samples.

Element data with more than 30% of the concentration measurements falling below the detection limit of that element on the ICP analyser was therefore not included in the statistical evaluation used to classify the data into spatial distribution groups.

Table 3.2. Comparison of 1st and 2nd analysis results of laboratory repeat samples for element concentrations that fell below/within detection limits. Concentrations are given in mg/l.

Metal	Detection limit	First analysis	Second analysis	Difference	Percent difference	Remarks
Cd	0.01	0.03	0.03	0.00	0.00	Precision is very good
Cu	0.01	129.58	168.50	38.92	30.04	Low precision
Ni	0.05	0.02	0.02	0.00	0.00	Precision is very good
	0.05	1.03	1.69	0.66	64.08	Close to lower detection limit
Pb	0.05	3.78	4.04	0.26	6.88	Precision is very good
	0.05	0.04	0.06	0.02	50.00	Close to lower detection limit
Sb	0.01	0.17	0.13	0.04	23.53	Close to lower detection limit

3.3.2. Scatter plots

Scatter plots were used to graphically display trends of 1st and 2nd sample results of field duplicates and to graphically display trends of 1st and 2nd analysis of laboratory repeat samples. The purpose of the graphical displays is to visually observe the scatter of sample pairs in relation to the ideal 45°-line, which is expected in a 1:1 relationship.

Water samples

Figure 3.3 shows the scatter plots of 1st and 2nd sample results of field duplicate data for Fe, Mn, Zn, Ca, Mg, Al, K, Na and sulphate, and figure 3.4 shows the scatter plots of the data from laboratory repeat samples. Linear trends are observed on the scatter plots and deviations from the 45°-line are observed on some of the data pairs.

Significant deviations from the ideal 45°-line are observed in the scatter plots of Al, Fe and sulphate duplicate data, showing that the data for these elements may not be very representative of the area. Low concentrations for Fe and Al, which were very close to the lower detection limits for these elements, may have contributed to the large deviations from the ideal 1:1 relationship. The deviation for sulphate is partly due to errors incorporated through several dilutions effected on some of the water samples with higher sulphate concentrations. The purpose of the dilutions was to lower sulphate concentrations in water samples to concentration levels detectable by the portable data logging spectrophotometer. The upper limit of the spectrophotometer is 70mg/l and any dilution of up to the square of the upper limit (490mg/l) is liable to an error of 100%. Large deviations are observed in the scatter plot of Na data from laboratory repeat samples.

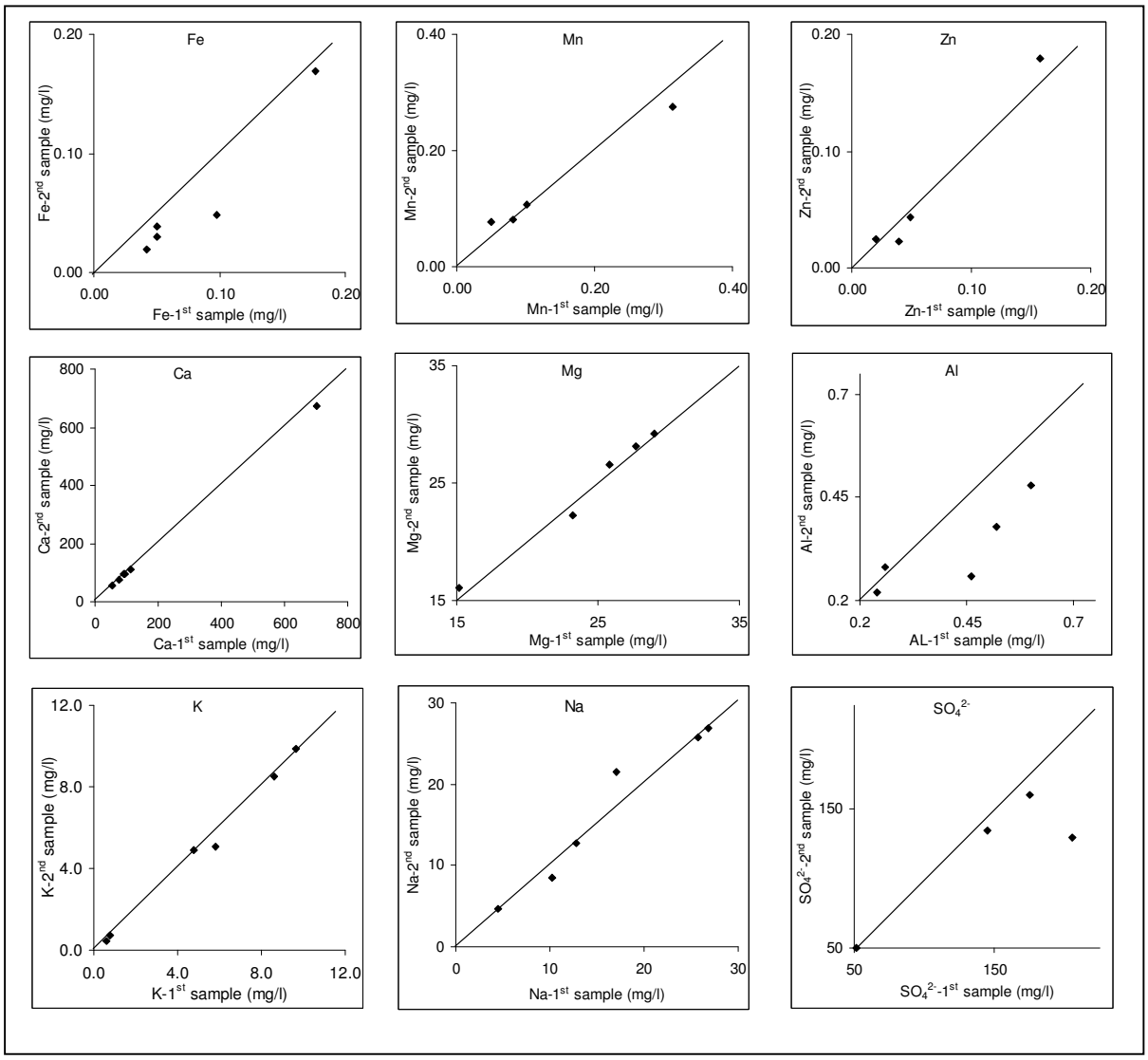

Figure 3.3. Scatter graphs showing plots of 1st and 2nd sample analysis of field duplicate water samples in the drainages of the area.

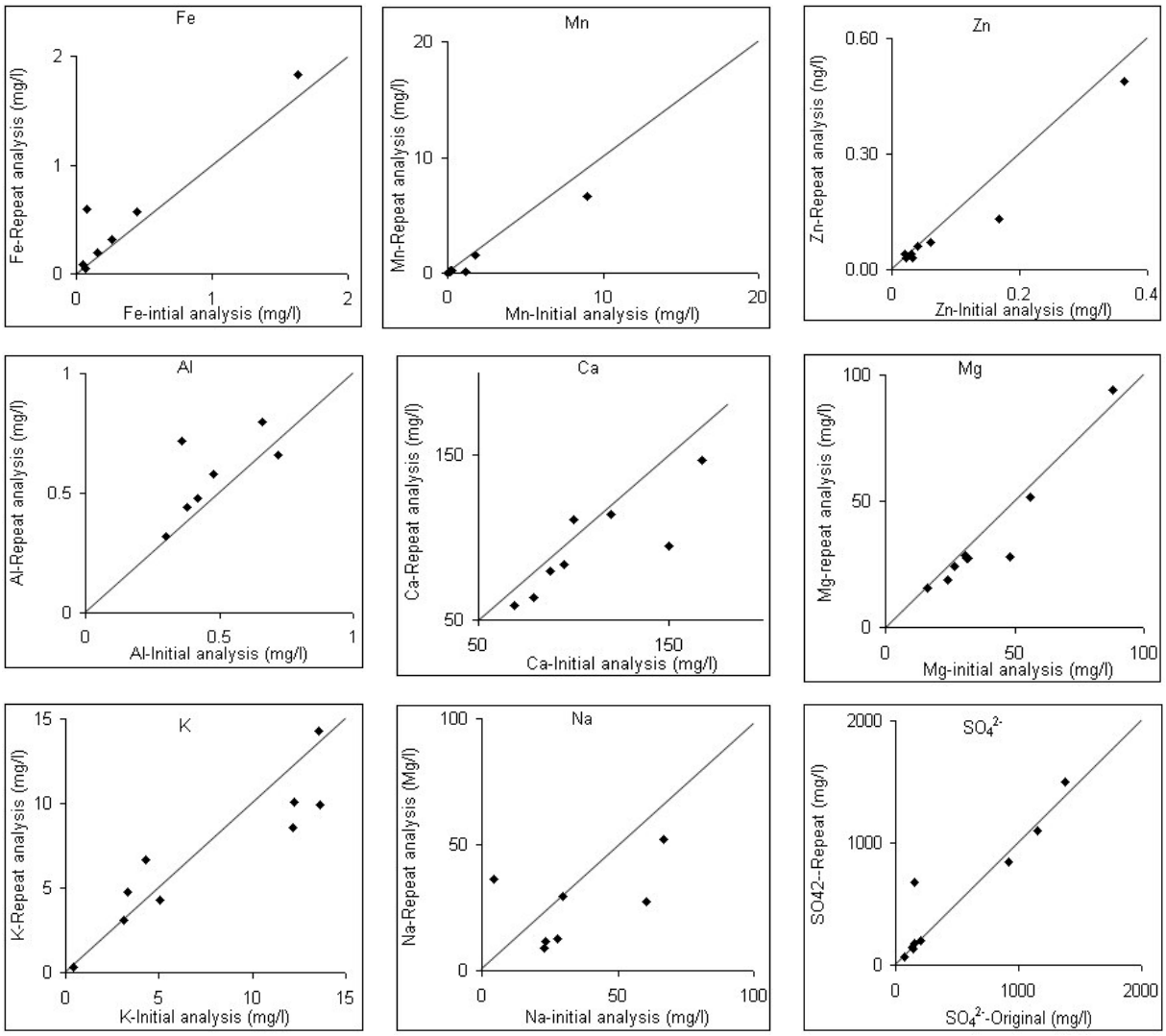

Figure 3.4. Scatter graphs showing 1st and 2nd analysis for laboratory repeat samples on some of the metal and sulphate concentrations in waters draining the area.

Stream sediments

Figure 3.5 shows the scatter plots of 1st and 2nd sample results of field duplicate data for the base metals. Linear trends are observed on the scatter graphs of field duplicate sample analysis of metal concentrations in the stream sediments of the waters draining the area. Large deviations are observed on the scatter plots of As and Sb data pairs. The deviations for these elements may be are due to their nature of occurrence in sediments whereby As and Sb can be locked in some minerals in their pure form, which give rise to large variations in analytical processing. Such deviations are more on sample level than on analytical level.

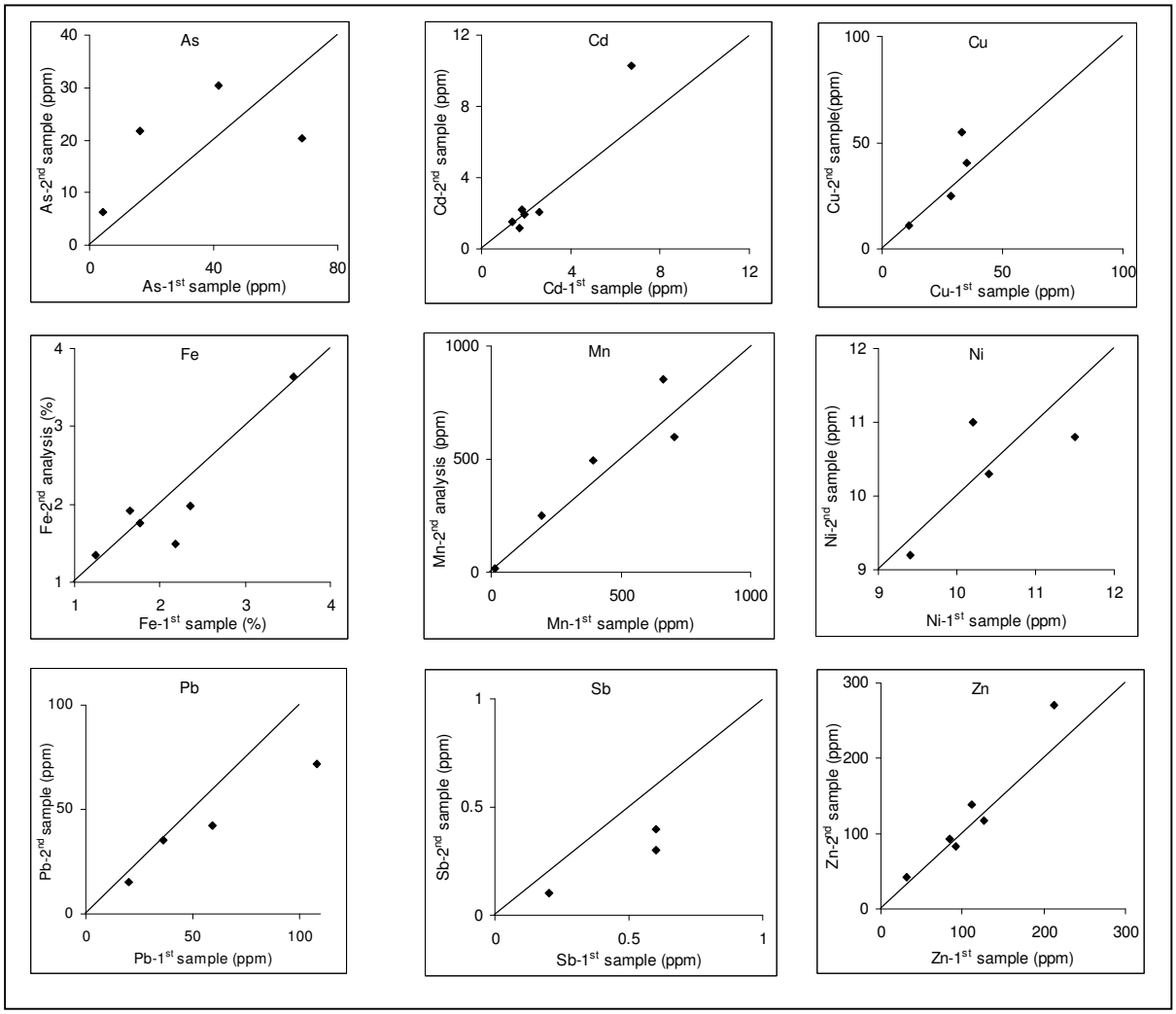

Figure 3.5. Scatter graphs showing plots of 1st and 2nd sample analysis of field duplicate stream sediments samples in the drainages of the area.

Repeat analysis for tailings and stream sediments samples

The tailings and stream sediment samples were analysed at the same time and in the same batches during analytical processing. Repeat sample analysis employed to determine the repeatability of analytical processes was therefore done collectively for tailings and stream sediment samples. Linear trends are observed on the scatter graphs of original-repeat plots of metal concentrations in the stream sediments and in the tailings (figure 3.6). Most of the initial-repeat data set pairs for the individual elements plot on the 45^{o}-line, which indicate that there is high precision in the analytical processes employed to determine the element concentrations in the stream sediments and tailings of the area.

Scatter plots area only used to subjectively draw conclusions on the variations in datasets. The analysis of variance is a more appropriate approach in analysing data variations because it is capable of classifying the variations according to their magnitudes and, at the same time, it separates these deviations into their respective components.

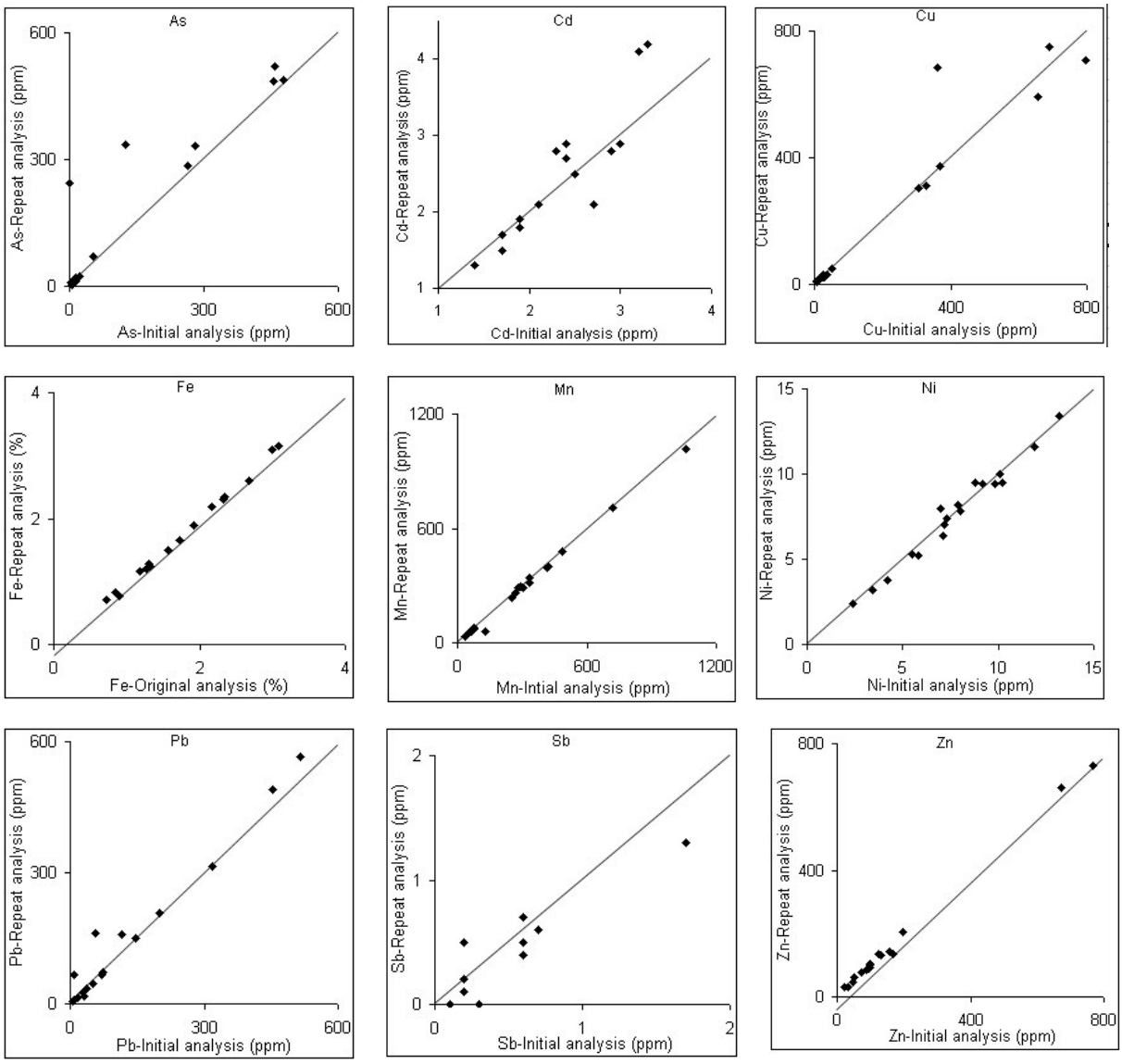

Figure 3.6. Scatter graphs showing plots of 1st and 2nd analysis of laboratory repeat samples for metal concentrations in the stream sediments and floatation tailings of the area.

3.3.3. Analysis of Variance

Whilst precision analysis by scatter plots is subjective, analysis of variance (ANOVA) can provide objective characterisation of data precision. The **variance** of a population is defined as a measure of the deviation or scatter of values about their mean and it is given as the average of the square of those deviations of values from their mean by the formula (from Swan and Sandilands):

$$\sigma^2 = 1/\mathrm{N}\sum_{i=1}^{N}(X_i - \mu)^2$$

where σ^2 is the variance, μ is the mean, and N is the sample population. Deviations from the mean are partly due to random variations in the sample population and partly due to procedural errors and sample inhomogeneity. Analysis of variance can be used to determine these deviation components.

The 1st and 2nd sample analysis of field duplicate data in the drainages of the area were analysed using the simple nested one-way ANOVA method (Hale M, 1990). The purpose was to decompose the total variance of sample measurements into variance due to procedural errors and sample inhomogeneity, and variance due to geochemical behaviour of the populations in the study area. Whilst the variance due to geochemical behaviour of the population can be exclusively determined, the variance introduced by procedural errors and by the inhomogeneity of the sample is not easily separated, except in water samples where the variance can be attributed to procedural errors because water is regarded as highly homogeneous. The total variance in this method can be described by the following relationship:

$$\sigma_t^2 = \sigma_w^2 + \sigma_b^2 ,$$

where σ_t^2 is the total variance measured in the data set, σ_w^2 is the sum of variances within groups and σ_b^2 is the total variance between groups.. In this study, σ_w^2 is equivalent to procedural errors and variations due to sample inhomogeneity, and σ_b^2 refers to geochemical variations in the sampled area. Because the calculation strictly involves the estimation of variances from a sample of the population, the relationship can be written as:

$$MS_t = MS_w + MS_b ,$$

where MS refers to mean squares. With the mean squares calculated, the corresponding percentages of procedural errors and geochemical variations can be determined. The "total mean squares" (MS_t) is the estimated variance of the observed measurements and comprises "mean squares between" (MS_b), which is the estimated variance between sample sites, and the "mean squares within" (MS_w), which is the estimated variance within sample sites. The mean squares between is expressed as a percentage of total mean squares estimates and represents the variance due to geochemical patterns, while the mean squares within is expressed as a percentage of total mean squares estimates and represents the variance due to procedural errors and sample inhomogeneity. According to Ramsey, geochemical data is acceptable when procedural errors fall below 20%, and the analytical component of procedural variance should not exceed 4% (Hale M, 1990).

The "mean squares terms" are calculated via the corresponding "sums of squares" (SS) as follows:

$$SS = \sum x^2 - (\sum x)^2 / n \qquad \text{……..……..(1)}$$

$$SS_b = \sum_1^i (\sum_1^J x)^2 / j - (\sum x)^2 / n \qquad \text{……..(2)}$$

$$SS_w = SS_t - SS_b \qquad \text{…….……(3)}$$

$$MS_b = (SS_b)/(i-j) \qquad \text{…….……..……..……(4)}$$

$$MS_w = (SS_w)/i(j-1) \qquad \text{..……...…..……(5)}$$

where i is the number of duplicate groups (pairs), j is the number of measurements within each duplicate group, and n is the product of i and j.

The F-test, which is the ratio MS_{max} / MS_{min} can be used to determine significances of estimated variances. With known degrees of freedom for the mean square-within and mean square-between (given by (i(j-1)) and (i-j) respectively), a critical F value can be determined from the reference Snedecor F statistical model at 5% level of variance ratio, or 95% significance level. In this study, the critical F value at 95% significance level is thus referred to as $F_{0.95}$. When F falls below the critical F-value, it implies that the populations, from which the two variances are drawn, are statistically indistinguishable. On the other hand, an F value that exceeds the critical value indicates that true geochemical patterns can be adequately reflected in the measurements (Hale, 1990), and therefore a decision can be made to reject or accept the hypothesis (Davis, 1986).

Water samples

Elements that were analysed for variance were arsenic, cadmium, copper, iron, manganese, nickel, lead, antimony, zinc, aluminium, potassium, calcium, magnesium and sodium (Table 3.3.).

Table 3.3. Summary of quality assessment for water sample data using simple nested one-way ANOVA.

Element	Geochemical Variation (%)	Procedural Error (%)	F	$F_{0.95}$	Data quality
As	99.06	0.94	105.65	4.96	satisfactory
Cd	99.45	0.55	180.75	4.96	Satisfactory
Cu	99.17	0.83	119.36	4.96	satisfactory
Fe	99.99	0.01	1654041284	4.96	Satisfactory
Mn	99.99	0.01	9683	4.96	satisfactory
Ni	99.93	0.61	163.46	4.96	Satisfactory
Pb	95.62	4.37	21.84	4.96	Good
Sb	99.46	0.54	182.82	4.96	satisfactory
Zn	99.94	0.06	1731.66	4.96	Satisfactory
Al	99.07	0.93	106.74	4.96	satisfactory
Ca	99.95	0.05	2119.92	4.96	Satisfactory
K	99.82	0.17	578.60	4.96	satisfactory
Mg	98.82	1.18	84.09	4.96	Satisfactory
Na	98.83	1.16	84.88	4.96	Satisfactory
SO_4	93.21	6.79	13.74	4.96	Good

The degrees of freedom are 5 and 6 for the mean square-between and mean square-within, respectively, and the critical value of F from the Snedecor F-statistic model is 4.96 at 95% significance level.

A large percentage of the variances in the analytical data for the water samples is due to geochemical patterns. Lead and sulphate analytical data have procedural error variation percentages of more than 4% while the other analytical data have procedural errors of less than 4%. The high procedural error in sulphate is mainly attributed to several dilutions of the samples as explained earlier on. All the calculated F values are greater than the critical F value at 95% significance level, which implies that true

geochemical patterns can be adequately reflected in the data. Overally, the results of laboratory procedures are good and quite satisfactory. Results of the analysis of water sample measurements can therefore be confidently used to reject or accept the hypotheses of the research.

Stream sediments

Table 3.4 shows that all analytical data except Zn are characterised by variances due to procedural errors and sample inhomogeneity which are higher than the maximum acceptable analytical variance of 4%. For Pb and Sb, the procedural errors exceed the maximum acceptable procedural variance of 20%. Lead and antimony data gave F-values lower than the critical F value at 95% level of significance, which implies that true geochemical patterns are not adequately reflected by the data obtained. The datasets are therefore considered to be poor and very poor for Pb and Sb respectively, good for As, Cd, Cu, Fe, Mn, Ni and Pb, and satisfactory for Zn.

Table 3.4. Summary of quality assessment for stream sediment sample data by simple nested one-way ANOVA.

Element	Geochemical Variation (%)	Analytical/ Sample Error (%)	F	$F_{0.95}$	Data quality
As	88.83	11.17	7.96	4.96	Good
Cd	92.98	7.01	13.27	4.96	Good
Cu	95.67	4.33	22.09	4.96	Good
Fe	95.57	4.43	21.57	4.96	Good
Mn	94.12	5.88	15.99	4.96	Good
Ni	86.67	13.32	6.50	4.96	Good
Pb	60.36	39.64	1.52	4.96	Poor
Sb	28.15	71.85	0.39	4.96	Very poor
Zn	96.24	3.76	25.58	4.96	Satisfactory

The degrees of freedom are 5 and 6 for the mean square-between and mean square-within, respectively, and the critical value of F from the Snedecor F-statistic model is 4.96 at 95% significance level.

Tailings samples

Summary of data quality assessment for tailings samples shows very poor quality for most of the elements (table 3.5.). Manganese and nickel are the only elements with variances due to procedural errors and sample inhomogeneity of less than 4% and F values greater than the critical F value of 4.96; hence these data sets are considered satisfactory. Zinc has an F value that is close to the critical F value and the variance due to procedural errors and sample inhomogeneity is 19.28%, which is slightly less than the maximum acceptable procedural variance of 20%; hence its data is considered good. Procedural variance for Cd data is higher than the variance due to geochemical patterns; therefore the data has been considered very poor. The quality of data for As, Cu, Fe, Pb and Sb is considered to be poor.

The observed high variability in the tailings data is mainly due to the sampled surface tailings materials, which, in some areas, is mixed with soil used to cover the tailings piles during remediation. Whilst every effort is put to sample only those surfaces of the tailings re-exposed by erosion, chances of incorporating soil into the samples are very high due to the strong mixing which occurs during erosion.

Table 3.5. Summary of quality assessment for tailings sample data by simple nested one-way ANOVA.

Element	Geochemical Variation (%)	Analytical/ Sample Error (%)	F	$F_{0.95}$	Data quality
As	66.04	33.96	1.94	4.96	Poor
Cd	39.40	60.61	0.65	4.96	Very poor
Cu	74.08	25.92	2.86	4.96	Poor
Fe	67.62	32.38	2.09	4.96	Poor
Mn	97.13	2.87	33.80	4.96	Satisfactory
Ni	99.26	0.74	134.84	4.96	Satisfactory
Pb	79.38	20.62	3.85	4.96	Poor
Sb	68.27	31.73	2.15	4.96	Poor
Zn	80.72	19.28	4.19	4.96	Good

The degrees of freedom are 5 and 6 for the mean square-between and mean square-within, respectively, and the critical value of F from the Snedecor F-statistic model is 4.96 at 95% significance level.

3.4. Remarks

A regular sampling interval of approximately 250m for stream waters and stream sediments was based on the distribution of spatial features which were thought to influence the geochemistry of the drainages in the area. Some of the proposed sampling locations were inaccessible, making it difficult to maintain the 250m sampling interval. In some of the sample locations, stream sediments sampling was not possible due to lack of sediment deposits, or due to big depth of the stream channel which made it impossible to collect stream samples. As a result, deductions of geochemical patterns in the drainage systems of the area are compromised due to lack of stream sediments data in some of the sample locations.

Water and stream sediment samples which were collected from locations that lie on the downstream side of the confluence of Parad Bikk and Parad Tarna are likely to be influenced by the strong flooding which occurred the night before sampling. The less acidic waters of Parad Tarna, which drains a larger catchment area, are likely to dominate the geochemistry of the waters and sediments of this area over the waters of Parad Bikk. The element concentrations of these samples are therefore likely to be lower than they usually are in normal conditions.

3.5. Conclusions

The data quality assessment revealed good quality for water analytical data. Therefore, water data analysis can reveal true geochemical patterns, and can be used to reject or accept the research hypothesis. Stream sediment data quality analysis showed that most of the data is good except for Pb and Sb. Analysis of the other element data may adequately reveal true geochemical patterns. Most of the floatation tailings analytical data is not representative due to the inhomogenety of the sampled material. Only Mn and Ni data revealed good quality and representativeness. The floatation tailings data, however, can be appropriately used as indicators of the amount of metal remaining in the tailings piles and as point source of contamination rather than revealing any other geochemical pattern.

Many of the samples for water geochemical data analysis have extremely low base metal concentrations, most of which were below the lower detection limits for those metals. This may give rise to low procedural variations due to the influence of the samples below detection limit.

Comparing deviations of the plots of duplicate/repeat data pairs with the "ideal" 45^{o}-line cannot precisely determine the quality of data but only serve the purpose of visualising those deviations. The Thompson and Howarth (1978) method is more appropriate in analysing data quality using the 10% precision model control chart. However, the small number of duplicate/repeat samples used for data quality assessment in this research could not allow the application of the Thompson and Howarth method.

Analysis of geochemical data obtained from water, stream sediments and tailings can now be used to determine element associations, processes and distributions that are useful in determining sources and levels of heavy metal contamination in the area.

4. DRAINAGE HYDROGEOCHEMICAL DATA ANALYSIS

The discipline of hydrogeochemistry deals with understanding the complex factors that influence both chemical and physical properties of water like element concentrations, hardness, pH, electrical conductivity and many others (Fortescue, 1979). In areas where the influence of anthropogenic factors to water chemistry is nil, metal element abundances for example can only be attributed to geogenic factors. Maps and graphs are useful tools used to correlate hydrogeochemical data and to present data analysis results for visualisation. The geochemical data obtained from water samples collected from the research area was analysed to determine physical property trends of waters draining the area, correlations among metals, similarities and differences, concentration changes, anomaly zones, and to classify water bodies according to their properties and geologic sources. The analysis of hydrogeochemical data of the area is separated into drainage hydrogeochemistry, which analyses data collected from the main streams of the area, and mine hydrogeochemistry, which analyses data collected from areas influenced by mining operations, for the sole purpose of determining geochemical trends which can be used as pointers of heavy metal contamination in the area.

4.1. Univariate data analysis

Analysis of individual element concentration data enables the determination of properties and parameters of elements distributions, which can be useful in exploratory and descriptive methods. It is also useful in determining population groupings, which are usually associated with certain environmental features in space. Population groups are therefore used in generating point maps, which are used in the analysis and visualisation of spatial distribution of element data.

4.1.1. Element data structure

Summary statistics

Summary descriptive statistics of the analytical data for water elements is shown in table 4.1.The summary statistics of Electrical conductivity and pH are also included in the table. Statistics for most of the base metal elements indicate that their concentrations in drainages are very low, while the concentrations for major cations are generally higher except for Al. The number of concentration measurements below detection limit for the analysed elements are also included in the statistics table. The spatial distributions of As, Cd, Cu, Pb and Sb concentrations could not be fully determined by statistical methods because the data for these elements have more than 50% of the concentration measurements falling below their lower detection limits.

Positive skews for the measured constituents indicate the existence of anomalous higher element concentrations while the negative skew for pH implies anomalous pH values in the low pH range. The coefficients of skewness show inverse relationship between pH and the other measured constituents. Because skewness influences results of statistical analysis of element data due to the influence of the high anomalous values, $\log_{10}$-transformed data, which is less skewed (table 4.1), is used in univariate data analysis for most of the constituents.

Table 4.1. Summary of descriptive statistics for water sample measurements (n=63). Concentrations are given in mg/l for the metals and sulphate ions while EC is given in µs/cm.

	No. of samples below detection limit	Min	Max	Average	Skew	log_{10}Skew
As	40	0.050	0.650	0.056	3.092	-0.510
Cu	24	0.010	0.070	0.013	1.487	-0.990
Fe	8	0.050	38.676	1.231	5.562	2.190
Mn	7	0.050	4.753	0.396	3.966	-0.230
Sb	44	0.020	0.210	0.020	3.192	0.140
Zn	0	0.010	0.420	0.064	2.740	0.770
Al	3	0.075	1.840	0.473	1.186	-0.360
K	0	0.750	21.900	8.503	0.268	-1.380
Ca	0	0.900	185.580	98.063	0.532	-4.870
Mg	0	0.620	118.410	32.508	2.195	-2.900
Na	0	8.250	275.260	56.980	1.852	0.690
SO_4^{2-}	0	34.000	430.000	167.714	1.573	-0.370
pH	0	5.000	8.000	6.630	-0.560	-0.980
EC	0	408.000	1887.000	896.330	1.140	0.650

4.1.2. Element distributions

Univariate statistical methods were employed to determine element population groups and their spatial distributions. In populations with normal distributions, quartile and mid percentiles of the population histograms were used to classify the population into subgroups, while "natural breaks" on the cumulative frequency curve were used in populations not normally distributed. The small size of the datasets could not allow the construction of probability graphs, which are best used to determine the sub-population groups, and as a result, thresholds were arbitrarily chosen for most of the datasets. The thresholds used to classify data into distribution groups are determined from the histogram as log_{10}-transformed values, which are converted to their equivalent antilogarithmic values in mg/l for the elements and in µs/cm for EC. Slicing of element data into groups used to generate point maps was achieved by the use of the "iff" statements in ILWIS GIS software. Due to the strong influence of water acidity on element mobility and distribution, univariate data is analysed alongside with pH measurements.

pH Data

Three populations are observed on the pH histogram (figure 4.1). Population A, which is about 8 % of the total population, is distributed in pH range from 5 to 6. The largest sub-population constitutes about 90% of the total population and is distributed in the near-neutral pH range from 6 to 7.5. Sub-population C, which constitutes about 5% of the total population, is distributed between pH values of 7.5 and 8. Displayed in figure 4.1 are the spatial distributions of pH in the waters draining the area.

Most of the waters draining the area are neutral or near neutral as indicated by sub-population B with the largest population ranging from 6 to 7.5. Slightly acidic waters with pH values ranging from 5 to 6 are distributed in tributaries of Parad Tarna draining hydrothermal alteration zones. Colloids of iron (III) precipitates (yellow boy) like those shown in figure 2.13 in chapter 2 have been observed in these sites. An area downstream of Recsk tailings in Parad Bikk is also characterised by slightly acidic waters indicating the influence of acidic waters draining the tailings and discharging into Parad Bikk. Two sample locations have waters with pH values between 7.5 and 8. The sample location with pH of 8 on the upstream of Parad Bikk is characterised by carbonate precipitates, which are believed to have crystallised from groundwater pumped out of the underground mine workings into a reservoir that drains into Parad Bikk (Zelenka and Carranza, field observations, 2002). The carbonate precipitates are likely to have influenced pH to slightly alkaline levels. The other high pH site is located in Parad Tarna just before the confluence with Parad Bikk. Table 4.2 summarises the observed spatial distributions of pH in the waters draining the area.

Table 4.2. Summary of observed spatial distribution of pH in the waters draining the area.

pH group	Upper percentile	pH range	Environmental association
C-Slightly alkaline	100	7.5 – 8.0	Parad Bikk with observed carbonate precipitates
B-Neutral	95	6.0 – 7.5	Areas with no significant influence from lithology.
A-Slightly acidic	8	5.0 – 6.0	Hydrothermal alteration zones and Recsk tailings

Electrical Conductivity(EC) data

Three populations are observed on the EC histogram (figure 4.2). The bulk of EC data is distributed in population group A ranging from EC values of 400 to 891µs/cm. Population B ranges from 891 to 1,288µs/cm while population C ranges from 1,288 to 1,887µs/cm. Displayed in figure 4.2 are the spatial distributions of EC in the area.

Waters with EC values ranging from 400 to 890µs/cm are distributed in Parad Tara and its tributaries. Some of the tributaries emanating from Oligocene clayey-marl geological units have waters with higher EC values ranging from 890 to 1290µs/cm. Population group C comprised of waters with EC values above 1290µs/cm is predominantly distributed in Parad Bikk, which indicate that there is more ion activity in Parad Bikk than the other drainages. The high EC which persist upstream of the Lahoca tailings indicate that EC in Parad Bikk is not only influenced by mine areas but by other sources as well. The headwaters of Parad Bikk streams originate in the Oligocene clayey-marl, which most likely influences the EC properties of waters draining through it. Table 4.3 summarises the observed spatial distribution of EC in the waters draining the area.

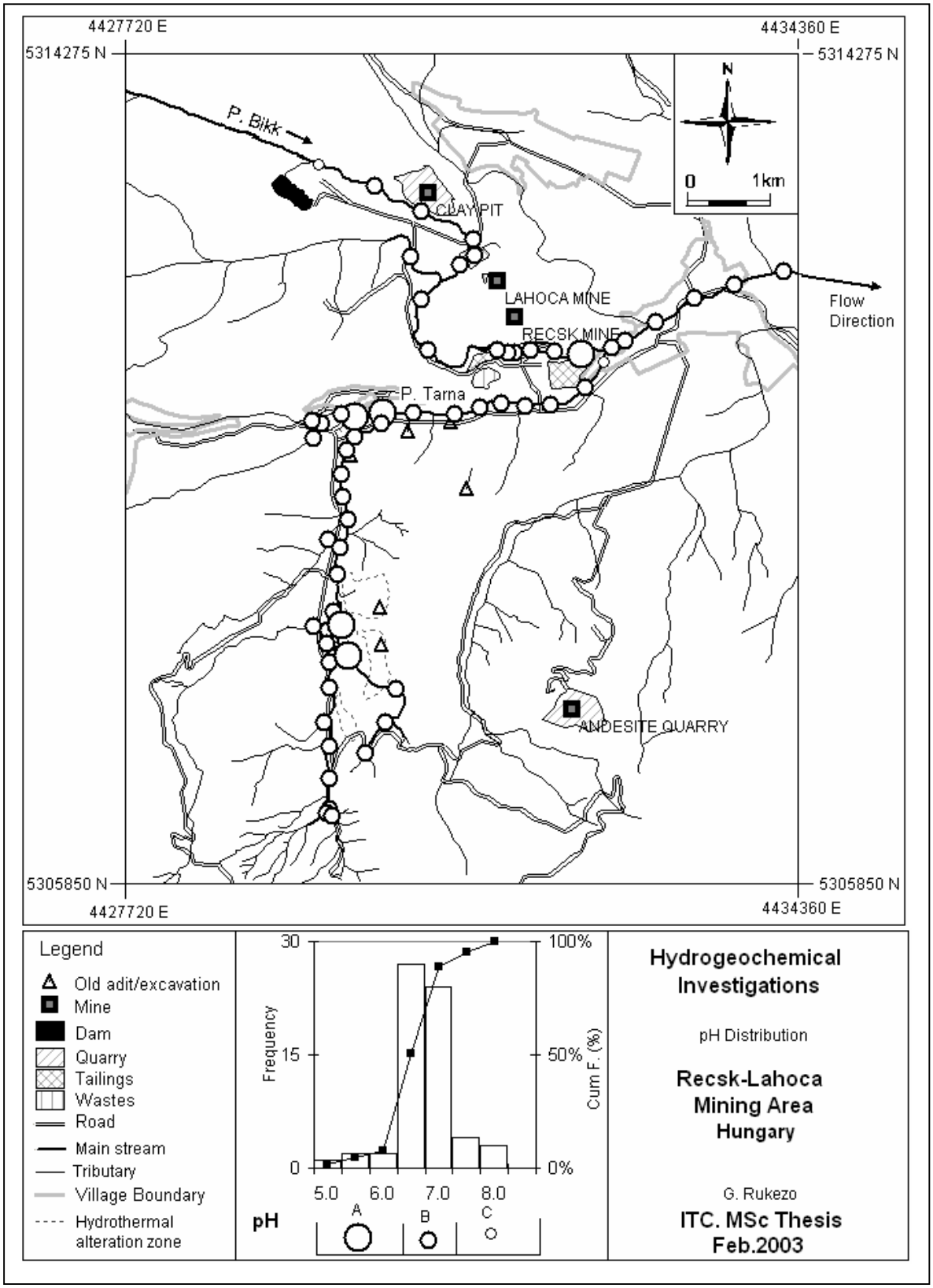

Figure 4.1. Spatial distributions of observed pH of the stream-waters draining the area.

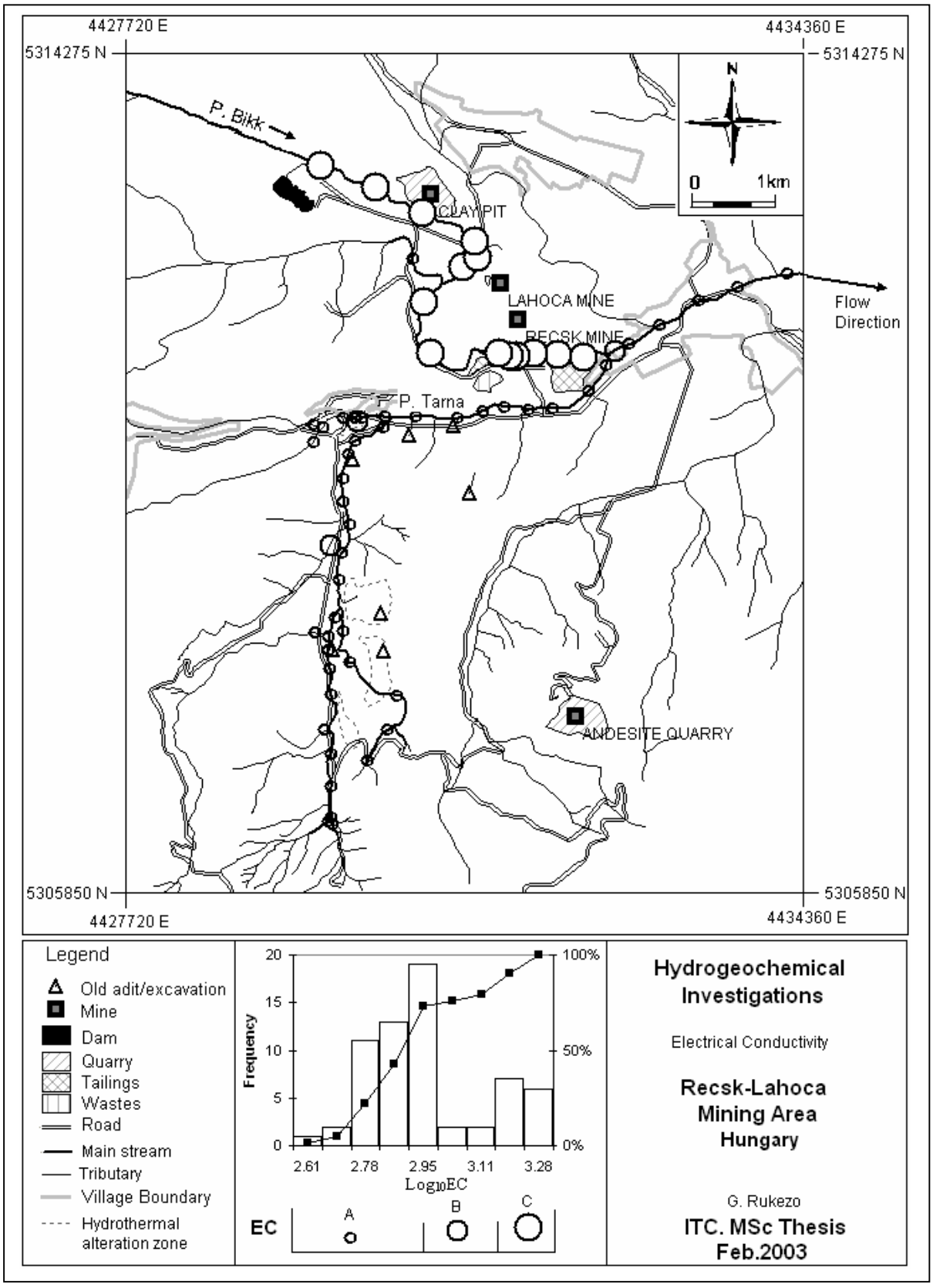

Figure 4.2. Spatial distributions of observed EC of the waters draining the area.

Table 4.3. Summary of observed spatial distribution of EC in the waters draining the area.

EC group	Upper percentile	EC range (µs/cm)	Environmental association
C	100	>1290	Parad Bikk.
B	95	890-1290	Parad Tarna tributaries
A	8	400-890	Parad Tarna

Sulphate data

Sulphate data is divided into three population groups. Group A is comprised of sulphate concentrations below 120mg/l, group B is comprised of sulphate concentrations ranging from 120 to 230mg/l, and group C is comprised of sulphate concentrations above 230mg/l. Displayed in figure 4.3 are the spatial distributions of sulphate concentrations in waters draining the area.

Sulphate concentrations below 120mg/l are distributed on the headwaters of Parad Tarna and its tributaries close to the water divide. Sulphate concentrations ranging from 120 to 230mg/l dominate most of the drainages in the area depicting that the normal sulphate concentrations due to geogenic factors fall within this concentration range. The above 230mg/l sulphate concentrations are predominantly distributed in the waters draining the Recsk tailings area indicating that the mine wastes influenced sulphate concentrations in waters draining through them. In Parad Tarna, sulphate concentrations above 230mg/l are only found in waters draining through or near hydrothermal alteration zones, which have been found to be mineralised with metal sulphides common to the area. Weathering and subsequent leaching of these sulphide minerals is likely to be loading sulphate in these areas giving rise to elevated concentrations. Table 4.4 summarises the observed spatial distribution of sulphate concentrations in waters draining the area.

Table 4.4. Summary of observed spatial distribution of sulphate concentrations in waters draining the area.

Sulphate group	Upper percentile	Sulphate range (mg/l)	Environmental association
C	100	>230	Parad Bikk in the Recsk tailings area.
B	87	120-230	Parad Tarna and Parad Bikk
A	17	<120	Headwaters of Parad Tarna

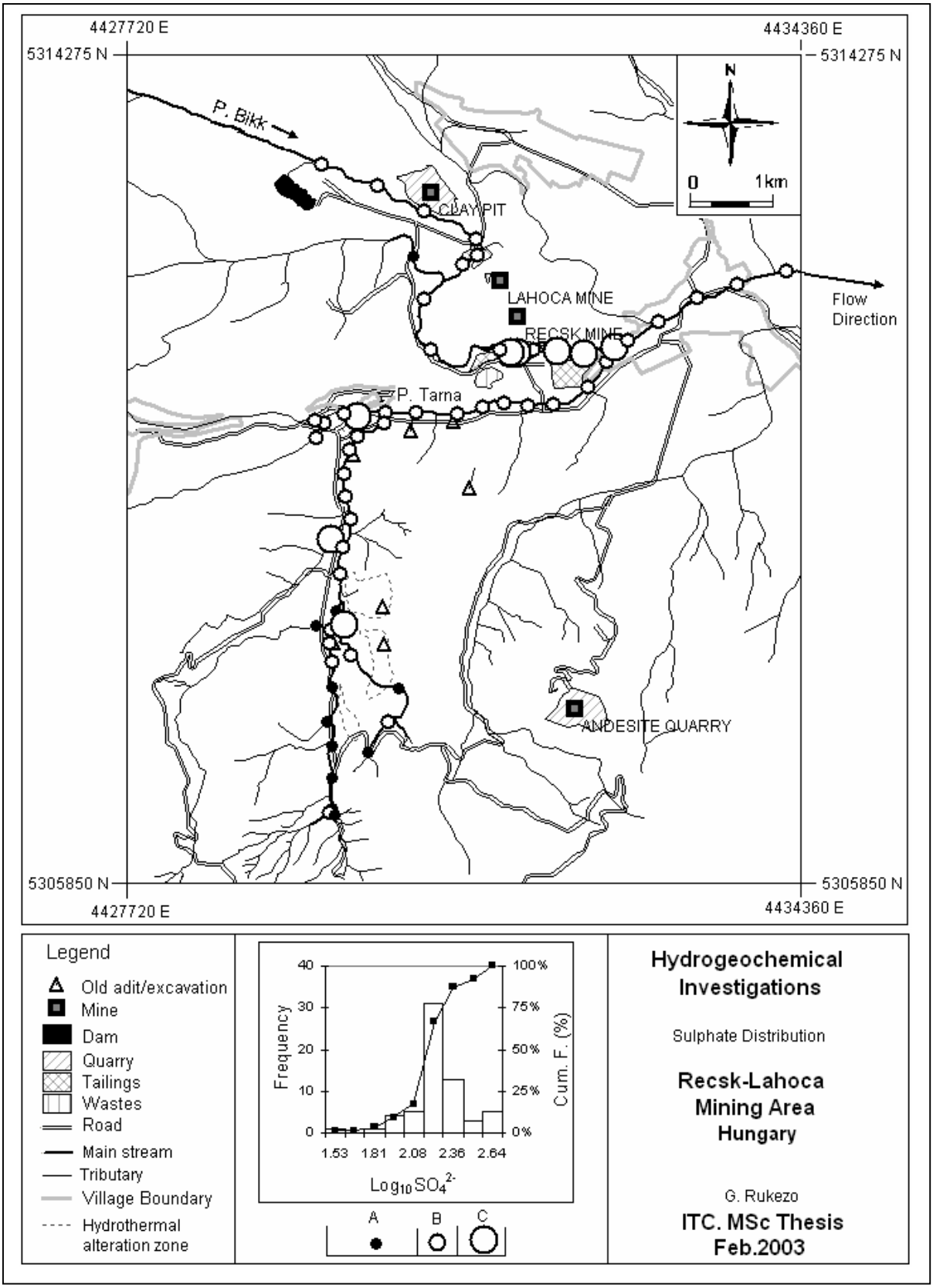

Figure 4.3. Spatial distributions of observed sulphate concentrations in waters draining the area.

Iron(Fe) data

The 92 cumulative percentile, which is equivalent to Fe concentration of 0.45mg/l, was taken to separate background and anomalous Fe concentrations, giving rise to two groups. Figure 4.4 shows the spatial distributions of Fe concentrations.

Iron concentrations above 0.45mg/l are associated with waters draining hydrothermal alteration zones in the tributaries of Parad Tarna. The high organic content in the drainages of the tributaries may have given rise to reducing conditions, which facilitate the hydrolysis of Fe^{3+}-oxides to the more mobile Fe^{2+} ions. Colloids of Fe^{3+}-hydroxides, which are easily reduced to Fe^{2+} in slightly low pH waters, are observable in these areas of elevated Fe concentrations. The rest of the drainages in the area are characterised by Fe concentrations of less than 0.45mg/l.

Manganese(Mn) data

The histogram and cumulative frequency plot of the Mn analysis has the form of a unimodal density distribution, which is near-normal with a slight negative skew. The data is divided into three groups at the 35 and 87 percentiles (i.e. 0.12 and 0.76mg/l) in order to depict the spatial distributions of Mn concentrations. Figure 4.5 displays the spatial distribution of these groups.

Population group A, which is comprised of the lowest Mn concentrations below 0.12mg/l, is distributed in Parad Tarna while population group B (0.12-0.76mg/l) is distributed in both streams. Population group C with the highest Mn concentrations above 0.76mg/l is distributed mainly in the tributaries of Parad Tarna. The higher Mn concentrations observed in Parad Bikk near Recsk tailings piles may be a result of leaching from the tailings. Table 4.5 summarises the spatial distributions of Mn concentrations in drainage waters of the area.

Table 4.5. Summary of observed spatial distribution of Mn concentrations in waters draining the area.

Mn group	Upper percentile	Mn range (mg/l)	Environmental association
C	100	0.76-4.75	P. Tarna, mainly in hydrothermal alteration zones.
B	87	0.12-0.76	Parad Tarna and Parad Bikk
A	35	<0.12	Parad Tarna

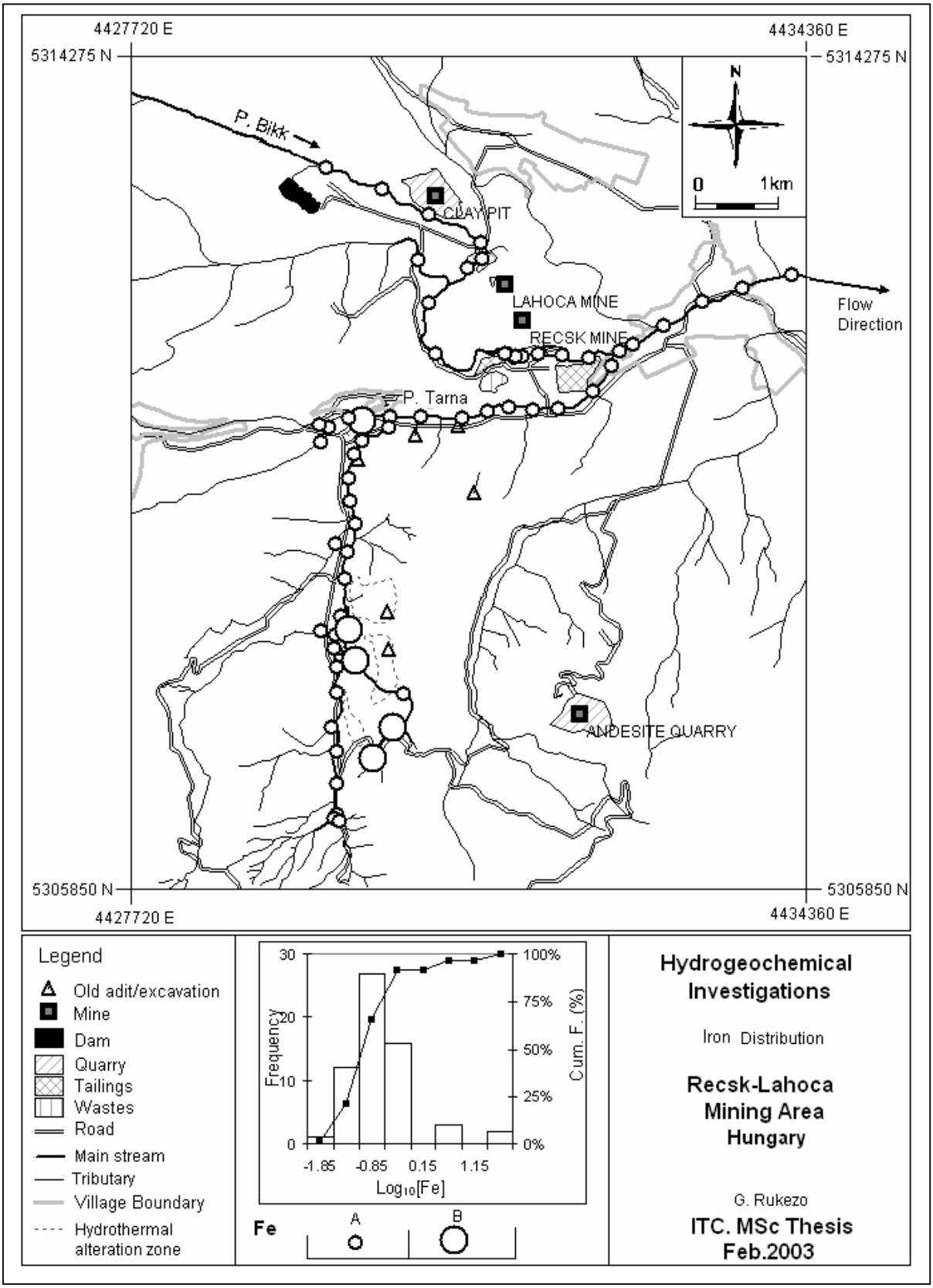

Figure 4.4. Spatial distributions of observed Fe concentrations in waters draining the area.

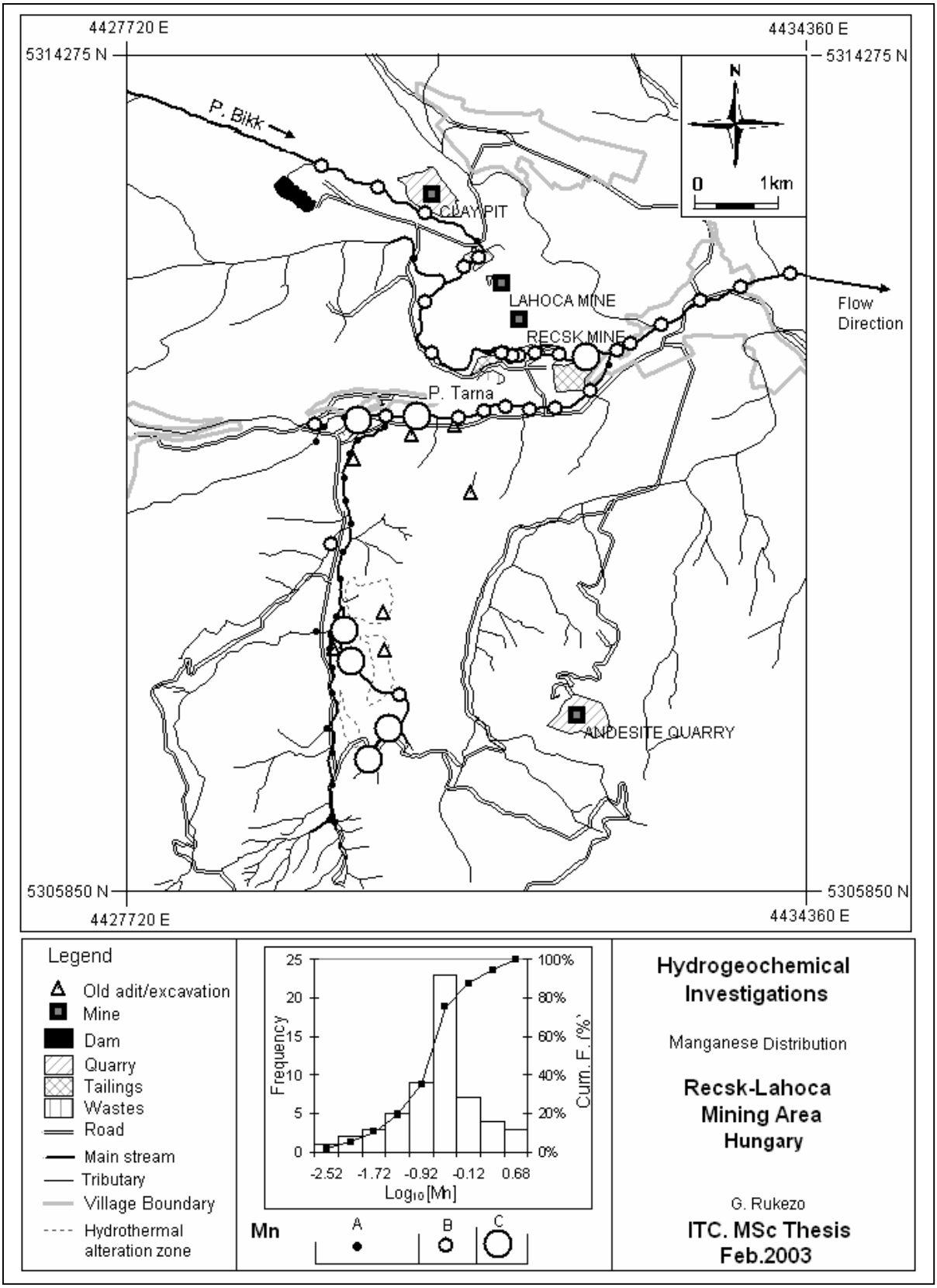

Figure 4.5. Spatial distributions of observed Mn concentrations in waters draining the area.

Zinc(Zn) data

Zinc concentrations range between 0.01 and 0.4 mg/l. The histogram for the Zn analysis has the form of a trimodal density distribution as indicated by the breaks at the 64 and 93 cumulative percentiles, which are equivalent to Zn concentrations of 0.06 and 0.22mg/l respectively. Population group A is thus comprised of Zn concentrations below 0.06mg/l, population group B is comprised of concentrations between 0.06 and 0.22mg/l and population C is comprised of concentrations between 0.22 and 1.4mg/l. Displayed in figure 4.6 are the spatial distributions of the Zn population groups.

Zinc concentrations below 0.06mg/l are mainly distributed in Parad Bikk and Parad Tarna headwaters. Concentrations ranging from 0.06 to 0.22mg/l are distributed in drainage waters close to the confluence of the two streams. The higher Zn concentrations of population C are distributed in drainage waters close to ancient adits and hydrothermal alteration zones in Parad Tarna. Table 4.6 summarises the spatial distributions of observed Zn concentrations.

Table 4.6. Summary of observed spatial distribution of Zn concentrations in waters draining the area.

Zn group	Upper percentile	Zn range (mg/l)	Environmental association
C	100	0.22-0.4	P. Tarna (Old adits & hydrothermal alteration zones).
B	93	0.06-0.22	Parad Tarna
A	64	<0.04	Parad Tarna and Parad Bikk

Arsenic, Cu, Ni, Pb and Sb data

Concentrations of As, Cu, Ni, Pb and Sb are very low in the drainage waters of the area. Concentrations were below detection limit for Ni and Sb while the four sample locations with Pb concentrations ranging from 0.57 to 3.1mg/l are distributed in Parad Bikk in the area the stream drains the Lahoca tailings. The few Cu concentrations above detection limit are intermittently distributed in Parad Bikk. Drainages in the area are dominated by As concentrations below 0.1mg/l except on the headwaters of Parad Tarna and its tributaries, which are characterised by concentrations between 0.1 and 0.2mg/l. The geochemical alteration zones in this part of the stream are likely to have contributed to the slightly higher concentrations. Two locations have As concentrations above 0.2mg/l. One location lies in Parad Bikk below the Lahoca tailings indicating that drainage from the tailings could have resulted in elevated As concentrations. The location in Parad Tarna lies on the downstream side of hydrothermal alteration zones.

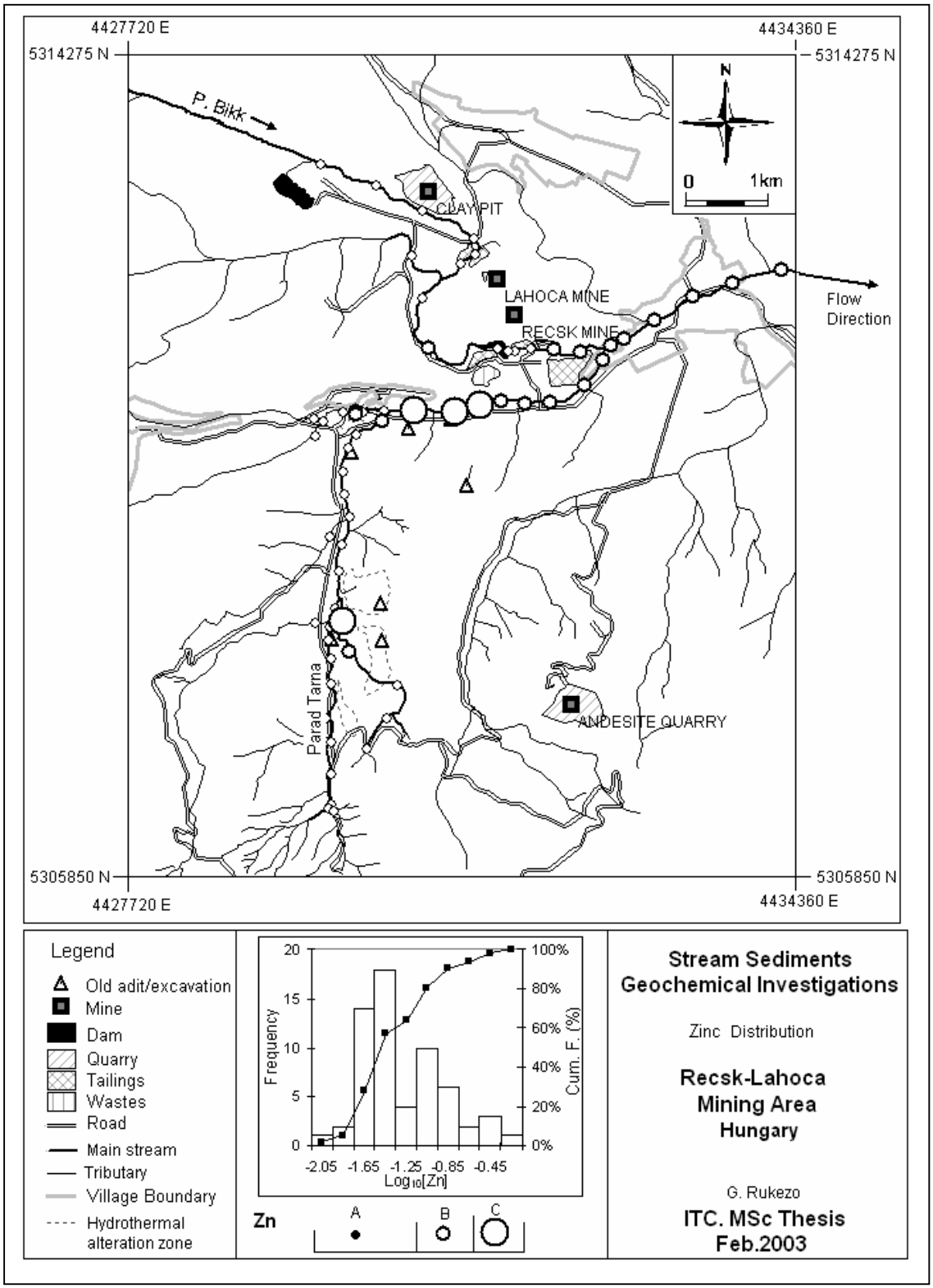

Figure 4.6. Spatial distributions of observed Zn concentrations in waters draining the area.

Calcium(Ca) data

A near-normal density distribution, with a slight positive skew due to the existence of a smaller sub-population with higher Ca concentrations, is observed on the Ca histogram. The quartiles and mid percentile are used to classify the population into four groups (i.e. 75, 92, and 112ppm). Displayed in figure 4.7 are the spatial distributions of the Ca concentrations.

Population group A, which is comprised of Ca concentrations below 75mg/l is mainly distributed in the upstream parts of Parad Tarna and its tributaries. Population group B with Ca concentrations ranging between 75 and 92mg/l is also distributed on the upstream side of Parad Tarna but in the areas where the stream drains close to hydrothermal alteration zones. Population group C is distributed in Parad Tarna in areas the stream drains close to the old adits. Calcium concentrations above 112mg/l are predominantly distributed throughout the stream profile of Parad Bikk. High concentrations on the upstream side of the mine workings indicate that Ca loading into the stream is not only due to mine operations but other geological factors. High Ca concentrations in the areas the stream drains Oligocene clayey-marl rock formation indicate that the rock unit contribute significantly to the loading of Ca in the stream. The carbonate precipitates observed upstream of the Lahoca tailings, which are believed to have precipitated from groundwater pumped out of underground mines during the production days of the mine (Zelenka and Carranza, field observations, 2002), may have contributed to the high Ca concentrations. High Ca concentrations are also observed in the tributaries of Parad Tarna emanating from the Oligocene clayey-marl, which further makes this rock unit a strong pointer towards the loading of Ca into the streams. Summarised in table 4.7 are the spatial distributions of Ca concentration and their environmental associations.

Table 4.7. Summary of observed spatial distribution of Ca concentrations in waters draining the area.

Ca group	Upper percentile	Ca range (mg/l)	Environmental association
D	100	112-186	P. Bikk and P. Tarna tributaries from Oligocene clay.
C	75	92-112	P. Tarna (Old adits & hydrothermal alteration zones).
B	50	75-92	Parad Tarna near hydrothermal alteration zones
A	25	<75	Headwaters of P. Tarna and its tributary.

Remarks

The distribution of Ca concentrations in drainage waters is observed to be similar to the distribution of EC indicating that EC of drainage waters is strongly influenced by Ca concentrations. An abrupt change in Ca concentrations observed downstream of the confluence of Parad Tarna and Parad Bikk suggests chemical processes that attenuate Ca from the stream. There is likely to be some bicarbonate ions which react with Ca to form immobile $CaCO_3$ precipitates. Further investigations are required to determine these processes.

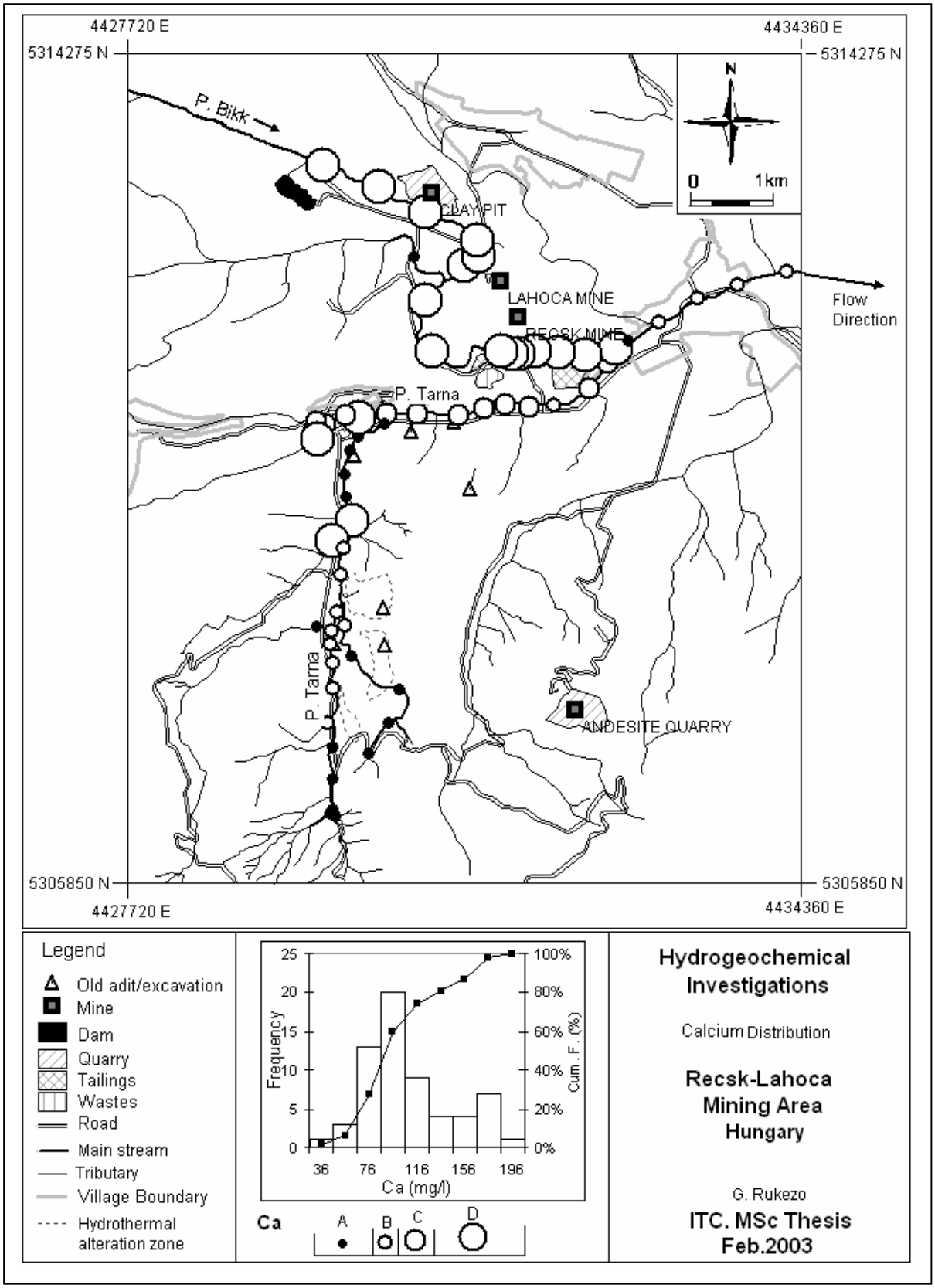

Figure 4.7. Spatial distributions of observed Ca concentrations in drainage waters of the area.

Magnesium(Mg) data

Two points of inflection observed on the cumulative frequency curve of the histogram are used to separate Mg data into three population groups. Group A is comprised of Mg concentrations less than 32mg/l and group B is comprised of Mg concentrations ranging from 32 to 63mg/l, while group C has Mg concentrations above 62mg/l. Figure 4.8 shows the distribution of Mg concentrations in the study area.

Population A is predominantly distributed in Parad Tarna while population B is distributed mainly in Parad Bikk. Higher Mg concentrations are distributed throughout Parad Bikk indicating that the Oligocene clayey-marl from which Parad Bikk emanates also influences Mg concentrations. The tributaries of Parad Tarna that are also observed to have high Mg concentrations emanate from Oligocene clayey-marl. Summarised in table 4.8 are the Mg distributions and their environmental associations.

Table 4.8. Summary of observed spatial distribution of Mg concentrations in waters draining the area.

Mg group	Upper percentile	Mg range (mg/l)	Environmental association
C	100	63-119	Parad Tarna tributary.
B	97	32-63	Parad Bikk and tributaries of Parad Tarna.
A	58	<32	Parad Tarna at stream confluence.

Remarks

The distribution of Mg concentrations is similar to those of Ca concentrations and EC distributions depicting that both Ca and Mg are leached from same sources and their concentrations strongly influence the EC of the stream waters.

Aluminium(Al) data

The histogram of Al data has the form of a normal density distribution. Four population groups were determined using the 25, 50 and 75 cumulative percentiles, resulting in group A with Al concentrations below 0.32mg/l, group B with concentrations ranging from 0.32 to 0.4mg/l, group C with concentrations ranging from 0.4 to 0.61mg/l and population D with concentrations above 0.61mg/l. Displayed in figure 4.9 are the distributions of Al concentrations in drainage waters of the area.

Aluminium concentrations below 0.32mg/l are predominantly distributed in Parad Tarna in areas close to old. Concentrations ranging from 0.32 to 0.4mg/l are also distributed in Parad Tarna. The Sub-population groups C and D are intermittently distributed in Parad Bikk, which indicate the attenuation of Al to insoluble complexes in some of the areas of the stream profile. Distribution of the highest Al concentrations points to the Oligocene clayey marl as a major source. High concentrations are also observed in the drainages near hydrothermal alteration zones. Table 4.9 shows the spatial distributions of Al concentrations.

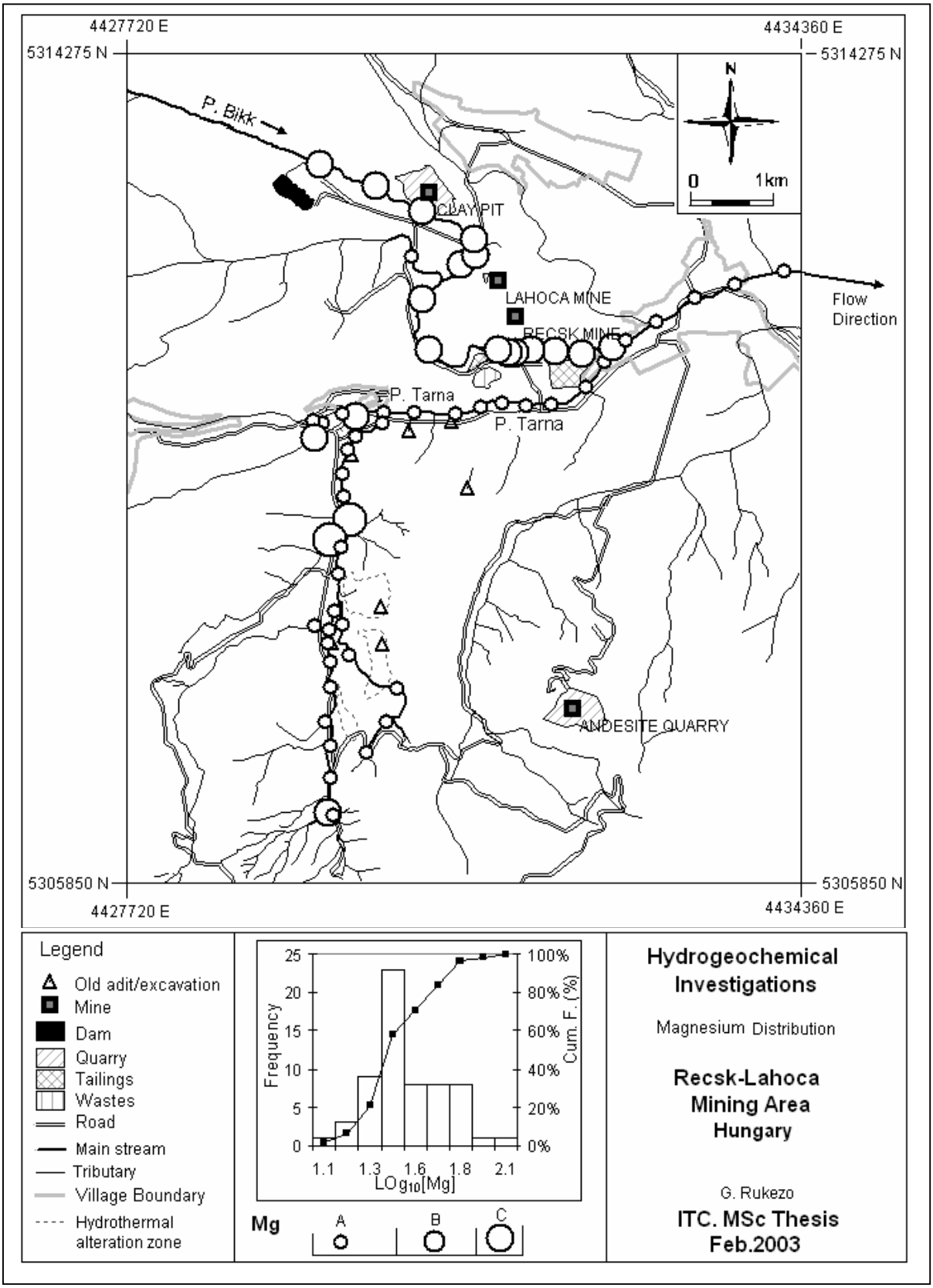

Figure 4.8. Spatial distributions of observed Mg concentrations in drainage waters of the area.

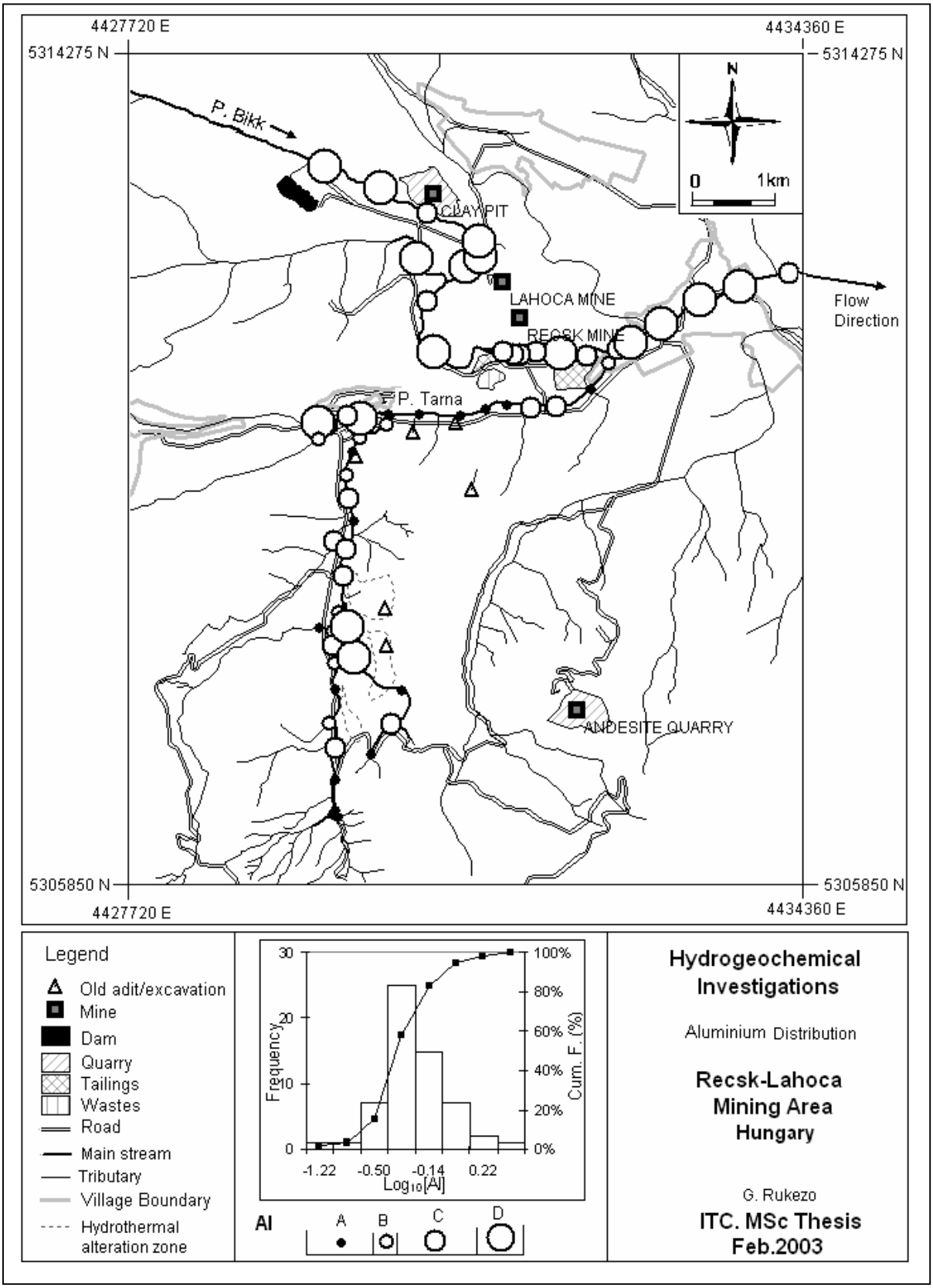

Figure 4.9. Spatial distributions of observed Al concentrations in drainage waters of the area.

Table 4.9. Summary of observed spatial distribution of Al contents in the waters draining the area.

Al group	Upper percentile	Al range (mg/l)	Environmental association
D	100	>0.61	P. Bikk and P. Tarna in hydrothermal alteration zones.
C	75	0.40-0.61	Parad Bikk and Parad Tarna
B	50	0.32-0.40	Parad Tarna.
A	25	<0.32	Parad Tarna.

Potassium(K) data

The 13 and 48 cumulative percentiles were used to divide the population into three distribution groups. Group A is comprised of K concentrations below 4.22mg/l, and group B is comprised of concentrations ranging from 4.22 to 8.41mg/l, while group C is comprised of concentrations above 8.41mg/l. Figure 4.10 shows the spatial distribution of K concentrations in drainage waters of the area.

The highest concentrations of more than 9.41mg/l are mainly distributed in Parad Bikk. The drainage of Parad Tarna is also characterised by high K concentrations in geochemical alteration zones and the area around the confluence with Parad Bikk. Concentrations below 8.41mg/l are distributed in the rest of Parad Tarna drainage. High concentrations in the tributaries of Parad Tarna are seen to disappear after the confluence with the main stream indicating that conditions in the main stream favours precipitation of K ions into insoluble complexes. Summarised in table 4.10 are the spatial distributions of K concentrations in the streams.

Table 4.10. Summary of observed spatial distribution of K contents in the waters draining the area.

K group	Upper percentile	K range (mg/l)	Environmental association
C	100	>8.41	Parad Bikk and tributaries of Parad Tarna.
B	48	4.22-8.41	Parad Tarna.
A	13	<4.22	Parad Tarna.

Sodium(Na) data

Three inflection points on the cumulative frequency curve are used to classify Na concentrations into four population groups. Table 4.11 shows the sub-population groups and their environmental association. The spatial distributions of the Na concentration groups are displayed in figure 4.11.

Population groups A and B are distributed in Parad Tarna while population groups C and D are predominantly distributed in Parad Bikk. Group D with Na concentrations above 126mg/l are observed in Parad Bikk in those parts the stream drains the Oligocene clayey-marl areas, the Recsk tailings area and the Lahoca tailings area indicating that these are the environments contributing most of the Na in the stream. Lower Na concentrations are observed between the Recsk and the Lahoca tailings indicating that chemical processes on this part of the stream favour the precipitation of Na into insoluble compounds.

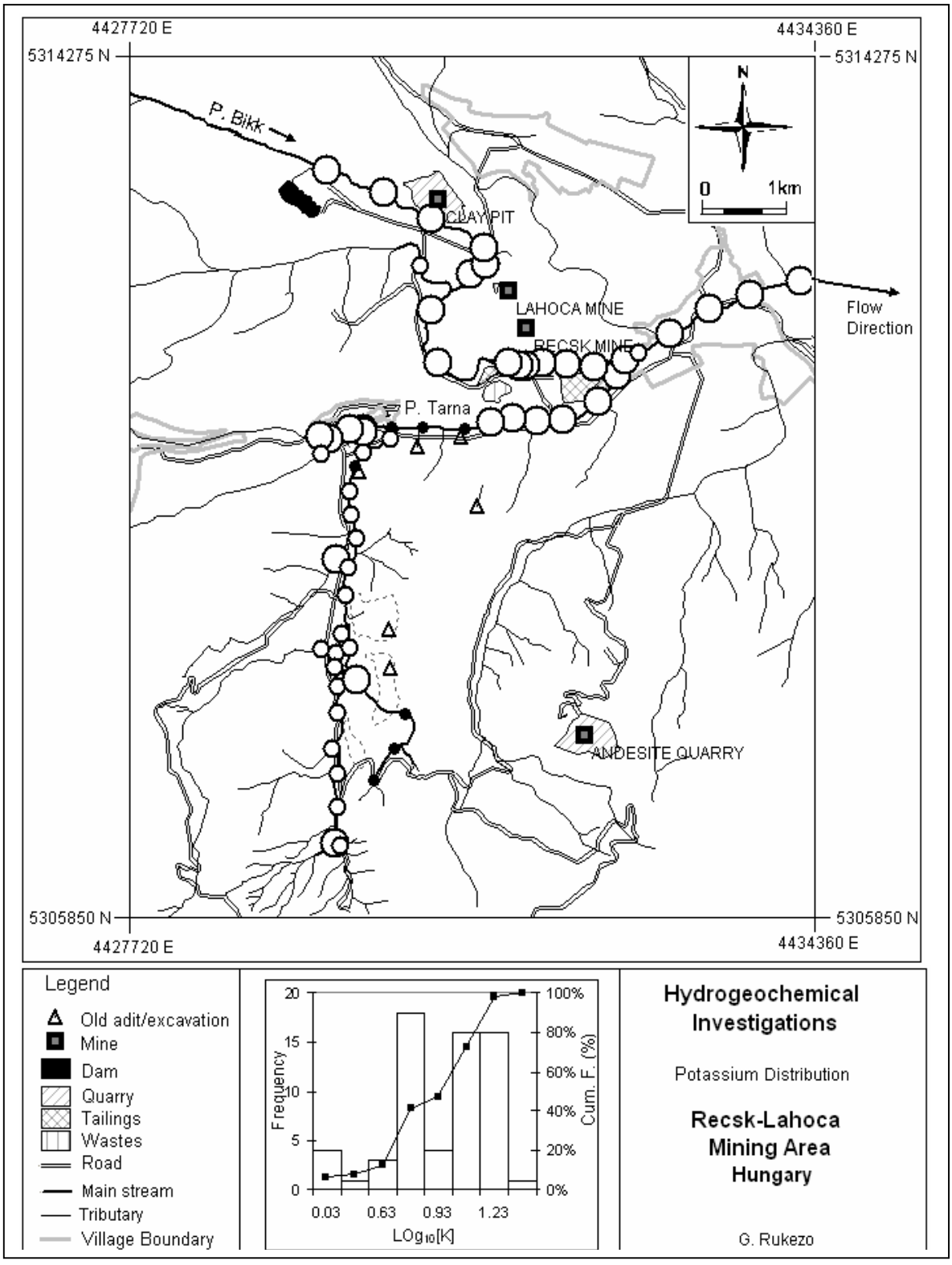

Figure 4.10. Spatial distributions of observed K concentrations in drainage waters of the area.

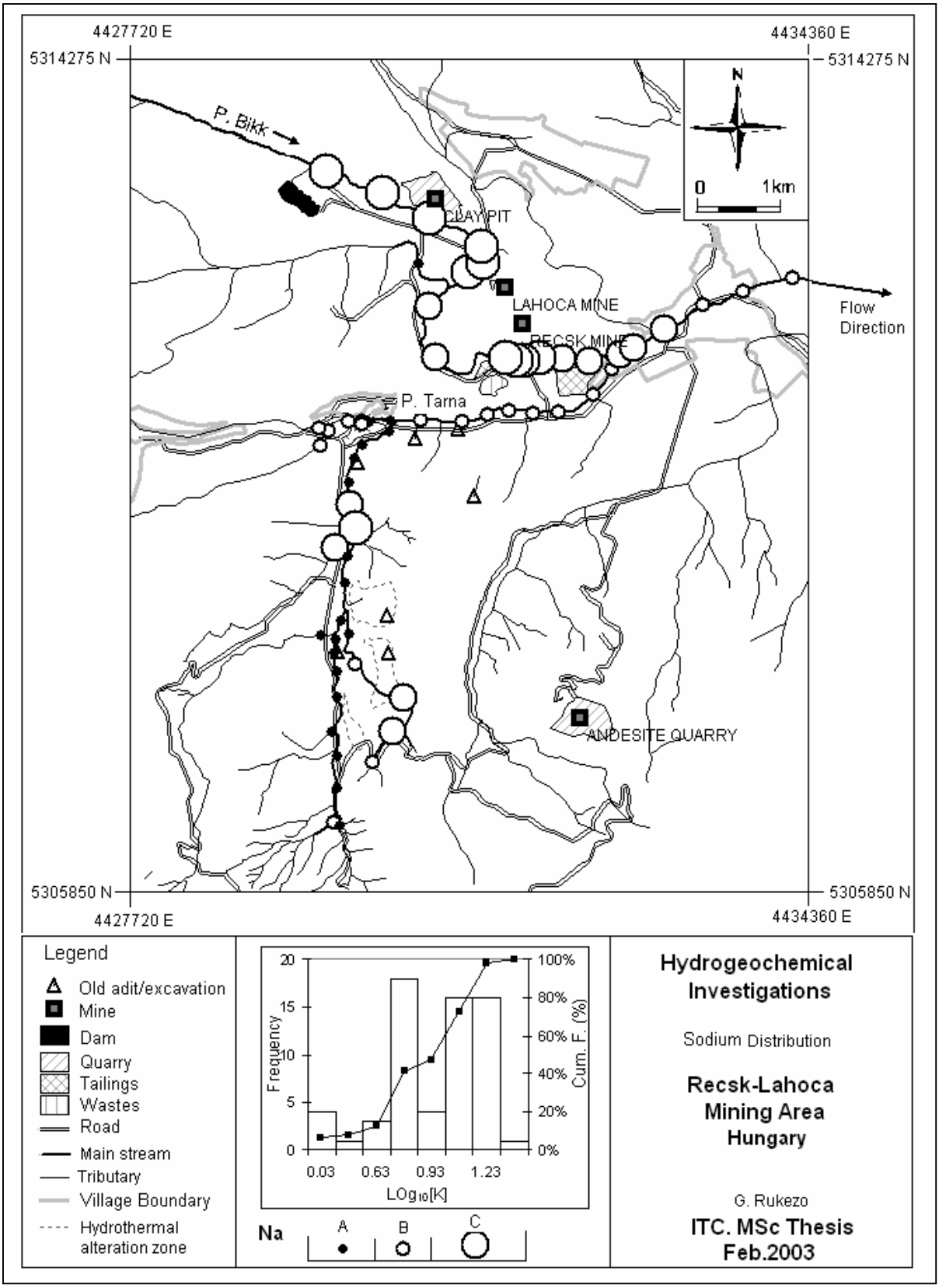

Figure 4.11. Spatial distributions of observed Na concentrations in drainage waters of the area.

Table 4.11. Summary of observed spatial distribution of Na concentrations in waters draining the area.

Na group	Upper percentile	Na range (mg/l)	Environmental association
D	100	>126	Parad Bikk and tributary of Parad Tarna.
C	83	32-126	Parad Bikk and Parad Tarna.
B	65	20-32	Parad Tarna.
A	33	<20	Parad Tarna.

Total major cation

The total concentrations of major cations were analysed to determine their spatial distributions in the drainage waters. The total major cation concentrations are comprised of Al, Ca, K, Mg and Na concentrations that were determined on every sample location in the streams.

The 65 and 78 cumulative percentiles, which are equivalent to concentrations of 159 and 316mg/l, were used to classify the population into three groups. Table 4.12 shows the population groups and their environmental distributions.

Total cation concentrations range from 10 to 603mg/l. Concentrations below 159mg/l and most of the concentrations ranging between 159 and 316 mg/l are distributed in Parad Tarna whereas the higher concentrations above 316mg/l are distributed in Parad Bikk. The Oligocene clayey marl and the Recsk and Lahoca tailings are most likely to be loading major cations in Parad Bikk. Displayed in figure 4.12 are the spatial distributions of total cation concentrations in drainage waters of the area.

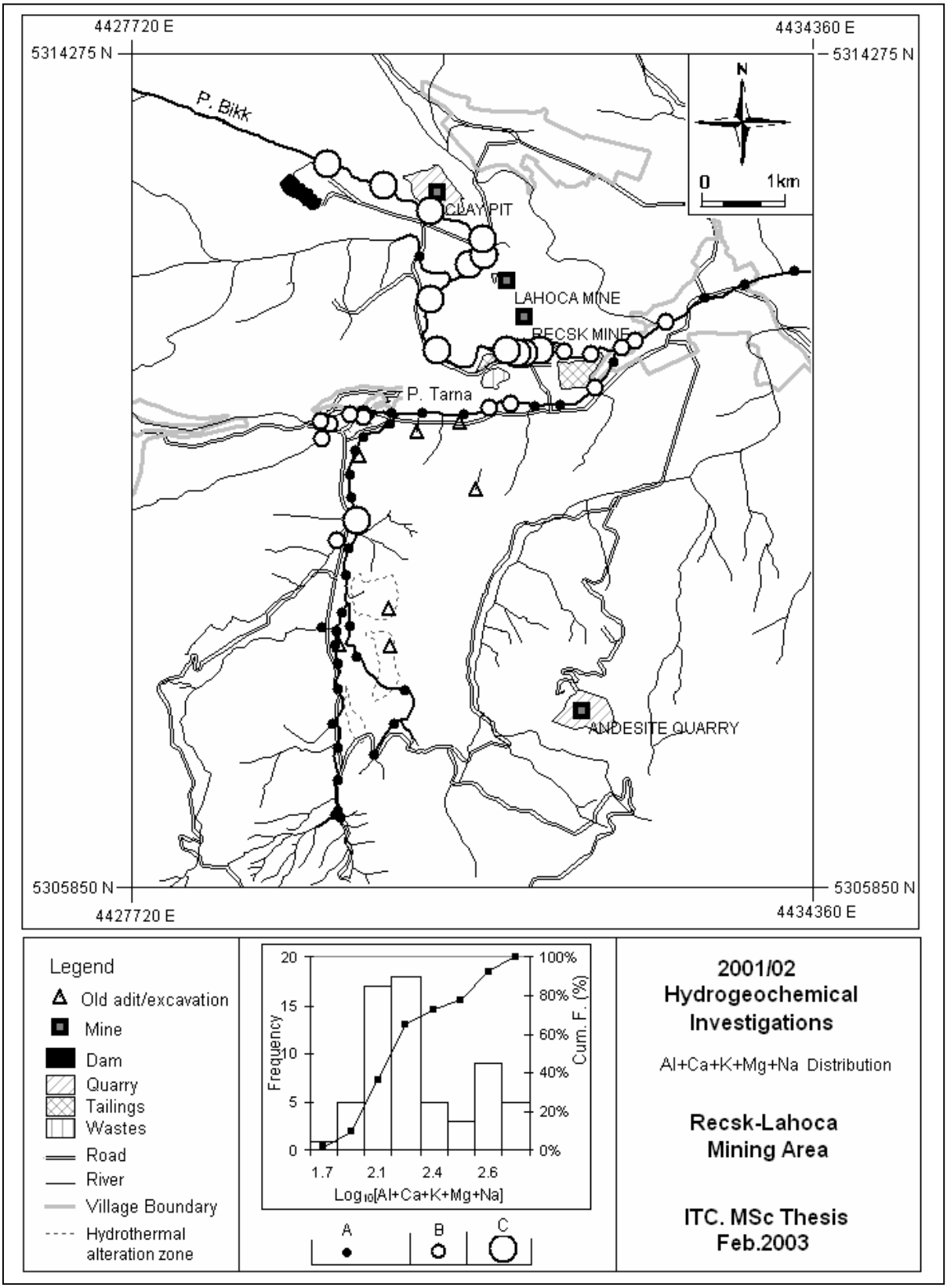

Figure 4.12. Spatial distributions of observed total major cation concentrations in drainage waters of the area.

Table 4.12. Summary of observed spatial distribution of total major cation concentrations in waters draining the area.

Group	Upper percentile	range (mg/l)	Environmental association
C	100	>316	Parad Bikk.
B	65	159-316	Parad Tarna.
A	33	<159	Parad Tarna.

4.1.3. Summary of the univariate data analysis

Element concentrations are observed to be related to the environments the waters drain through, like lithologies, geochemical alteration zones and mine areas. Spatial distributions of major cation are observed to be similar indicating that they are from similar sources and the processes that leach them into solution are also similar. Some of the base metal distributions are also observed to be similar, which indicate similar sources or similar environmental associations. Potassium and Al are quite high downstream of the confluence while Ca, Mg and Na are very low when the compared with the concentrations immediately above the confluence.

The relationships observed between element concentrations and the environments the streams drain through can further be compared graphically by plotting concentrations against distance along the stream profiles. The similarities of the element distributions are also indicative of interrelationships, which can be studied to fully determine the factors responsible for loading metals in the drainage waters of the area. Multivariate data analysis methods are useful in establishing these element associations and the factors that contribute to their mobility in stream waters.

4.2. Metal concentrations along stream profiles

Stream water geochemical data was plotted against distance along the stream profiles in order to determine changes in metal concentrations from upstream downwards. The sample locations on the uppermost parts of the streams were taken as points of origin. Metal concentrations on sample locations downstream of the points of origin were plotted against the distances of the sample locations from the point of origin. Figure 4.13A to I shows metal concentrations along stream profiles. Due to the high variations in the element concentrations, the y-axis is plotted on a logarithmic scale. Index bars highlighting areas of interest along the stream profiles are included as footnotes on the graphs of the two streams in order to compare element concentrations with environmental features. The abbreviations used to describe the environmental features are: H = hydrothermal alteration zone; TC = tributary confluence; H/A = hydrothermal alteration/ancient adits area; C = confluence of Parad Tarna and Parad Bikk; L = Lahoca tailings piles area; W52 = Sample location with extreme acidic waters; R = Recsk tailings piles area.

Element concentrations are observed to be generally higher in Parad Bikk than in Parad Tarna when the graphs of the same element are compared. The environmental features indicated on the footnote bars have significant influence on the concentrations of the elements as indicated by either a rise or a fall in element concentration. Iron and Mn are seen to increase significantly in the hydrothermal alteration zones (H) and the area with ancient adits (H/A). A sharp rise in Zn concentration in the old

adits area indicates that the waters oozing out of the old adits and/or the sulphidised and hydrothermally altered andesite in that area have high Zn content, which is leached into Parad Tarna. The ore, which was accessed by the old adits, is likely to contain sphalerite, (Zn,Fe)S, which is one of the major mineralization in the area. Slight kinks of increase in Cu concentrations are observed in the same areas. In Parad Bikk, all the base metals show positive kinks in the area the stream drains Recsk and Lahoca tailings (R and L respectively), which indicate that the leaching of base metals is taking place in these tailings piles. Extremely high element concentrations are observed on a sample site that is located between the Recsk and Lahoca tailings piles (W52). The water of this location is highly acidic with pH of 2. The lack of vegetation within the vicinity of the acidic waters of this area is a clear indication of vegetation poisoning due to extremely high metal and acidic conditions. The acidic conditions are likely to be due to processes of acid mine drainage taking place on some transported tailings materials, which were deposited on this site during erosion, or acidic mine water from some other area surfacing on this site. While most of the metal concentrations are high on this site, K, and Na concentrations are extremely low, with concentration values in the ranges of their lower detection limits. This behaviour is also observed in the old adits area, the Recsk tailings area and the Lahoca tailings areas where Na and k are low while the other element concentrations are high. The low concentrations of K and Na are likely to be due to their high sorbance, which result in them getting sorbed on the immobile hydroxyl complexes that form in acidic waters through ion exchange (Krauskopf., 1995). An example of a process that depletes K from water is the precipitation of Fe-hydroxide complexes like jarosites, where K, due to its high reactivity, is easily incorporated into the complex ahead of the other metals. Aluminium is also observed to be low in the old adits area depicting that it reacts with constituents of the acidic waters at the interface with stream water to give rise to immobile mineral complexes.

The graphs of most of the major element cations show a general decline in concentration along the stream profile of Parad Bikk. Highest concentrations are observed in the headwaters where the stream drains the Oligocene clayey marl. This trend is typically observed in the Na profile (figure 4.15I). This further confirms the Oligocene clay as a major source of major element cations as observed in the spatial distribution maps in the earlier section. The sample location immediately below the confluence of Parad Tarna and one of its tributaries (TC), which originating from the Oligocene clay, is characterised by sharp increases in major element cation concentrations, which further indicates that the Oligocene clay is a major source for major element cations.

The area downstream of the confluence of Parad Tarna and Parad Bikk does not show much variation in element concentrations except immediately below the confluence where a positive kink is observed on the element profiles from Parad Tarna and a negative kink is observed on element profiles from Parad Bikk as the two streams mix.

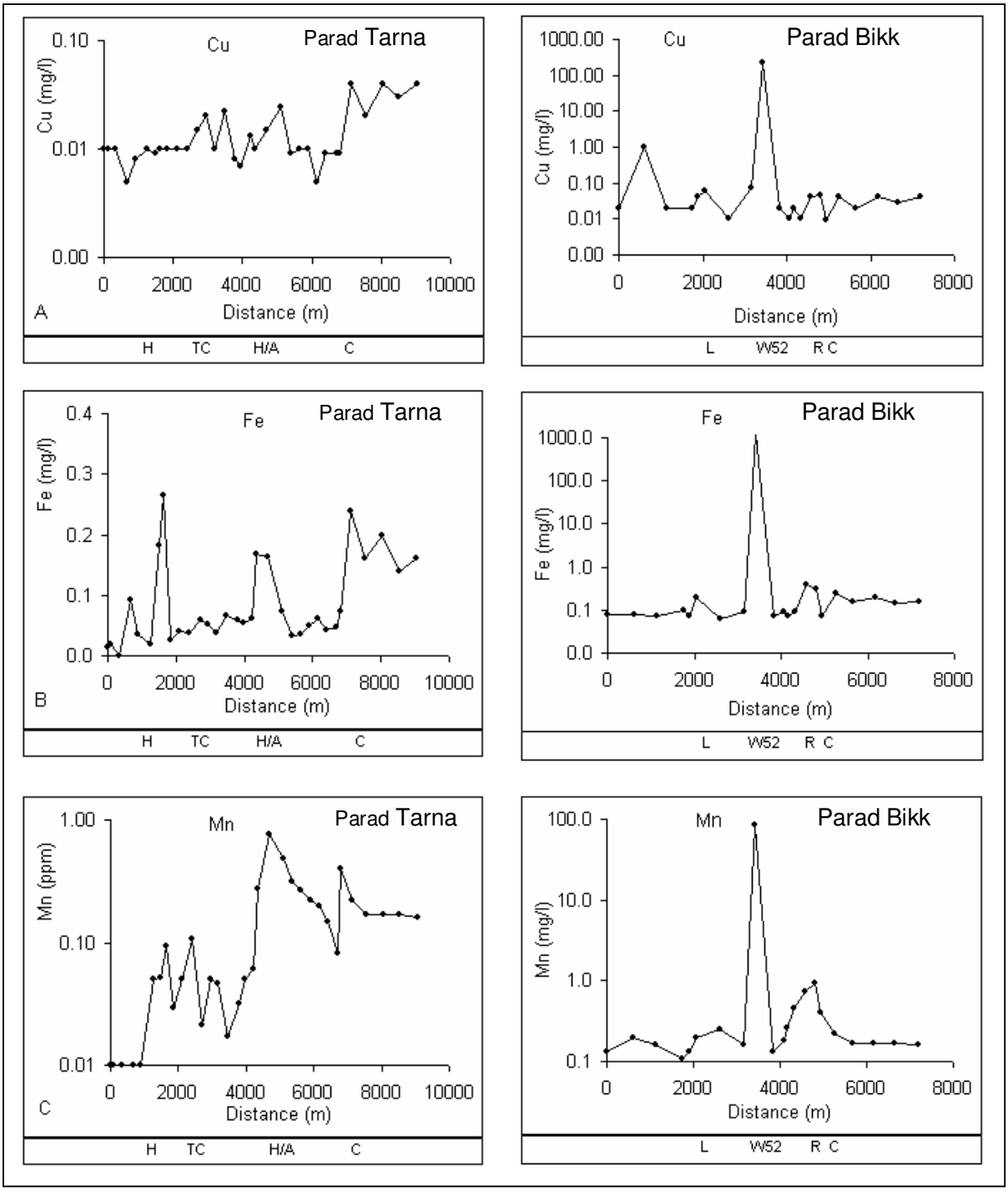

Figure 4.13. Graphs of element concentrations as functions of distance along stream profiles. Row A = Cu; B = Fe; C = Mn; H = hydrothermal alteration zone; TC = tributary confluence with P. Tarna; H/A = hydrothermal alteration/ancient adits area; C = confluence of P. Tarna and P. Bikk; L = Lahoca tailings area; W52 = sample location with extreme acidic waters; R = Recsk tailings piles area.

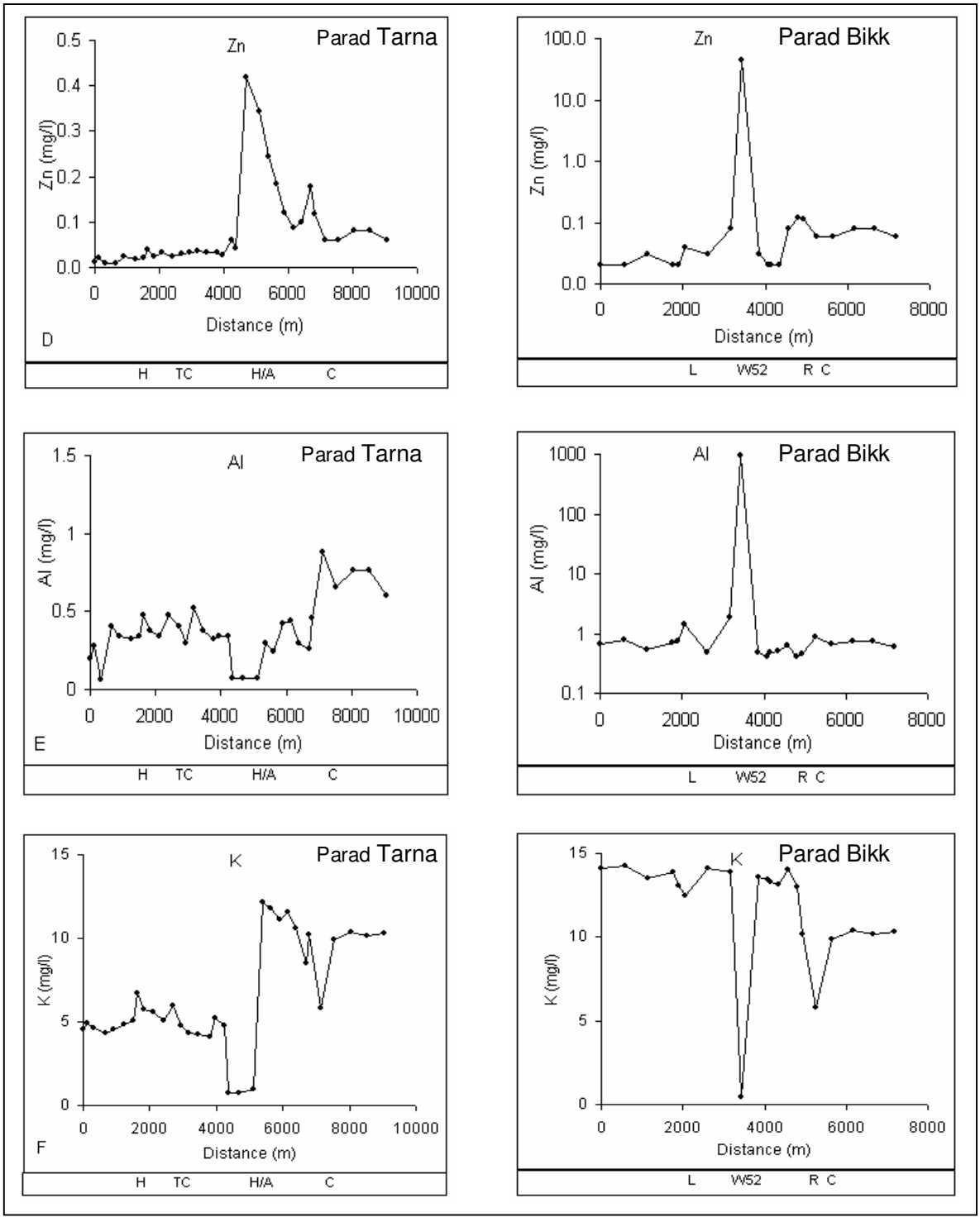

Figure 4.13 (continued). Graphs of element concentrations as functions of distance along stream profiles. Row D = Zn; E = Al; F = K; H = hydrothermal alteration zone; TC = tributary confluence with P. Tarna; H/A = hydrothermal alteration/ancient adits area; C = confluence of P. Tarna and P. Bikk; L = Lahoca tailings area; W52 = sample location with extreme acidic waters; R = Recsk tailings piles area.

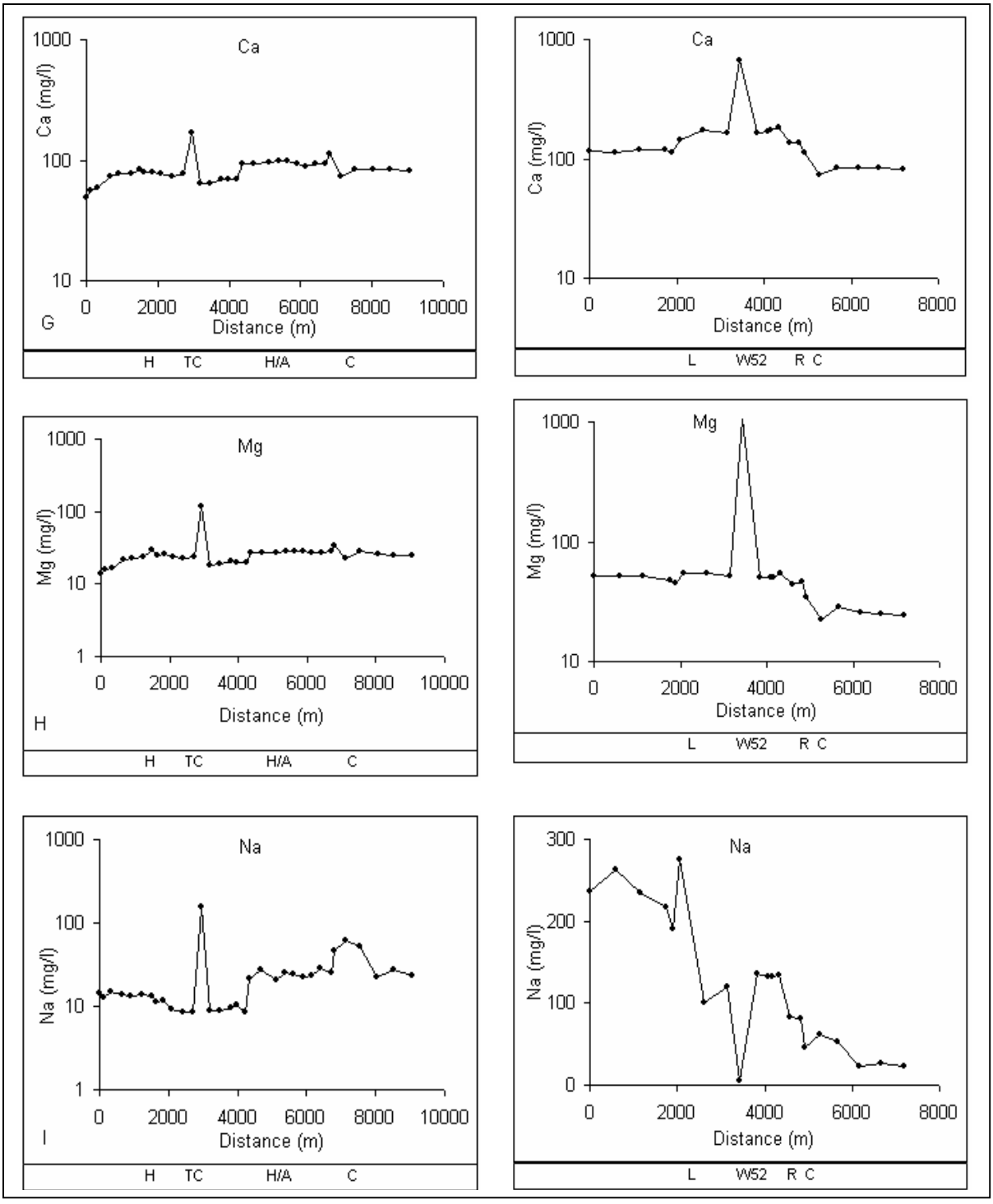

Figure 4.13 (continued). Graphs of element concentrations as functions of distance along stream profiles. Row G = Ca; H = Mg; I = Na; H = hydrothermal alteration zone; TC = tributary confluence with P. Tarna; H/A = hydrothermal alteration/ancient adits area; C = confluence of P. Tarna and P. Bikk; L = Lahoca tailings area; W52 = sample location with extreme acidic waters; R = Recsk tailings piles area.

4.3. Multivariate data anlysis

In hydrogeochemical data analysis, multivariate data analysis methods are employed in order to simultaneously determine detailed interrelationships and associations of variables not fully revealed by univariate methods, and by so doing, factors influencing the properties of water and the distribution of metals in water are fully established. Correlation coefficient analysis was used to determine element interrelationships in the streams.

4.3.1. Correlation analysis

In order to estimate the degree of interrelationship between variables in a manner not influenced by measurement units, the correlation coefficient (r), which is the ratio of the covariance of two variances to the product of their standard deviations is used, and is given by the formula(Davis., 1986):

$$r_{xy} = COV_{xy}/s_x s_y$$

where r_{xy} is the correlation coefficient, COV_{xy} is the covariance, and s_x and s_y are the standard deviations of the x and y variables. The correlation coefficient is a unitless ratio number, which ranges between –1 and +1, where a correlation of +1 indicates a perfect direct rectilinear relationship between two variables, and a correlation coefficient of –1 indicates that the variables have an inverse rectilinear relationship. Between the two extremes is a spectrum of less-than-perfect relationships, including zero, which indicates lack of linear relationship at all (Swan and Sandilands., 1995).
The Pearson (or product moment) correlation coefficient was used in estimating the degree of interrelationship between water constituent variables. The Correlations were calculated for elements with not less than 50% of the measurements falling below detection limit. These were Cu, Fe, Mn, Zn, Al, K, Ca, Mg, Na and SO_4^{2-}. Electrical conductivity and pH were included in the correlation analysis in order to determine their interrelationships with element concentrations. Table 4.13 is the correlation coefficient matrix table showing the correlation coefficients of the constituents.

Table 4.13. Correlation coefficient matrix for the stream water geochemical data.

	Cu	**Fe**	**Mn**	**Zn**	**Al**	**K**	**Ca**	**Mg**	**Na**	**SO_4^{2-}**	**pH**	**EC**
Cu	1											
Fe	-0.05	1										
Mn	-0.01	0.89	1									
Zn	0.14	0.07	0.24	1								
Al	0.51	0.28	0.26	-0.17	1							
K	0.27	0.07	0.05	-0.12	0.50	1						
Ca	0.28	-0.03	0.02	0.00	0.23	0.60	1					
Mg	0.23	-0.09	-0.09	-0.12	0.18	0.55	0.82	1				
Na	0.33	-0.08	-0.10	-0.20	0.42	0.54	0.56	0.64	1			
SO_4^{2-}	0.25	0.14	0.31	0.20	0.22	0.58	0.58	0.48	0.25	1		
pH	0.02	-0.47	-0.60	-0.28	-0.03	0.25	0.25	0.28	0.44	-0.16	1	
EC	0.33	-0.02	0.01	-0.06	0.35	0.69	0.73	0.60	0.88	0.51	0.39	1

Only Mn and Fe are strongly correlated with each other among the analysed base metals. The high positive correlation on these two elements indicates similar element-water reaction control on the system due to similarities in their chemical properties.

A positive correlation coefficient of 0.51 observed on Cu and Al data is most likely an impression of their leaching from same mineralised lithological source. Most of the Cu is leached from the mineralised parts of the andesite, which are known to be argillised, and Al is leached into solution during the argillisation processes.

Potassium, Ca, Mg and Na are all positively correlated suggesting that they are all loaded into stream waters from similar sources and by similar leaching processes. The concentrations of these elements in the stream waters are probably enhanced by the weathering of the clay minerals in the Oligocene clayey marl from which most of the streams draining the area originate. Also, primary magmatic minerals of these elements are the major mineral constituents of the andesite rock which covers the bulk of the study area. Weathering of the andesite rock can therefore enhance the concentrations of these elements in the drainage waters of the area. Stronger positive correlation observed on Mg and Ca is most likely due to the weathering of the underlying carbonate rocks. Groundwater rich in Ca and Mg may manifest itself into stream waters through faults and fractures, which results in the loading of these two elements in surface drainages of the area. Carbonate precipitates have been observed in a stream which originates from a reservoir used for the storage of water pumped out of underground mine excavations during the active periods of the mine. The precipitation of carbonates from such waters shows that groundwater is laden with Ca and Mg which can easily drain into surface waters in areas where the groundwater comes to the surface.

Aluminium has a relatively high positive correlation with potassium among the other major cations, which, may be, is due to their strong association in the weathering of feldspars. Hydrolysis of k-feldspars results in the formation of Al-bearing clay minerals like kaolinite which co-exist in solid-liquid equilibrium with K^+ ions.

Positive correlations area observed between sulphate and major cations, which may be is a reflection of the chemistry of the rocks which host the sulphide deposits: an andesite rock with high silicate minerals of these major cations. The breakdown of metal sulphides and of the silicates of these elements in acidic waters leads to the uptake of major cations and sulphate in water, leaving a silica rich residue. Figure 4.14 shows the scatter graph of total major cation against sulphate concentrations. The Plots of data from Parad Tarna and the area downstream of the confluence of the streams show more linear relationships than plots of data from Parad Bikk, which may be indicative of the lithological sources of the element constituents. In Parad Tarna, most of the sulphate and major element cations are leached from the weathering of the andesite bedrock, giving rise to a linear relationship, whereas in Parad Bikk, a significant quantity of the major cations are leached from the Oligocene clay while the sulphate is leached from the andesite and tailings piles. The different sources may result in lack of correlation in this part of the stream environment.

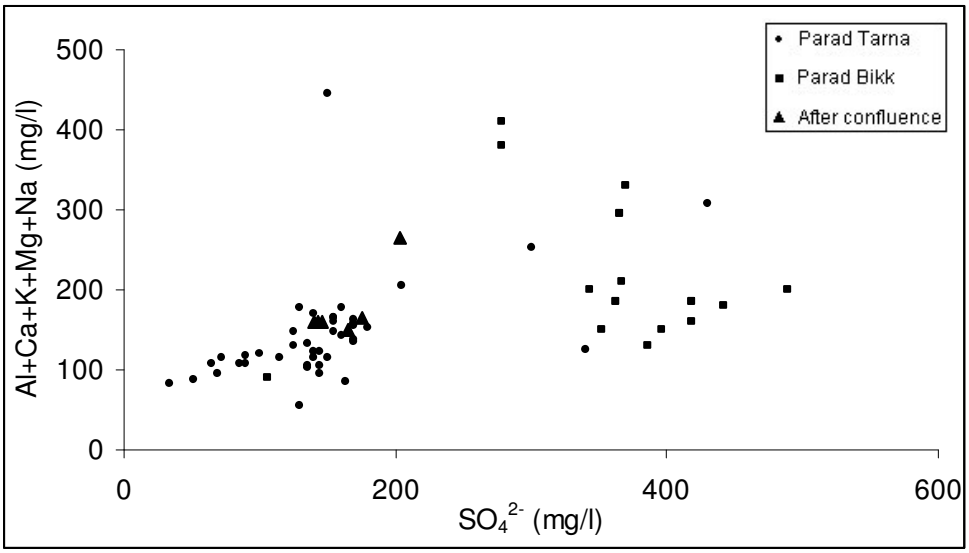

Figure 4.14. Scatter graph showing the relationship between sulphate and the total concentrations of major element cations.

Correlation coefficients between sulphate and base metals are positive but generally low indicating that the correlations are not strong. Sulphide minerals, which are oxidised and hydrolysed into solution, are the sources of base metals and sulphates in water. Their leaching into water explains the positive correlations, which are weak due to other surface geo-fluvial processes like co-precipitation of the base metals into insoluble compounds as a result of scavenging effects of precipitating Fe and Mn.

Negative correlations are observed between pH and base metals and are strongest with Mn and Fe. Sulphate also has weak negative correlation with pH. Hydrolysis of metal sulphide minerals requires acidic waters to produce mobile base metals and sulphate, which explains the negative correlations of these constituents with pH. The precipitation of Mn and Fe is mainly dependent on the pH of water while that for the other base metals is also dependent on co-precipitation, which explains why the inverse correlation is stronger between the two elements and pH, and why the inverse correlation is weaker between the other base metals and pH. Other surface processes similarly remove sulphate from water (e.g. ionic bonding with strongly alkaline metals to form sulphate salts), giving rise to weaker inverse correlation between sulphate and pH.

Weak positive correlations are observed between pH and the major cations, which indicate that high pH conditions are favourable for major element cation mobility.

Electrical conductivity is not correlated with base metals except Cu. The contribution of the low base metal ion concentrations towards the electrical properties of water are likely to be overshadowed by the high concentrations of major element cations. High positive correlations with major element cations indicate that EC is strongly influenced by the concentrations of major elements. A near perfect direct relationship is observed when EC is plotted against the total concentrations of major element cations (figure 4.15). The near perfect correlation for all the data from Parad Tarna, Parad Bikk and after the confluence shows that EC is mainly influenced by major element cation concentrations in the streams.

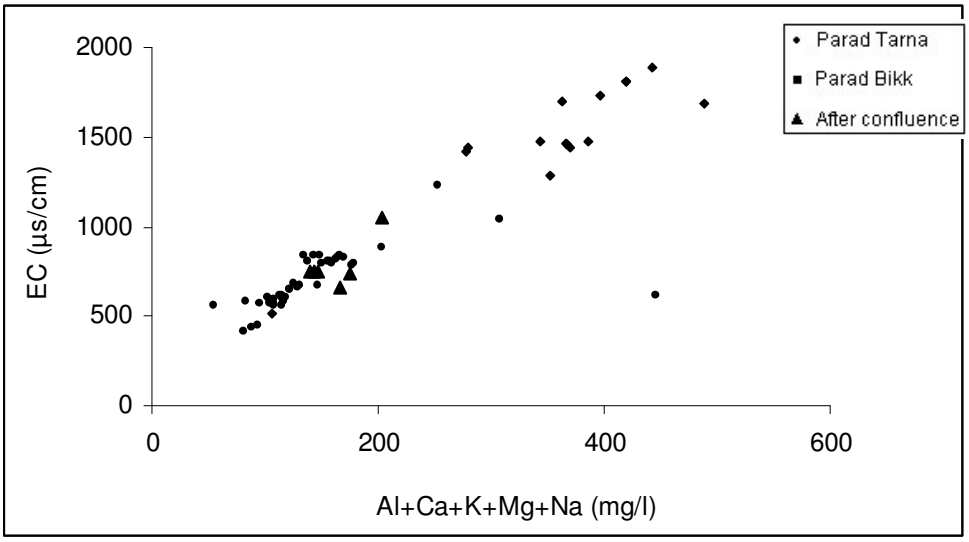

Figure 4.15. Scatter graph showing the relationship between EC and the total concentrations of major element cations.

A positive correlation of 0.51 between EC and sulphate indicates that EC properties of water are also dependent on sulphate concentrations. Figure 4.16 shows the EC-sulphate relationship on a scatter graph.

Electrical conductivity of water is known to increase with increase in element ion concentration and mobility in water through the following relationship:

$$TDS = kcEC \text{ or } EC = TDS/kc$$

where TDS is total dissolved solids, k_c is the correlation factor and EC is electrical conductivity (Lloyd and Heathcote., 1985). The dissolved solids-electrical conductivity formula approximates a linear relationship, which explains the strong correlations between EC and major cation concentrations and between EC and sulphate ion concentrations. Both major element cations and sulphate ions constitute the largest percentages of dissolved solids in the stream waters of the area.

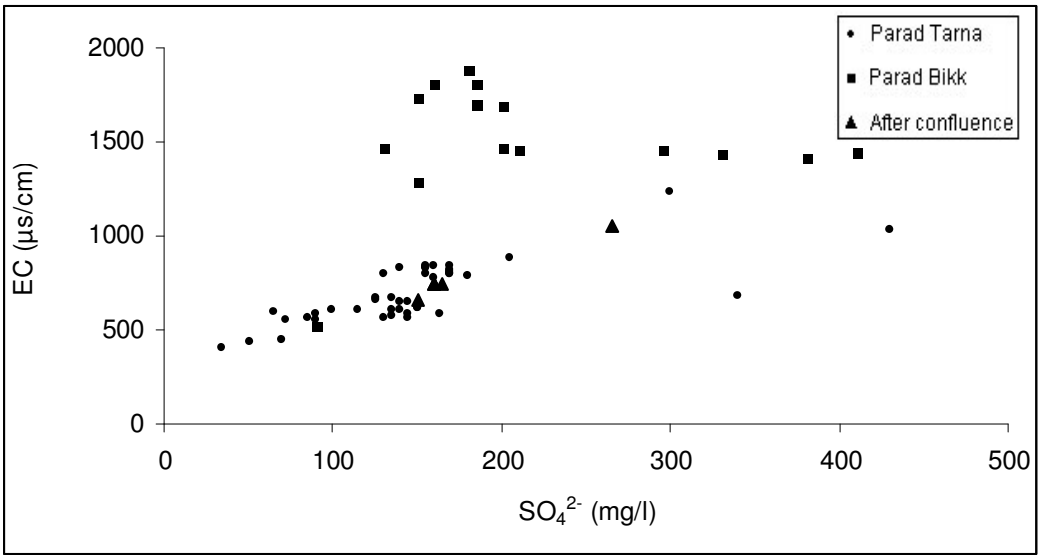

Figure 4.16. Scatter graph showing the relationship between EC and sulphate concentrations.

4.4. Conclusions

The extremely low base metal concentrations in the stream waters draining the area makes it difficult to fully established the correlations between these elements and the other measured constituents.

Higher concentrations of the base metals are mainly distributed in areas where the streams drain hydrothermal alteration zones and areas with old adits.

Similar spatial distributions of major elements suggest a similar source for these elements. The higher concentrations for these elements in the areas the streams drain the Oligocene clay indicate that this lithology is a major source for the major elements.

Graphical displays of element concentrations against distance along stream profiles clearly indicate the variations between element concentrations and the environmental features drained by the streams, which are otherwise difficult to visualise on element distribution maps.

The analysis of correlation coefficient can indicate the elements with dominant influence on the properties of water like EC.

The results of single element analysis, graphical displays of element concentrations as functions of distance and correlation analysis indicated the possible lithological sources of metal load in the stream waters and the possible surface geo-fluvial processes giving rise to the detected element concentrations. An analysis of the sediments of these streams may be helpful in further revealing stream characteristics which are indicative of the sources of metals in those streams and the surface processes that attenuate the metals.

5. STREAM SEDIMENTS GEOCHEMICAL DATA ANALYSIS.

Stream sediment geochemical data collected from Parad Tarna and Parad Bikk and their tributaries was collectively analysed using univariate methods, mainly to determine element distributions in the area, and multi-element methods used mainly to identify mineral associations in the area.

5.1. Univariate Data Analysis

5.1.1. Element data structure

Summary Statistics:
Summary descriptive statistics of the stream sediments elements is shown in table 5.1.

Table 5.1. Summary of descriptive statistics for stream sediments geochemical data (n=53). Concentrations are given in ppm except for Fe which is in percentage.

Element	Min.	Median	Max.	Mean	Std. Dev.	Skew	Log_{10}Skew
As	0.8	20.6	1965	131.04	328.39	4.17	0.86
Cd	0.8	1.7	8.1	2.01	1.16	3.32	1.25
Cu	7.2	31.8	1995	226.49	510.09	2.79	1.34
Fe	0.77	1.74	3.65	1.83	0.62	1.10	0.17
Mn	103	546.3	3303	600.27	488.92	3.53	-0.17
Ni	0.3	10	49.6	11.59	7.24	3.47	-2.93
Pb	4.1	29.9	157.3	37.19	30.42	2.06	-0.14
Sb	0.02	0.3	19.2	0.76	2.77	6.67	1.56
Zn	15	78.9	235.4	79.08	40.29	1.35	-0.42

Element concentrations range from low to high indicating high variability in the data. Statistics of the original data shows strong positive skew indicating the presence of highly anomalous concentrations. Because skewness influences results of statistical analysis of element data due to the influence of highly anomalous values, log_{10}-transformed data, which is less skewed (table 5.1), is used in univariate and multivariate data analysis for all the measured constituents.

5.1.2. Element distributions

Univariate statistical methods were employed to determine element population groups and their spatial distributions. Slicing of element data into groups used to generate point maps was achieved by the use of "iff" statements in ILWIS GIS software. Sub population groups were arbitrarily chosen using quartile and mid-percentiles in near-normal distributions, and natural breaks were used in distributions not normally distributed. The thresholds used to classify data into distribution groups are determined from the histogram as log_{10}-transformed values, which are first converted to their equivalent antilogarithmic values in ppm (or in % for Fe)

Arsenic(As) data

Two sub-populations are observed on the histogram of As data. The smaller sub-population is comprised of higher concentrations than the larger sub-population, which depicts a positive skew indicative of anomalous As values in the higher concentrations. Due to its near-normal distribution, the data is divided into four groups at the 25, 50 and 75 percentiles which are equivalent to 8.91, 23.99, and 79.43ppm (table 5.2). Displayed in figure 5.1 are the spatial distributions of the groups.

Arsenic concentrations of population groups A and B are all distributed in Parad Tarna and its tributaries. The concentrations less than 9ppm in group A are mainly distributed in the tributaries and headwaters of Parad Tarna while group B concentrations are distributed in the main stream. Group C concentrations are distributed in areas where Parad Tarna drains close to ancient adits and geochemical alteration zones. Two locations, one between Recsk and lahoca tailings areas and another on the upstream side of the Lahoca tailings area, are characterized by As concentrations within the concentration range of group C. Group D concentrations of above 79ppm are primarily distributed in Parad Bikk especially in areas where the stream drains through Lahoca and Recsk floatation tailings piles showing that the mine waste piles are the strongest pointers to As loading in the stream sediments. These high As concentrations persist downstream beyond the confluence with Parad Tarna. Summarised in table 5.2 are the spatial distributions of As concentration groups.

Table 5.2. As sub-population groups and their environmental associations.

As group	Upper percentile	As range (ppm)	Environmental association
D	100	>79	Parad Bikk in & downstream of tailings piles.
C	75	24 – 79	Parad Tarna near ancient adits.
B	50	9 - 24	Parad Tarna.
A	25	<9	Parad Tarna headwaters and tributaries.

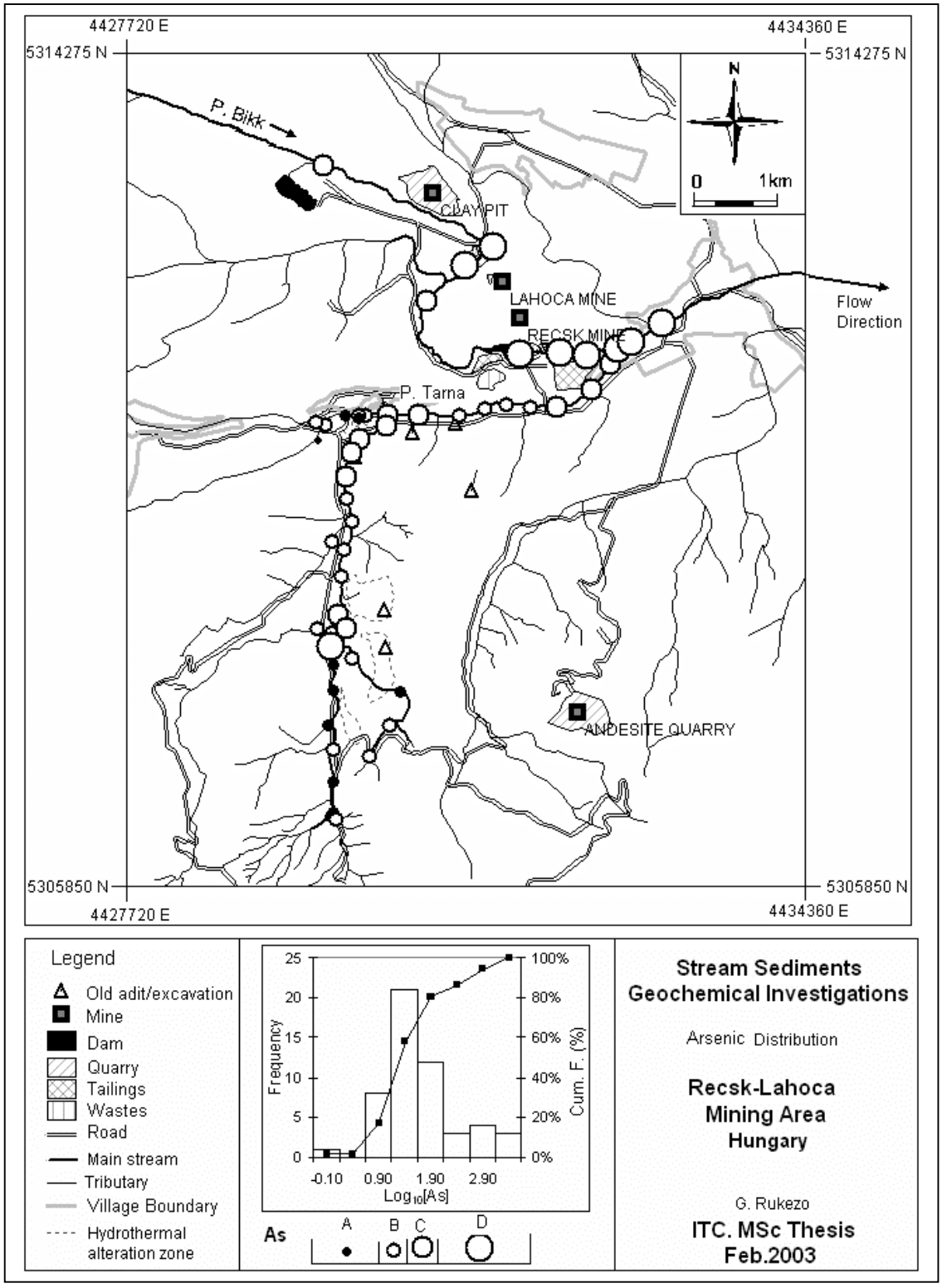

Figure 5.1. Spatial distributions of observed As concentrations in sediments of streams draining the area.

Cadmium(Cd) data

A unimodal distribution with a positive skew is observed on the Cd histogram (figure 5.2). Three population groups were determined on the histogram distribution. Figure 5.2 displays the spatial distributions of Cd concentration groups. Group A is comprised of Cd concentrations below 2.09ppm and group B is comprised of Cd concentrations ranging from 2.09 to 3.98 while group C is comprised of concentrations above 3.98ppm.

Cadmium concentrations above 3.98ppm are distributed in Parad Bikk downstream of Lahoca tailings and within the stream areas draining Recsk mining areas. Concentrations between 2.09 and 3.98ppm are predominantly distributed in the mine areas and in areas where Parad Tarna drains geochemical alteration zones. Concentrations below 2.09ppm are distributed in Parad Tarna and its tributaries. The stream sediments on the downstream side of the confluence of the two streams are characterized by concentrations below 2.09ppm, which indicate dilution due to the influence of Parad Tarna over Parad Bikk. Table 5.3 shows the population groups and their environmental associations.

Table 5.3. Cd sub-population groups and their environmental associations.

Cd group	Upper percentile	Cd range (ppm)	Environmental association
C	100	>3.98	Parad Bikk in the Recsk-Lahoca tailings area.
B	96	2.09 - 3.98	P. Bikk & P. Tarna in hydrothermal alteration areas.
A	77	<2.09	Parad Tarna.

Copper(Cu) data

A bimodal distribution is observed on the Cu histogram (figure 5.3) with a positive skew on the overall data distribution indicating the presents of anomalous high Cu concentrations in the area. Points of inflections at the 77 and 90 cumulative percentiles (i.e. 81 and 912ppm) are used to divide the Cu concentrations into three groups. Group A is comprised of Cu concentrations below 81ppm and group B is comprised of Cu concentrations between 81 and 912ppm while group C is comprised of concentrations above 912ppm. Displayed in figure 5.3 are the spatial distributions of the Cu concentrations in the area.

A distribution similar to that of As concentrations is observed, which indicates that Cu and As are likely to be from same sources and are attenuated into stream sediments by similar processes. Concentrations above 912ppm are only distributed in stream sediments of Parad Bikk in those areas it drains mine tailings areas indicating that these concentrations are mainly related to mine waste materials, which have high Cu-sulphide minerals. A similar trend to that of the highest Cd distribution in the Lahoca area is observed whereby highest Cu concentrations are observed after a distance of about 700m downstream of the Lahoca tailings. Only one sample location next to an area with old excavations has Cu concentrations above 912ppm in the Parad Tarna drainage. Copper concentrations ranging from 91 to 912ppm are distributed around the Lahoca tailings area and downstream of the stream confluence. The less than 81ppm concentrations are predominantly distributed in sediments of Parad Tarna drainages where little influence from mining is expected in the stream sediments. Table 5.4 shows the Summary of observed distributions of the Cu concentrations.

Table 5.4. Cu sub-population groups and their environmental associations.

Cu group	Upper percen-tile	Cu range (ppm)	Environmental association
C	100	>912	Parad Bikk in Recsk tailings areas.
B	90	81 - 912	P. Bikk in Lahoca tailings area & after confluence.
A	77	<81	Parad Tarna.

Iron(Fe) data

A near-normal unimodal density distribution is observed on the histogram of Fe concentration data (figure 5.4). The data is divided into four groups at the quartile and mid-percentile points of the histogram in order to depict the spatial distributions of Fe concentrations in the stream sediments of the study area. The resulting groups A, B, C and D have concentration ranges of < 1.38%, 1.38-1.74%, 1.74-1.95% and > 1.95% respectively. Figure 5.4 shows the spatial distribution of Fe concentrations in the stream sediments of the area.

Iron concentrations above 1.95% are predominantly distributed in the sediments of Parad Bikk and in the sediments of Parad Tarna in those areas the stream drainage is close to geochemical alteration zones and ancient adits. Fe concentrations in the inter-quartile range (1.38-1.95%Fe) are all distributed in the stream sediments of Parad Tarna. The less than 1.38% Fe concentrations are found in the sediments of the headwaters and tributaries of Parad Tarna. Concentrations are also observed to rapidly decline to less than 1.38%Fe after the confluence. Table 5.5 shows the summary of the spatial distributions of the Fe concentrations.

Table 5.5. Fe sub-population groups and their environmental associations.

Fe group	Upper percen-tile	Fe range (%)	Environmental association
D	100	>1.95	Parad Bikk & P. Tarna in hydrothermal alteration areas
C	75	1.74 – 1.95	Parad Tarna
B	50	1.38 – 1.74	Parad Tarna
A	25	<1.38	Parad Tarna & after confluence

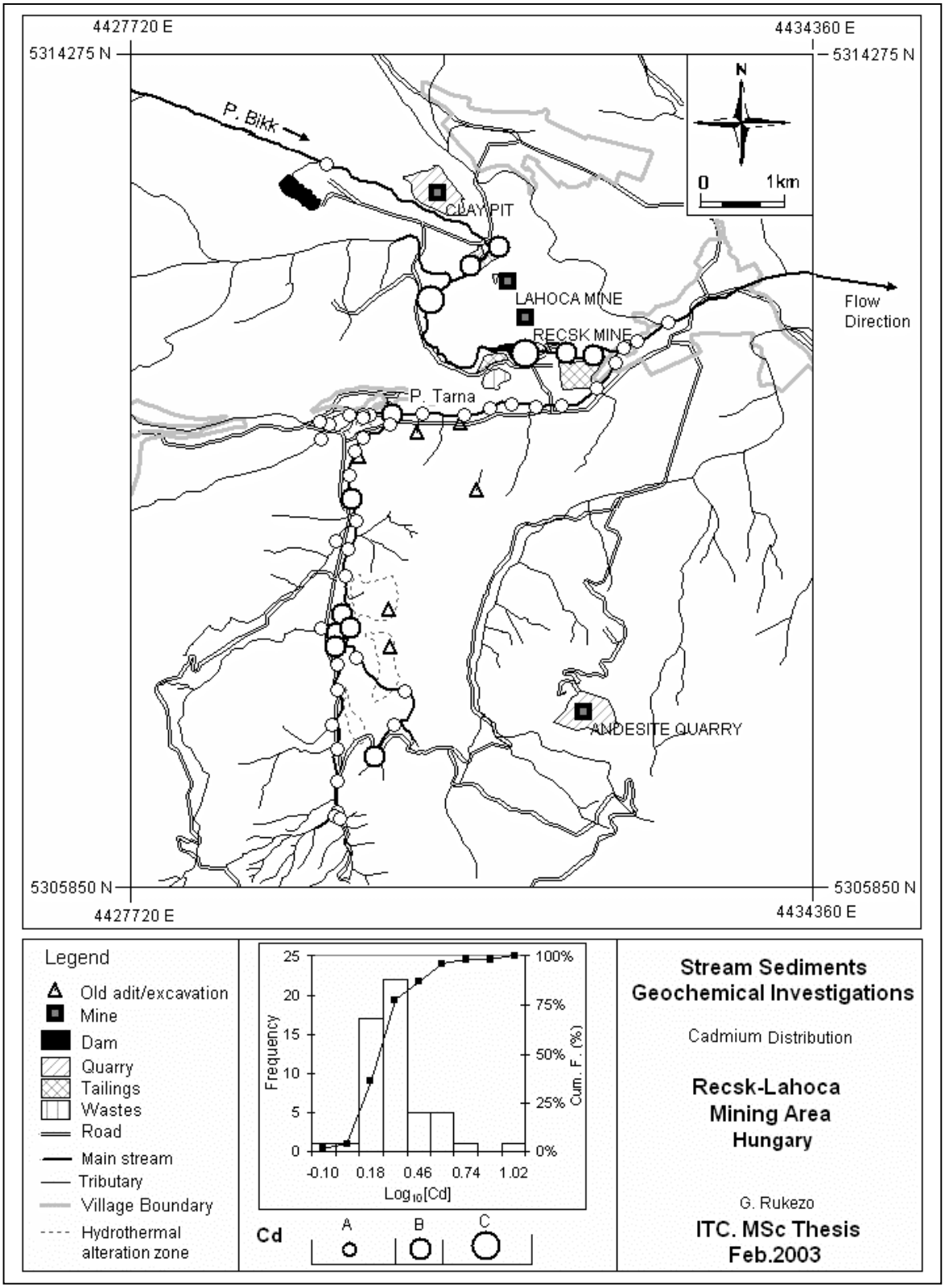

Figure 5.2. Spatial distributions of observed Cd concentrations in sediments of the streams draining the area.

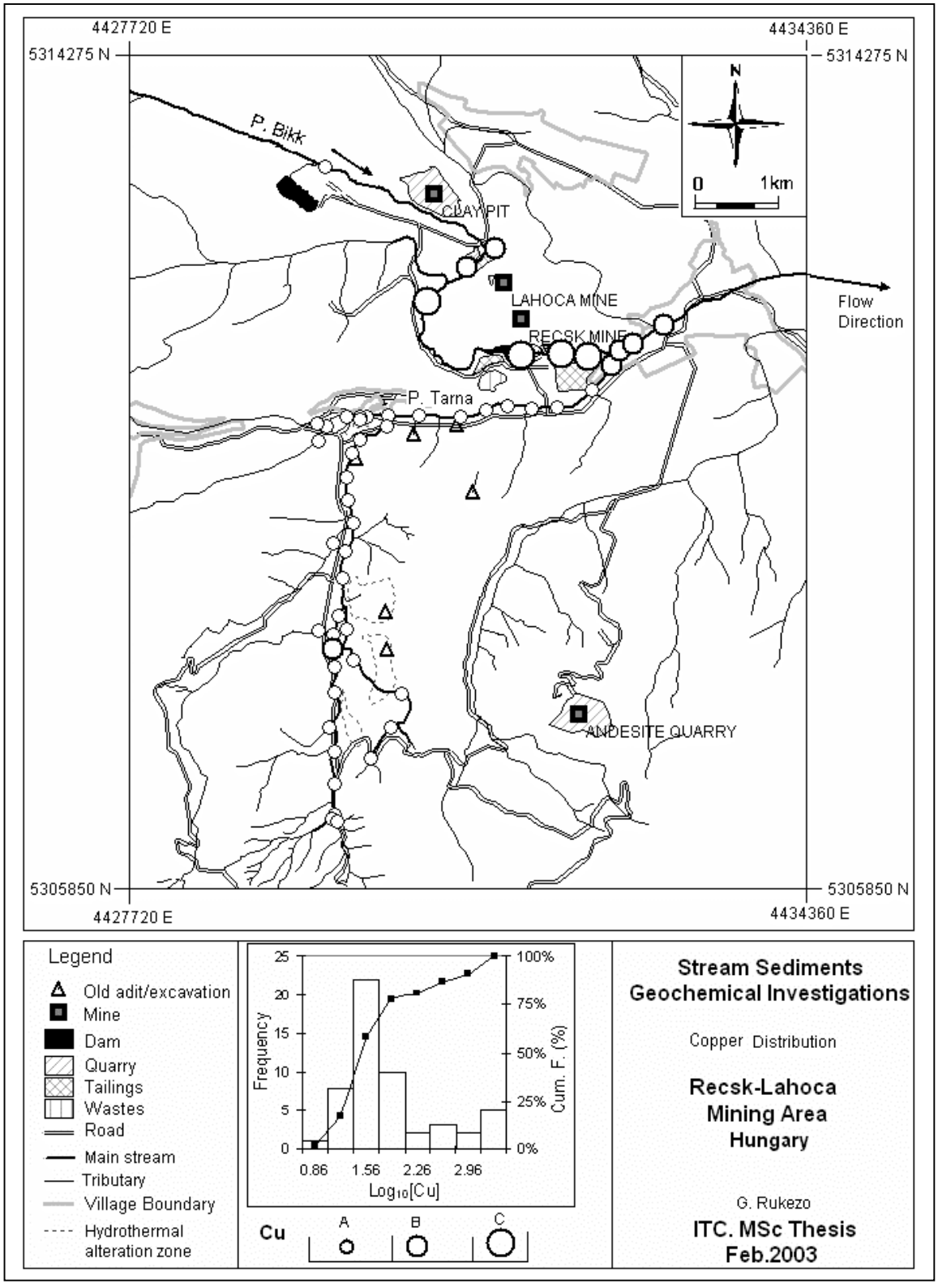

Figure 5.3. Spatial distributions of observed Cu concentrations in sediments of streams draining the area.

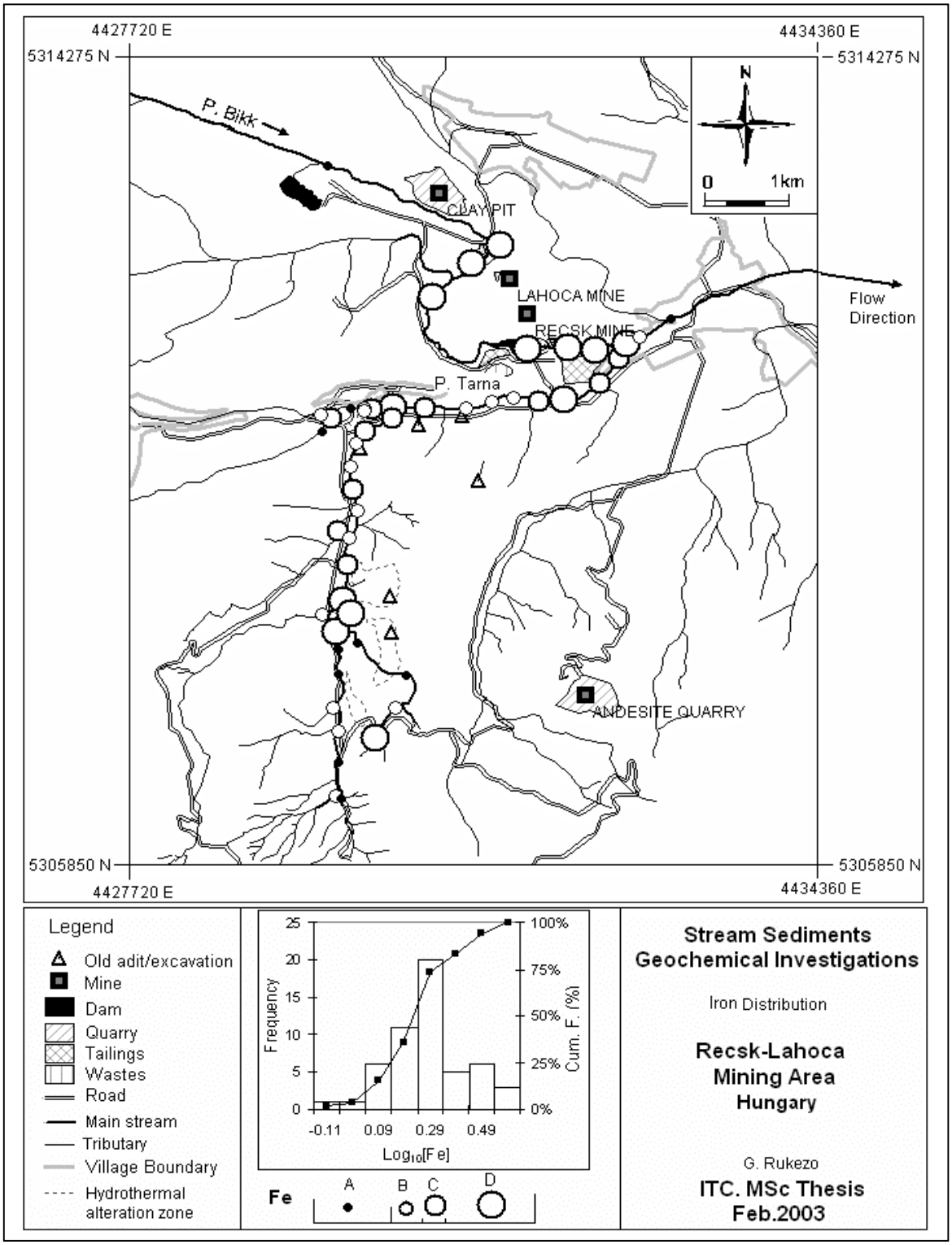

Figure 5.4. Spatial distributions of observed Fe concentrations in sediments of streams draining the area.

Manganese(Mn) data

The Mn histogram is in the form of a unimodal density distribution. The Mn data is divided into quartile classes with the corresponding Mn concentration ranges shown in table 5.6. Displayed in figure 5.5 are the spatial distributions of Mn concentrations in the stream sediments of the waters draining the area

Mn concentrations are observed to have a contrasting distribution to those of the other analysed elements. No particular pattern related to mine areas or geochemical anomaly zones is observed in the distribution of Mn concentrations above 933ppm except that most of them are observed at stream confluences. Concentrations between 562 and 933ppm are distributed in the larger part of the Parad Tarna drainage. Mn concentrations of the two lower groups below 562ppm are predominantly distributed in geochemical alteration zones. The Recsk and Lahoca mine areas are characterized by Mn concentrations below 302ppm. There is less Mn in sediments of drainages influenced by mining waste and in areas of hydrothermal alterations and ancient adits. Low Mn concentrations persist beyond the confluence of Parad Tarna and Parad Bikk. Summarised in table 5.6 are the spatial distributions of the Mn concentration groups.

Table 5.6. Mn sub-population groups and their environmental associations.

Mn group	Upper percentile	Mn range (ppm)	Environmental association
D	100	>933	Isolated locations in the streams & at confluences.
C	75	562 - 933	Parad Tarna
B	50	302 - 562	Parad Tarna mainly in hydrothermal alteration zones
A	25	<302	Parad Bikk

Hydrous Mn oxides are known to form at quite high pH values (typically > 8) unless there is bacterial mediation which can result in precipitation of Mn phases at pH values below 6-7 (Nordstrom and Alpers, 1999). The lower pH values in Parad Bikk, which drains the mine areas, result in Mn remaining in water as observed in the previous chapter. This explains the high Mn concentrations in the stream sediments of most of Parad Tarna, with higher pH values, and the lower Mn concentrations in Parad Bikk. Hydrothermal alteration areas and old mining areas are influenced by sulphide mineral oxidation and hydrolysis, which lower pH values, and as a result, Mn is not easily precipitated into stream sediments, hence low Mn concentrations in the stream sediments of drainages of these areas. Lower pH values which are not favourable for the precipitation of Mn are likely to persist downstream of the stream confluences resulting in sediments with less Mn concentrations in this area. A high pH location in Parad Tarna (pH=8) just before the confluence with Parad Bikk is characterised by sediments with Mn concentrations above 933ppm indicating that water pH controls the distribution of Ma in the area.

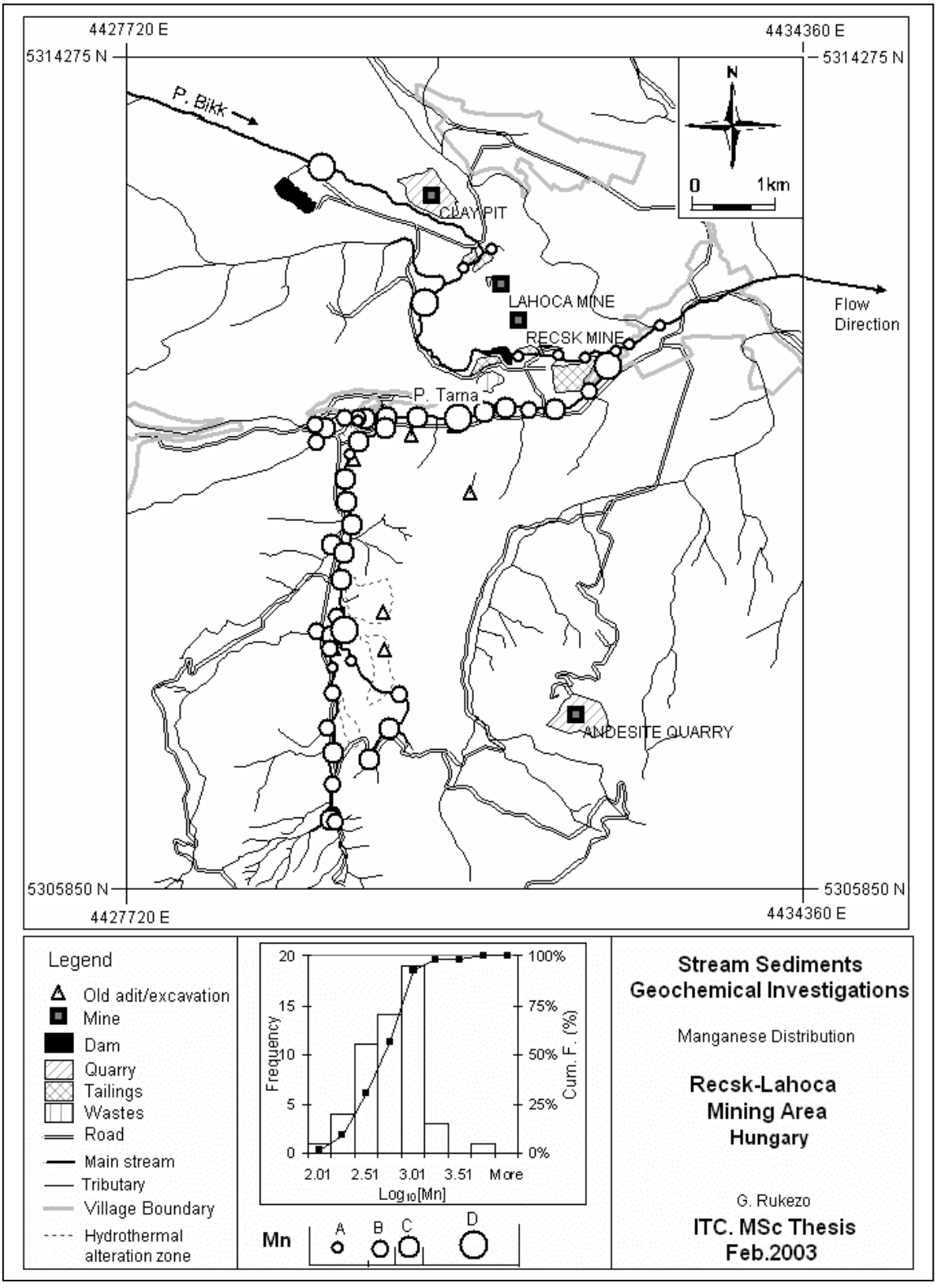

Figure 5.5. Spatial distributions of observed Mn concentrations in sediments of streams draining the area.

Nickel(Ni) data

The original $\log_{10}$-transformed Ni concentration data was characterized by high kurtosis and negative skew due to the presence of an extremely low Ni concentration on one of the sample locations, which, as a result, invalidated the univariate statistical procedures. The histogram of Ni data without the outlier value is in the form of unimodal density distribution with strong positive skew (figure 5.6). Three population groups (table 5.7) were determined using the 83 and 92 cumulative percentiles, which are equivalent to concentrations of 12.59 and 22.39ppm. Displayed in figure 5.6 are the spatial distributions of Ni concentrations.

Ni concentrations above the upper threshold value of 22.39ppm do not show any strong relation to the environmental signatures in the area besides their being distributed at confluences and stream headwaters. Population B is distributed only in the drainages of Parad Tarna and its tributaries. Most of the concentrations are in stream confluences. The rest of the concentrations below 12.59ppm, which constitute the largest population, are distributed in most of the drainage channels in the area. The low Ni concentrations in sediments of the drainages around the tailings indicate the absence of favourable precipitation conditions for Ni. Table 5.7 shows the Ni population groups and their spatial distributions.

Table 5.7. Ni sub-population groups and their environmental associations.

Ni group	Upper percentile	Ni range (ppm)	Environmental association
C	100	>22.39	Isolated locations in the streams (confluences).
B	75	12.59 – 22.39	Parad Tarna.
A	83	<12.59	Parad Tarna & Parad Bikk.

Lead(Pb) data

A near-normal unimodal distribution density is observed on the Pb histogram (Figure 5.7). The quartile classes are used to depict the spatial distributions of Pb concentrations in the stream sediments of the area (table 5.8).

Table 5.8. Pb sub-population groups and their environmental associations.

Pb group	Upper percentile	Pb range (ppm)	Environmental association
D	100	>45	Recsk dumps & P. Tarna hydrothermal alteration zones.
C	75	28 - 45	Parad Tarna.
B	50	17 - 28	Parad Tarna, Recsk & Lahoca dumps.
A	25	<17	Stream headwaters & tributaries.

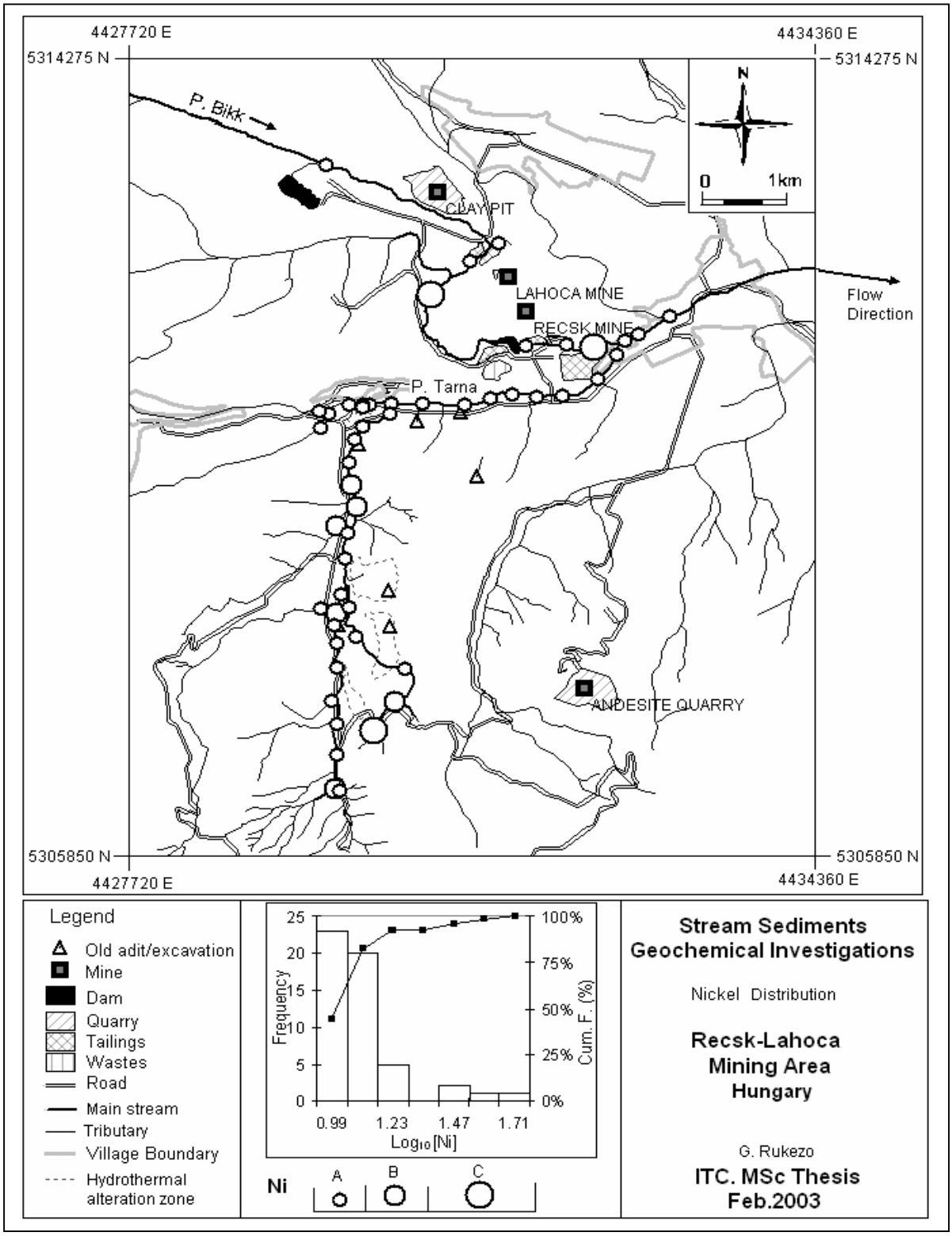

Figure 5.6. Spatial distributions of observed Ni concentrations in sediments of the streams draining the area.

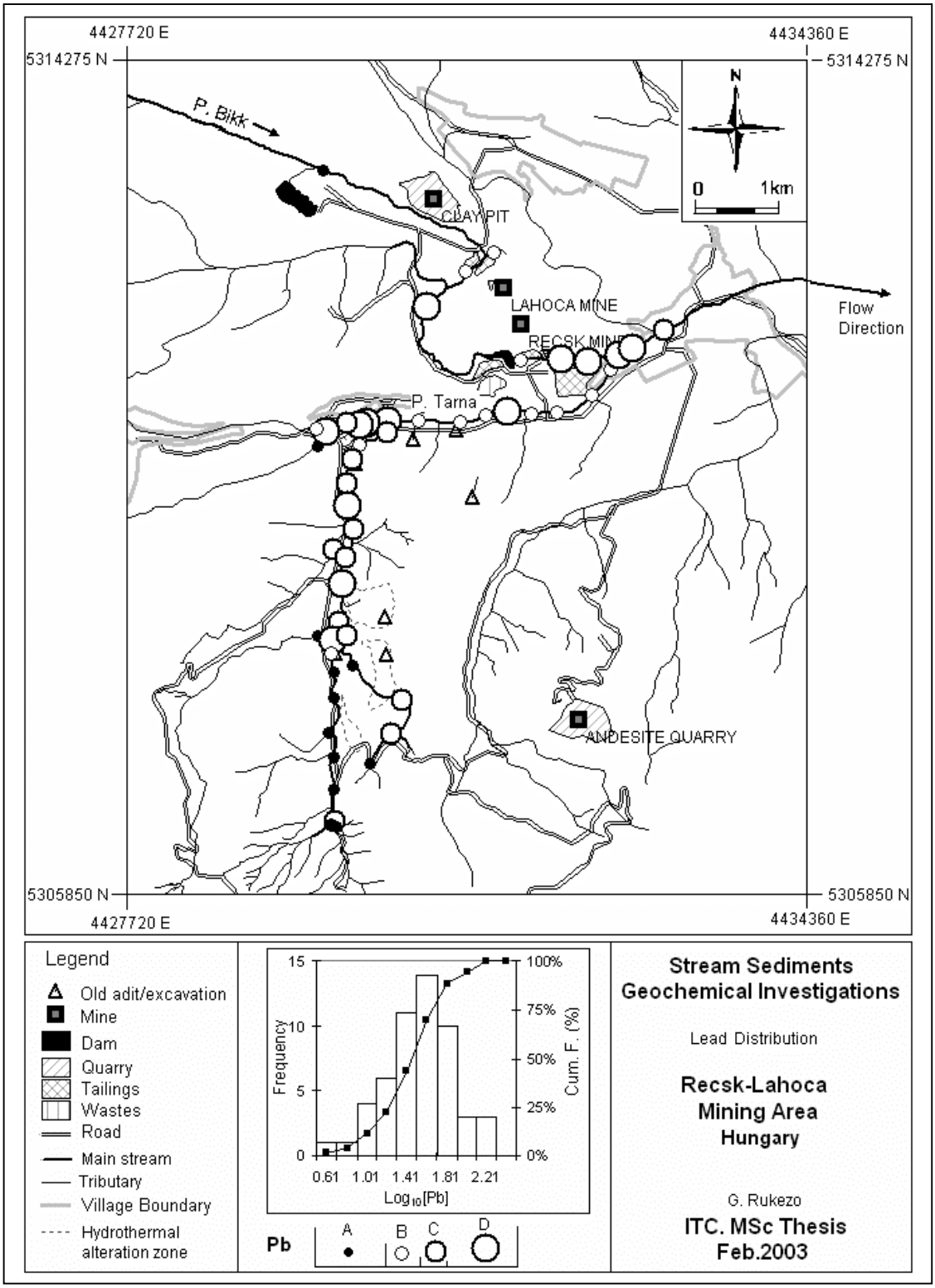

Figure 5.7. Spatial distributions of observed Pb concentrations in sediments of the streams draining the area.

Lead concentrations of above 45ppm are mainly associated with stream sediments in drainage areas around Recsk tailings piles, and in hydrothermal alteration zones (figure 5.7). Most of the concentrations in the inter-quartile range (17 – 45ppm) are distributed in Parad Tarna and they are most likely linked to ancient adits and alteration zones. The rest of the sediments with concentrations below 17ppm are distributed on the headwaters of the streams, with most of them related to the headwater drainages of Parad Tarna. Table 5.8 summarises the spatial distributions of Pb concentrations.

Antimony(Sb) data

Concentrations of antimony are very low in the stream sediments of the area. Except for one outlier with Sb concentrations of 19.2ppm, the other concentrations range from 0 to 1.6ppm. A strong positive skew is observed on the histogram indicating that the higher values are anomalous (figure 5.8). The 24 and 90 cumulative percentiles, which are equivalent to Sb concentrations of 0.2 and 1.38ppm, are used to determine the population groups used in the spatial distributions (table 5.9). Displayed in figure 5.8 are the spatial distributions of the Sb concentrations.

The more than 1.58ppm Sb concentrations are distributed in Parad Bikk intermittently with the less than 0.2ppm concentrations, which indicate abrupt changes of stream properties which attenuate Sb in the sediments. Population group B ranging between 0.2 and 1.58ppm is mainly distributed in Parad Tarna and is also intermittently distributed with the less than 0.2ppm concentrations. Table 5.9 summarises the population groups and their environmental associations.

Table 5.9. Sb sub-population groups and their environmental associations.

Sb group	Upper percentile	Sb range (ppm)	Environmental association
C	100	>1.58	Parad Bikk
B	90	0.2 – 1.58	Parad Tarna
A	24	<0.2	Parad Tarna & P. Bikk in Recsk & Lahoca dumps.

Antimony is likely to remain hydrolysed in solution in low pH drainages like Parad Bikk in the Recsk and Lahoca tailings areas, which result in less Sb concentrations in the stream sediments of these areas.

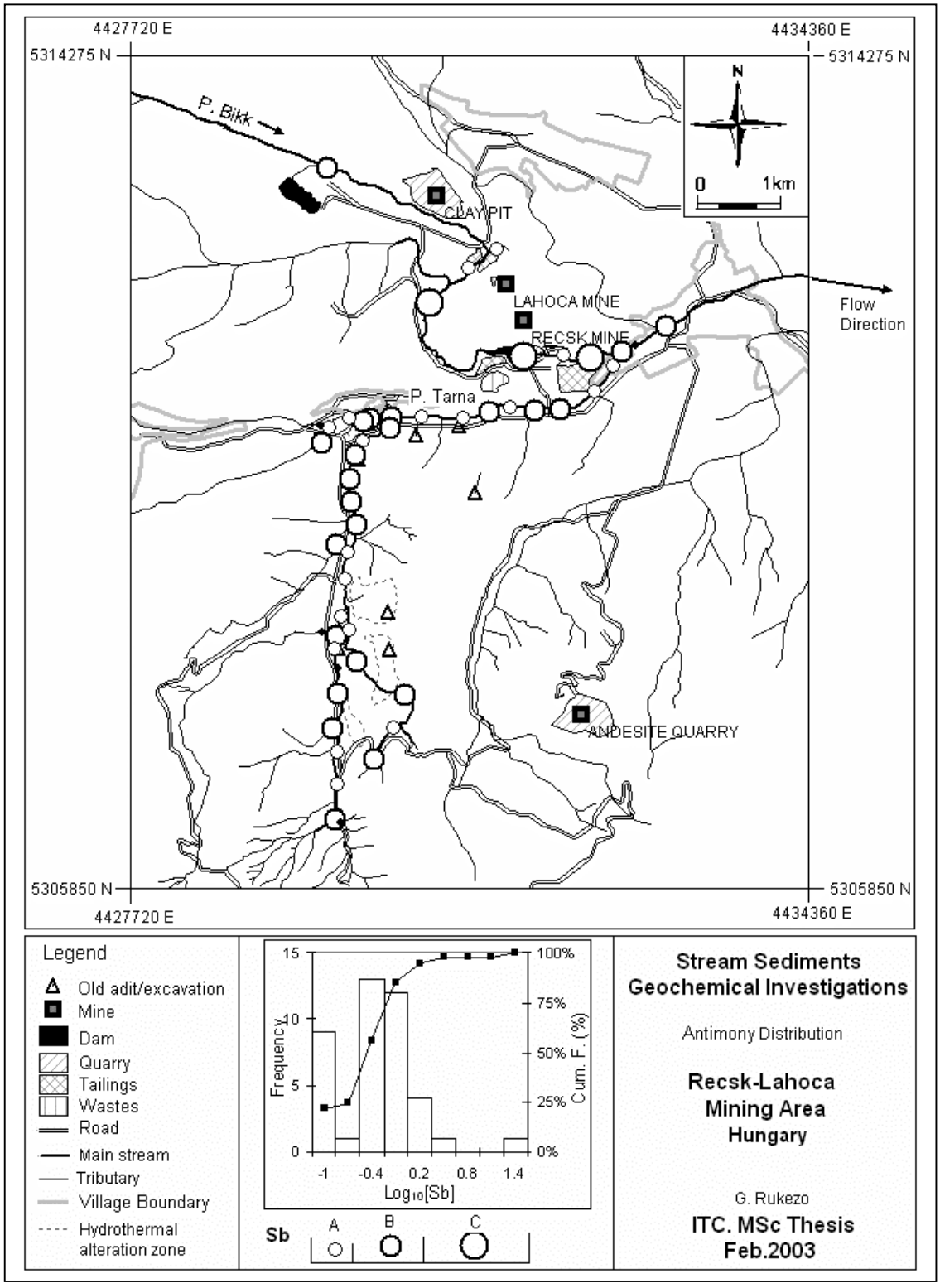

Figure 5.8. Spatial distributions of observed Sb concentrations in sediments of streams draining the area.

Zinc(Zn) data

Zn concentrations were classified using 34 and 87 cumulative percentiles, which are equivalent to concentrations of 60 and 120 ppm. Concentration ranges of the Zn groups are shown in table 5.10. Figure 5.9 displays the spatial distributions of Zn concentrations.

Concentrations of above 120ppm are mainly distributed in Parad Bikk. Two Zn concentrations above 120ppm in the sediments of Parad Tarna are distributed in parts of the stream draining argillised areas with precipitates of iron hydroxides. Iron is likely to have co-precipitated Zn into the sediments in these areas. Zn concentrations between 60 and 120ppm are predominantly distributed in Parad Tarna while concentrations below 60ppm are mainly distributed on the headwaters of Parad Tarna. Summary of the Zn groups and their spatial distributions are shown in table 5.10.

Table 5.10. Zn sub-population groups and their environmental associations.

Zn group	Upper percentile	Zn range (ppm)	Environmental association
C	100	>120	Parad Bikk & parts of P. Tarna
B	87	60 - 120	Mainly Parad Tarna
A	34	<60	Headwaters of Parad Tarna

5.1.3. Summary of element Data

The distributions of element concentrations in the stream sediments are observed to be strongly related to specific environmental features like hydrothermal alteration zones, mine tailings and lithologies drained by the streams in the area. The elements are similarly distributed, which suggests that there is association of elements in the stream sediments. Stream profile graphs are used to further investigate the observed influence of the environmental features on the element concentrations in the stream sediments while multivariate data analysis methods are used to further understand the inter-element relationships indicated in the univariate data analysis.

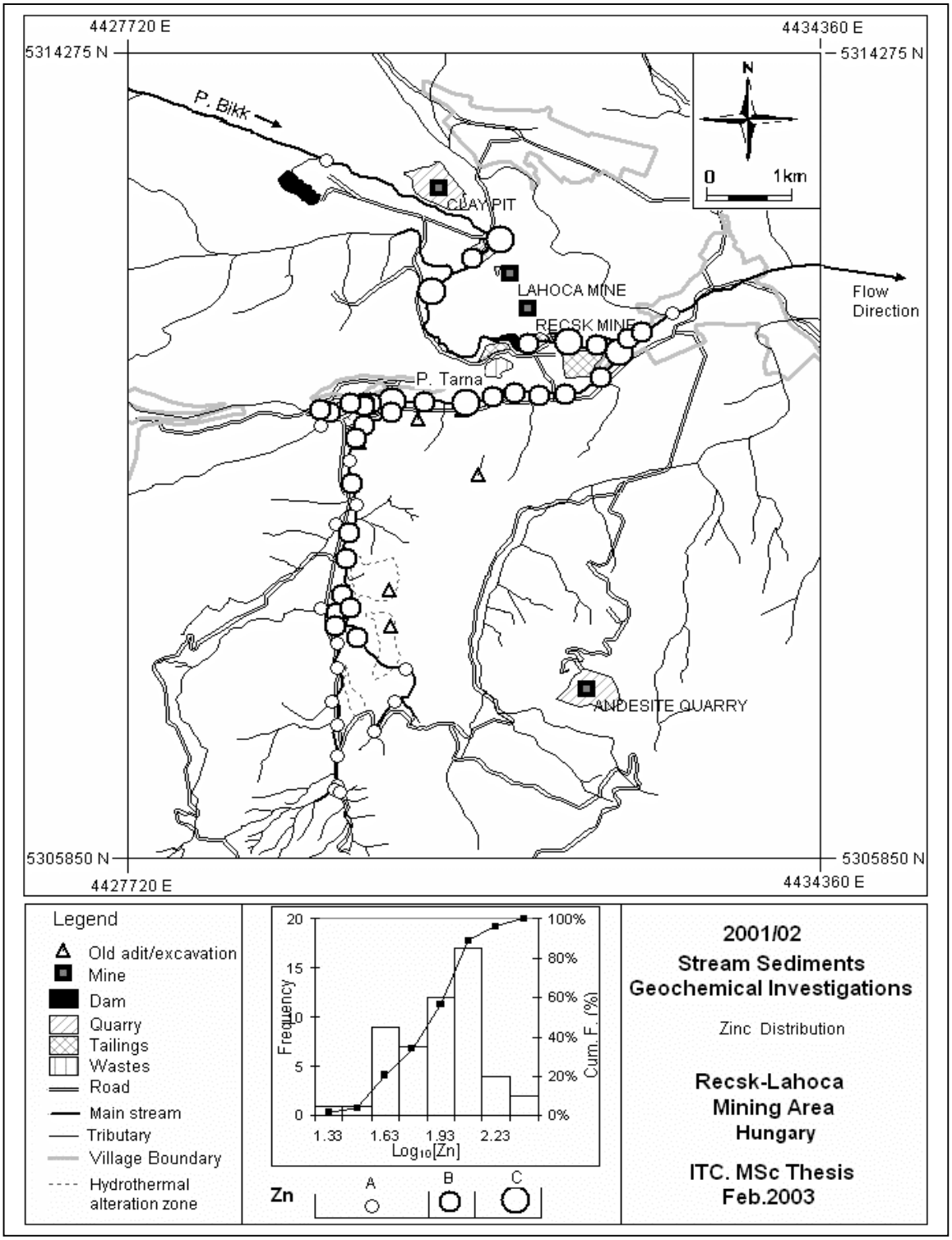

Figure 5.9. Spatial distributions of observed Zn concentrations in sediments of streams draining the area.

5.2. Metal concentrations along stream profiles

Stream sediments geochemical data was plotted against distance along the stream profiles in order to determine changes in metal concentrations from upstream downwards. The sample locations on the uppermost parts of the streams were taken as points of origin. Metal concentrations on sample locations downstream of the points of origin were plotted against the distances of the sample locations from the point of origin. Figure 5.10A to I shows metal concentrations along stream profiles. Some of the element concentrations with high variations were plotted on a semi-logarithmic scale. Index bars highlighting areas of interest along the stream profile are included as footnotes on the graphs of the two streams in order to compare element concentrations with environmental features. The abbreviations used to describe the environmental features are: H = hydrothermal alteration zone; TC = tributary confluence; H/A = hydrothermal alteration/ancient adit area; C = confluence of Parad Tarna and Parad Bikk; L = Lahoca tailings piles area; W52 = Sample location with extreme acidic waters; R = Recsk tailings piles area.

Element concentrations are generally higher in Parad Bikk than in Parad Tarna when graphs of the same element are compared. The environmental features indicated on the footnote bars have significant influence on the concentrations of the elements as indicated by either a rise or a fall in element concentrations, especially in the graphs of element concentrations along Parad Bikk. High variations observed on the graphs of sediments concentrations in Parad Bikk are mainly due to the influence of the tailings piles scattered along the stream profile. Element concentrations in the stream sediments of Parad Tarna are more evenly distributed because most of them are a result of the natural weathering of the bedrock.

In the area Parad Bikk drains floatation tailings piles, concentrations of As, Cd, Cu, Fe, Pb, Sb and Zn increase by as much as 10 times their concentrations in Parad Tarna or in those areas of Parad Bikk which are not influenced by the floatation tailings piles. This clearly indicates that the floatation tailings piles are the main sources of metal concentrations in sediments in this part of the stream. The similarities in the trends of the graphs of these elements are also indicative of the mineralization in the sulphidised andesite host rock in the mine areas. Except for Cd, all the other elements are the main constituents of the sulphide minerals found in the ore deposits of the area. Whilst the concentrations of these elements generally increase between the Recsk and Lahoca tailings piles, a negative kink indicating a decrease in concentration is observed in the profiles of As, Cu, Pb and Sb on sample location W52 with the highly acidic waters (figure 5.10). The stream profile graph for Cu concentration in water, displayed in figure 4.15 in chapter 4, shows a sharp increase in concentration on the same location. Asernic, Pb and Sb concentrations in water are also extremely high on this location. This revelation leads to the conclusion that the metals are hydrolysed into solution, and precipitation into stream sediments is minimal on this location due to the highly acidic waters.

The behaviours of Ni and Mn are opposite to those of the other elements. Their concentrations are lower in the area the stream drains the floatation tailings piles. The lower concentrations are mainly due to the slightly acidic conditions of the water in this part of the stream. Manganese is a highly mobile element, which precipitate at pH values of more than 8 under normal conditions and therefore most of it remain dissolved in water in this part of the stream. The stream profile graph for Mn con-

centration in water, displayed in figure 4.15 in the previous chapter, shows an increase in Mn in these tailings areas, which confirms that most of the Mn remains dissolved in water rather that precipitating into stream sediments.

A sample location immediately after the confluence between Parad Bikk and one of its tributaries (TC) is characterized by an increase in Mn, Ni, Pb and Sb. The tributary is likely to be draining bedrock with high content of minerals of these elements, or pH is elevated by the mixing waters resulting in precipitation of metals in the sediments.

In Parad Tarna, whilst element concentrations are more evenly distributed along the stream profile than in Parad Bikk, variations are observable, especially in the areas corresponding to the environmental features indicated on the footnote bar. Most of the element concentrations decrease in the hydrothermal alteration zone (H) followed by an increase downstream of this zone. This again is the opposite of what is observed in the stream profile graphs of element concentrations in water in the same areas (figure 4.15). The slightly lower pH in the hydrothermal alteration zone facilitates dissolution of elements more than precipitation. On the downstream side of the hydrothermal alteration zone, the rising pH facilitate precipitation of the metals, hence the increase in metal concentrations in the sediments. The sediments of the stream in the old adit area (H/A) are characterised by increases in element concentrations, which could be a result of precipitation of metals from the acidic waters oozing out of the old adits at the interface with surface stream waters.

After the confluence of Parad Tarna and Parad Bikk, element concentrations rapidly fall back to the more or less even concentrations observed in Parad Tarna. This indicates that dilution is strong from Parad Tarna. The other possibility is dilution from flood sediments since the stream sediment samples from the downstream side of the confluence of the two streams were collected a day after heavy rains and flooding.

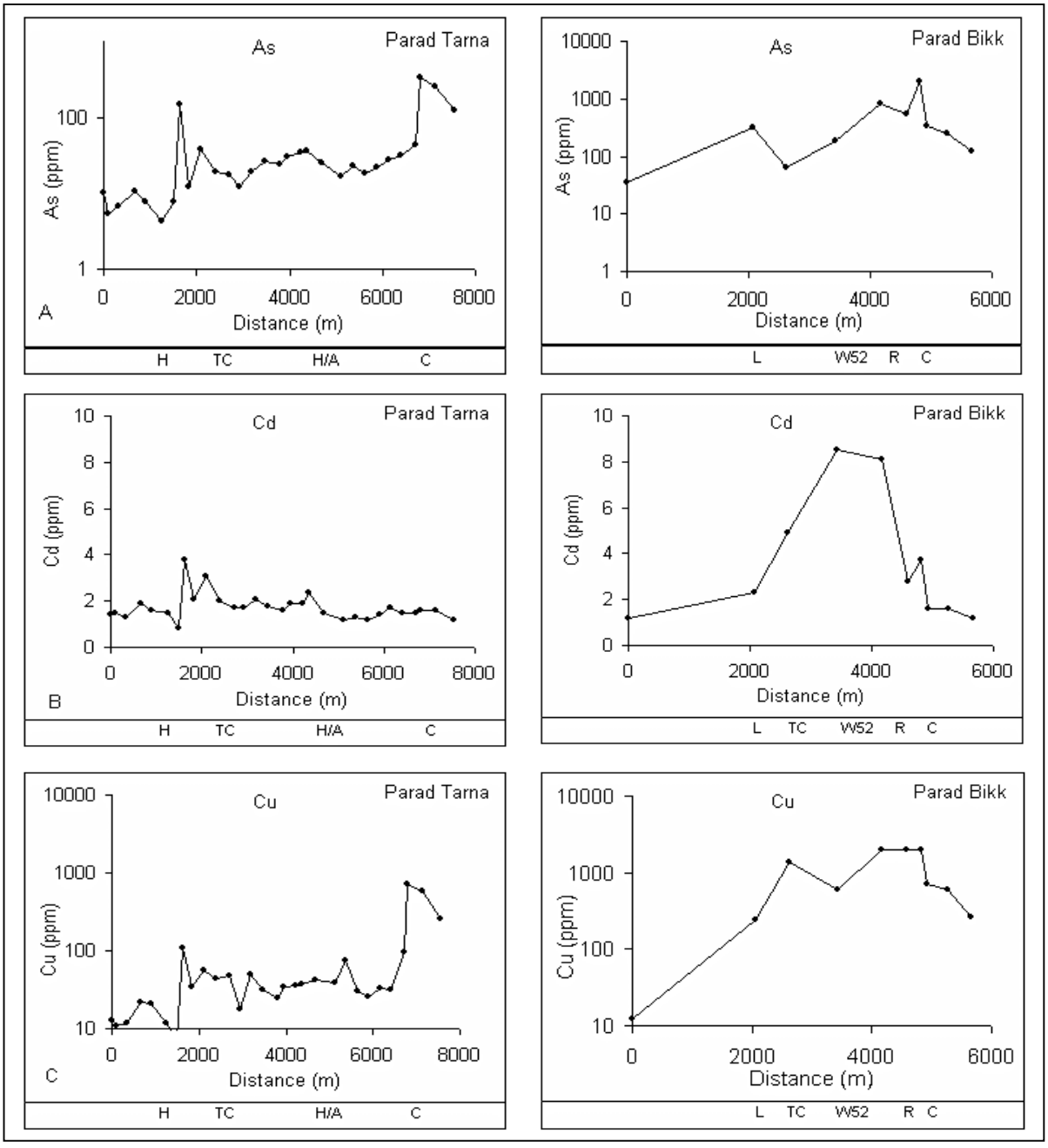

Figure 5.10. Graphs of element concentrations against distance along stream profiles. Row A = As; B = Cd; C = Cu; H = hydrothermal alteration zone; TC = tributary confluence with P. Tarna/P. Bikk; H/A = hydrothermal alteration/ancient adit area; C = confluence of P. Tarna and P. Bikk; L = Lahoca tailings area; W52 = sample location with extreme acidic waters; R = Recsk tailings piles area.

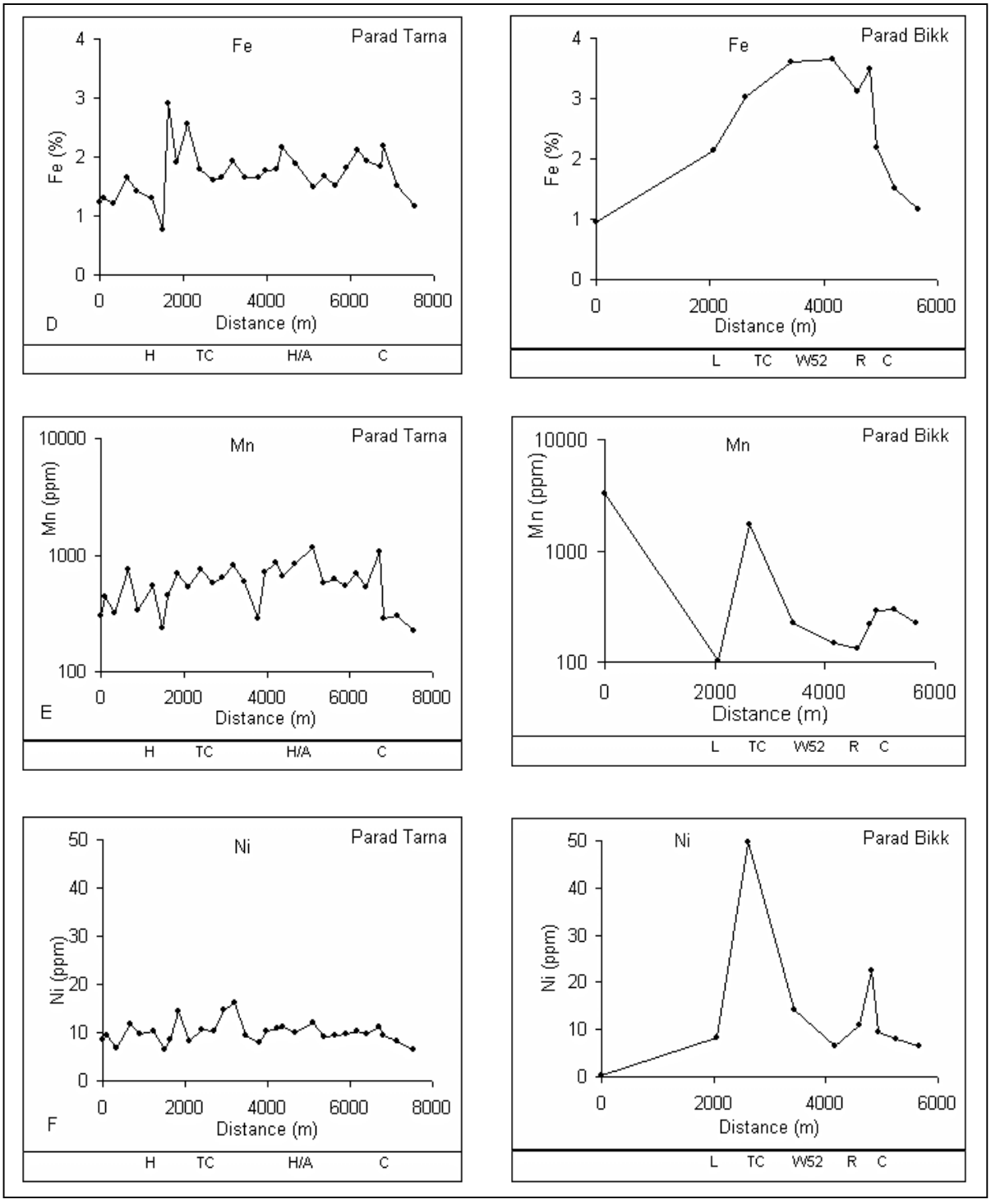

Figure 5.10 (continued). Graphs of element concentrations against distance along stream profiles. Row D = Fe; E = Mn; F = Ni; H = hydrothermal alteration zone; TC = tributary confluence with P. Tarna; H/A = hydrothermal alteration/ancient adit area; C = confluence of P. Tarna and P. Bikk; L = Lahoca tailings area; W52 = sample location with extreme acidic waters; R = Recsk tailings piles area.

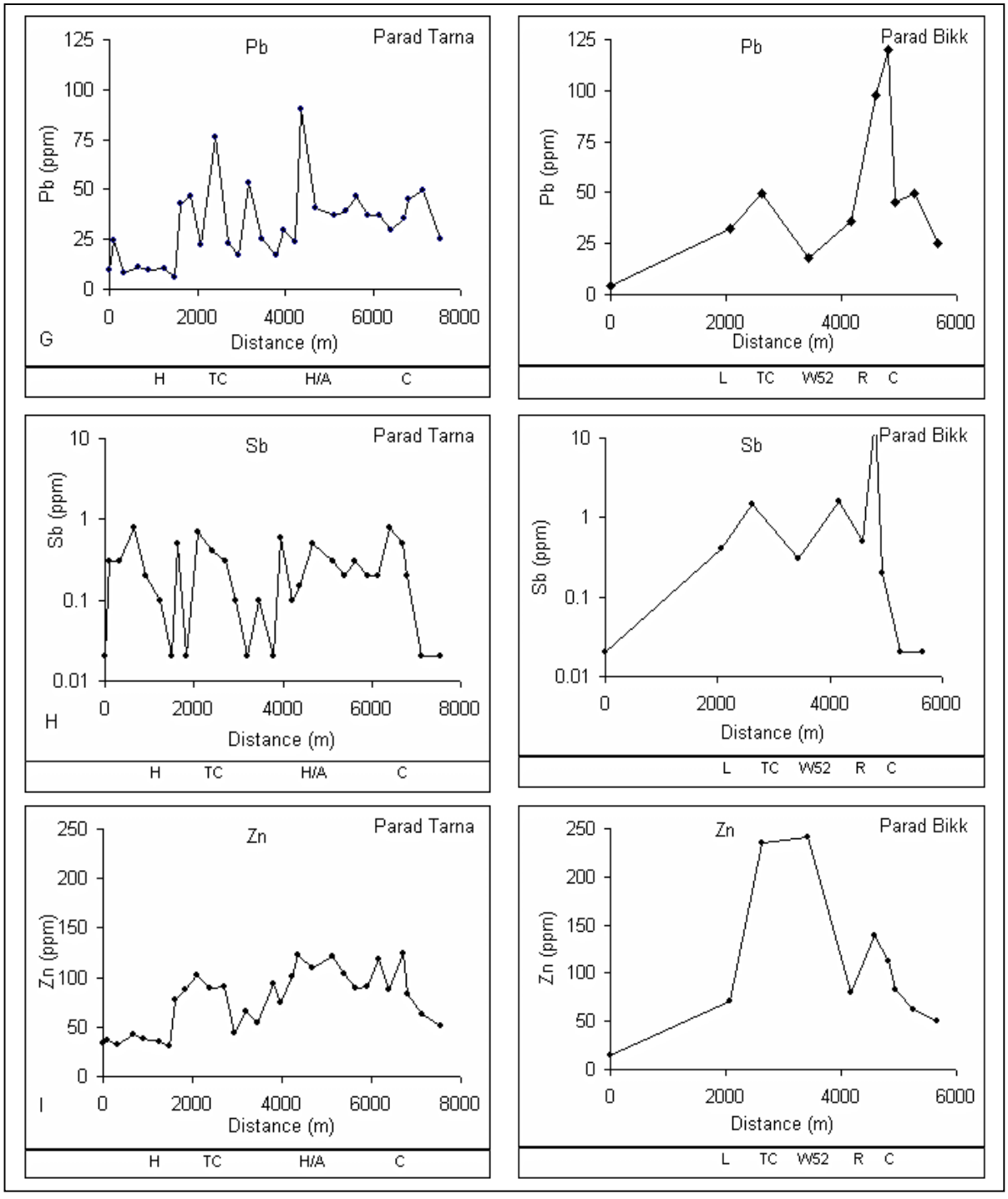

Figure 5.10 (continued). Graphs of element concentrations against distance along stream profiles. Row G = Pb; H = Sb; I = Zn; H = hydrothermal alteration zone; TC = tributary confluence with P. Tarna; H/A = hydrothermal alteration/ancient adit area; C = confluence of P. Tarna and P. Bikk; L = Lahoca tailings area; W52 = sample location with extreme acidic waters; R = Recsk tailings piles area.

5.3. Multivariate Data Analysis

5.3.1. Correlation Coefficient Analysis

The Pearson (or product moment) correlation coefficient was used in estimating the degree of interrelationship between stream sediments element variables. Table 5.11 shows the Pearson correlation matrix for the measured elements.

Table 5.11. Correlation coefficient(r) matrix for stream sediments data.

	As	Cd	Cu	Fe	Mn	Ni	Pb	Sb	Zn
As	1.00								
Cd	0.53	1.00							
Cu	0.82	0.72	1.00						
Fe	0.66	0.85	0.75	1.00					
Mn	-0.27	-0.04	-0.17	-0.11	1.00				
Ni	0.25	0.39	0.38	0.45	0.18	1.00			
Pb	0.53	0.29	0.49	0.52	-0.13	0.26	1.00		
Sb	0.84	0.29	0.56	0.46	-0.13	0.26	0.41	1.00	
Zn	0.27	0.42	0.43	0.64	0.05	0.50	0.50	0.17	1.00

Iron is strongly correlated with As, Cd, Cu and Zn and moderately correlated with Pb. The strong correlation could be due to the scavenging effect of iron on the more mobile elements. Pb is less co-precipitated than the other elements. Manganese shows weak negative correlations with As, Cd, Cu, Fe, Pb and Sb, and weak positive correlations with Ni and Zn. This indicates that Mn does not play a major role in element scavenging. As explained in the earlier uni-variate section on Manganese above, hydrous Mn oxides precipitate at higher pH values than Fe, which result in Fe being the sole scavenging element in slightly acidic waters giving rise to strong correlation of Fe with the other elements and negative correlation for Mn with Fe and the other elements scavenged by Fe. The significant Zn-Cu and Zn-Pb correlations are most likely caused by occurrences of minerals of these elements in the sulphidised andesite.

5.3.2. Principal Components Analysis (PCA).

Principal components analysis is used to separate the element associations inherent in the structure of the correlation matrix into a number of groups of elements that together account for the greater part of the observed variability of the original data, with the aim of representing the large numbers of elements in the original data by a smaller number of factors, each of which is a linear function of the element concentrations, thus giving greater efficiency in terms of information compression over the original data, and be able to interpret it (Howarth., 1983).

From the 9 elements analysed, 9 principal component loadings are observed (table 5.12). According to Howarth, it can be reasonably assumed that 5% of the total variability of the data is due to random errors inherent in the data. The first 6 of the 9 principal component loadings (PCL), which account for 95.72% of the total variability, are therefore due to patterns in the element associations. Emphasis on

element associations is put on the first three loadings, which account for more than 75% of the total variability.

Table 5.12. Principal Component Loadings (PCL) for stream sediments geochemical data.

	PC1	PC2	PC3	PC4	PC5	PC6	PC7	PC8	PC9
As	0.84	-0.43	0.23	-0.03	0.02	-0.04	-0.07	-0.13	0.16
Cd	0.77	0.18	-0.21	-0.50	0.12	0.10	0.16	0.14	0.07
Cu	0.89	-0.12	0.00	-0.19	0.05	0.07	-0.38	0.05	-0.09
Fe	0.91	0.15	-0.20	-0.16	0.11	-0.06	0.18	-0.18	-0.11
Mn	-0.15	0.67	0.60	-0.09	0.39	-0.01	-0.03	-0.02	0.01
Ni	0.54	0.55	0.21	0.06	-0.57	0.21	0.01	-0.02	0.01
Pb	0.66	-0.05	-0.08	0.61	0.28	0.31	0.07	0.04	0.00
Sb	0.66	-0.42	0.53	0.10	-0.11	-0.20	0.17	0.11	-0.07
Zn	0.63	0.50	-0.27	0.34	-0.01	-0.39	-0.08	0.05	0.04
% of Var	50.12	15.98	9.99	9.19	6.55	3.88	2.71	0.96	0.62
Cum. % of Variance	50.12	66.10	76.10	85.29	91.84	95.72	98.43	99.38	100.00

The first principal component (PC1) is very strong and it explains about 50.12% of the total variance. High positive loadings for As, Cd, Cu, Fe, Ni, Pb, Sb and Zn are observed, and Fe has the highest positive loading. The high positive loadings reflect co-precipitation processes that take place in the drainage waters due to the scavenging effect of Fe. Scavenging is higher on As, Cd and Cu than on Ni, Pb and Zn as indicated by the higher loadings for the former. Manganese is negatively loaded indicating that it is slightly antipathetic with the other elements, which depicts less scavenging effect of Mn than Fe on the other elements. The antipathetic relationship between Mn and the other elements further indicates different precipitating environments for these elements. All the other elements are co-precipitated with Fe at lower pH and Mn remain in solution. Because this principal component loading explains over 50% of the variance, it follows that most of the stream sediments are a result of precipitation from stream waters than mechanical weathering of the bedrock. It therefore follows that a lot of metal is leached into solution in the area but due to scavenging by Fe, most of those leached sediments are attenuated into stream sediments.

The second principal component explains about 15.98% of the total variability. High positive loadings are observed on Mn, Ni and Zn and negative loadings are observed on As, Cu, and Sb. Iron and Cd have weak positive loadings while Pb is almost not correlated with the other elements. The element associations probably reflect variations in mineral associations of these elements in the primary andesite rock they are leached from. The Cu-As-Sb association probably reflects sulphidised parts of the andesite where Cu-As association is known to be present in the form of Enargite and luzonite mineralisation. The antipathetic behaviour reflected by Mn-Ni-Zn and As-Cu-Sb element associations depicts that rocks enriched in As, Cu and Sb are depleted in Mn, Ni and Zn. The weak loadings for Fe, Cd and Pb reflect that the occurrence of the two elements is neither influenced by the Mn-Ni-Zn or As-Cu-Sb element associations. The variations in the element-mineral associations of the source rock are reflected in the stream sediments through leaching of elements or by mechanical weathering of the

rocks. Plotting the element concentrations of these associations can reveal more information on this variability.

PC3 explains about 9.99% of the total variability. An antipathetic behaviour is also observe between the negatively loaded Cd, Fe and Zn and the positively loaded As, Mn, Sb and Ni. Loadings of zero for Cu and –0.5 for Pb indicate little to no variability for these elements in this principal component. PC3 is possibly due to leaching of elements from parent rocks enriched in Cd, Fe and Zn and depleted in As, Mn, Sb and Ni or vise-versa. Manganese and Sb have much higher loadings depicting that the two have much higher association than their association with As and Ni. Copper and Pb are depleted in both situations resulting in little to no correlation, which suggests that these mineral associations are likely to occur in non mineralized parts of the andesite whereas those of PC2 are more likely in the mineralized parts of the andesite.

The variations explained by the PCs can be spatially outlined by calculating and mapping the principal component scores. In this way, the spatial distributions of the geochemical processes attenuating the elements into the stream sediments of the waters draining the area can be fully explained and visualised. The PCs are calculated according to the formula (by George and Bonham-Carter, 1989):

$$S_{ci} = \sum_{j=1}^{n} l_{cj} z_{ij} \quad \text{for } i = 1, 2, \ldots, n \text{ samples}$$

where S_{ci} = score for sample i on component c; l_{cj} = loading on element j on component c; Z_{ij} = concentration of element j for sample i.

PC1 Scores

The scores which range from -1.3 to 4.3 were directly plotted onto a point map which was overlaid with the base map to determine the spatial relationships of the scores with other environmental features of the area. PC1 scores were enhanced by stretching the representation scale within the limits of the score range using ILWIS GIS software. Displayed in figure 5.11 are the spatial distributions of the scores from PC1 analysis.

High scores, which are predominantly distributed in Parad Bikk in the Recsk tailings area, are indicative of areas characterised by the strong association of Fe, As, Cd, Cu, Ni, Pb, Sb and Zn. These are the areas where co-precipitation due to scavenging effect of Fe is prevalent. The drainage on the Lahoca tailings area and the downstream side of the tailings is also characterised by this element association, depicting that scavenging of elements is prevalent in mine areas. Drainages in mine areas are characterised by acidic waters which hydrolyse minerals of these elements into solution. Because of the high solubilities of the elements, their precipitation is only achieved through co-precipitation by ferric iron, which precipitates at low pH due to its low solubility. Manganese, which is found to be antipathetic to the Fe and other elements association, is likely to be in solution in these acidic areas of the drainage with high scores. Drainage parts with low and negative scores are characterised by higher pH waters favourable for the precipitation of Mn. This distribution is found to be similar when compared with Mn distributions displayed in figure 5.5, which shows lowest Mn concentrations in lower pH waters draining the Recsk and Lahoca tailings areas and highest concentrations in the neutral to

slightly alkaline waters. The Fe-elements association rapidly disappears after the confluence of Parad Tarna and Parad Bikk due to higher pH waters from Parad Tarna.

PC2 Scores

In order to spatially portray the distributions of the element associations derived from the positive and negative loadings of PC2, the scores were sliced into two groups of the negatively loaded elements and the positively loaded elements followed by stretching the representation scale (in ILWIS GIS software) in order to enhance those areas of increased geochemical signatures of the element associations. Displayed in figure 5.12 are the spatial distributions of the scores for the two element associations. The As-Cu-Sb element association is distributed mainly in Parad Bikk between the Recsk and Lahoca mine tailings area. The highest geochemical signature of this association is observed near the Recsk east tailings pile. Copper-bearing minerals are the main mineralisation of the ore bodies mined at these mines giving rise to tailings piles rich in copper. Arsenic and Sb are also found in association with Cu sulphide minerals like enargite. Stream sediments of these areas are therefore characterised by variability of this association inherent in the mineralization of the andesite in the area. This element association is also observed near ancient adits and in hydrothermal alteration zones in Parad Tarna where anomalies of Cu have been detected. The Mn-Ni-Zn association is observed in the other parts of Parad Tarna suggesting that this association is predominant in stream sediments of waters draining non-mineralised andesite rock, and also in drainages with elevated pH values. The highest geochemical signature for the Mn-Ni-Zn observed downstream of Lahoca tailings is most likely a result of the tributary which increases pH on mixing with Parad Bikk waters resulting in the precipitation of elements of the Mn-Ni-Zn association. The associations compare very well with element distributions displayed in the previous sections, especially that of Zn.

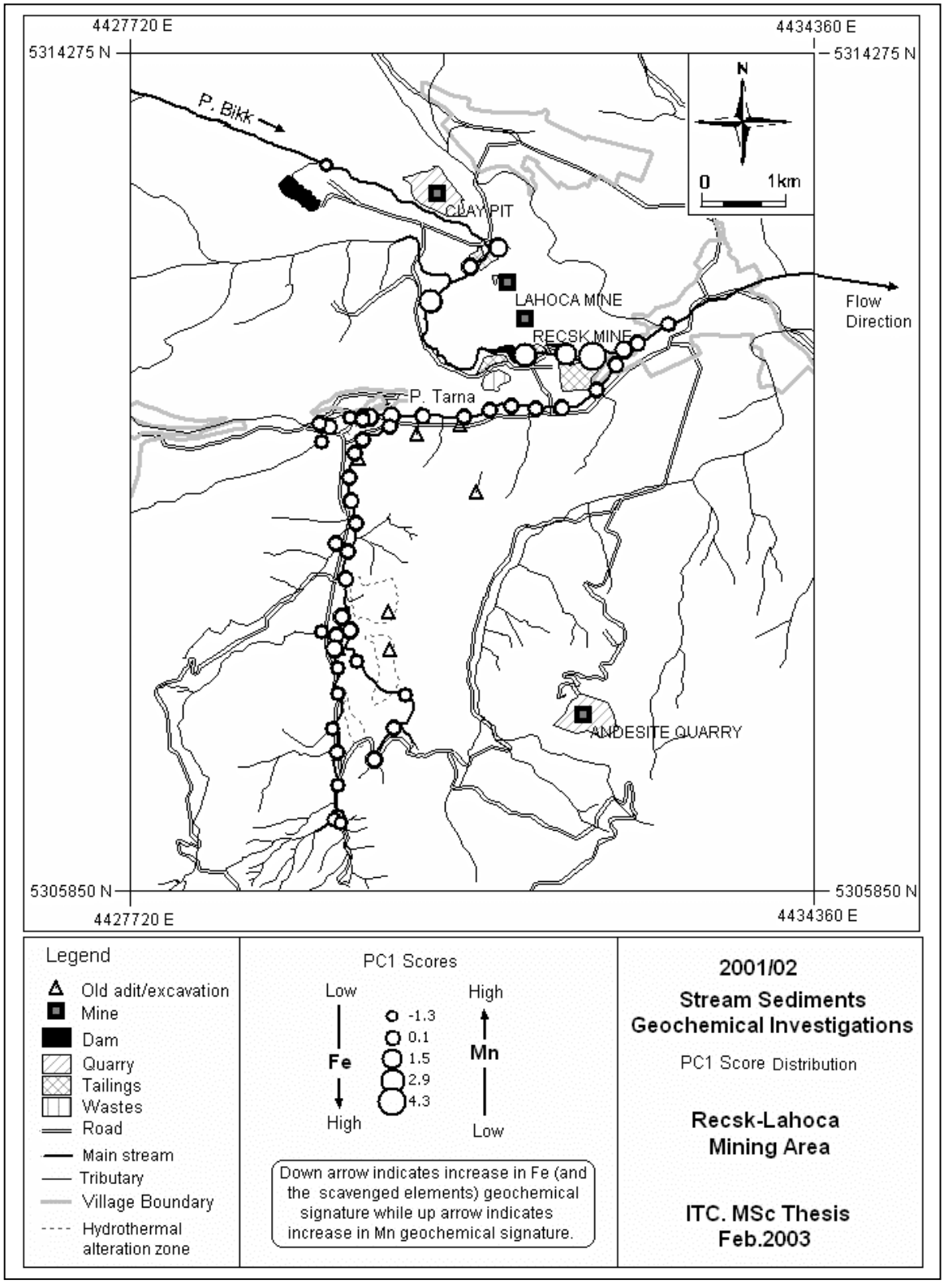

Figure 5.11. Spatial distributions of the calculated scores from PC1 showing the antipathetic relationship between Fe (and the scavenged elements) and Mn.

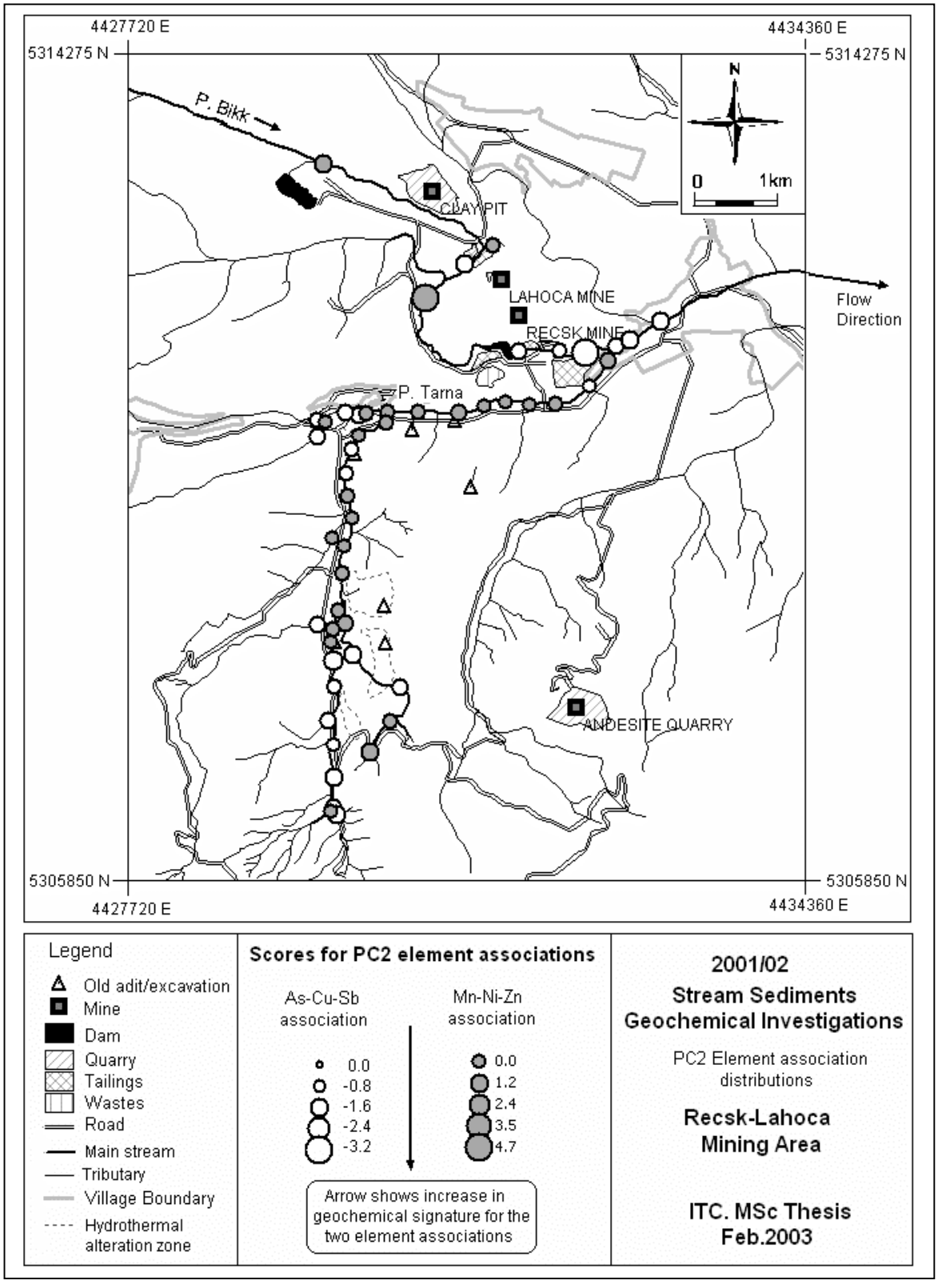

Figures 5.12 Spatial distributions of the element associations explained by PC2 scores.

5.4. Conclusions

Spatial distributions of univariate data indicate that there are strong relationships between the distributions of element concentrations and the environments drained by the streams. High element concentrations are predominantly distributed in the floatation tailings area between the Lahoca and the Recsk mines, which indicate that most of the element concentrations in this part of the stream are from the floatation tailings piles. Higher element concentrations are also observed in those parts of the stream close to hydrothermal alteration zones and old mine workings. Manganese and Ni are the only elements which showed low concentrations in these areas, most likely due to lower pH values which facilitate the dissolution of these two elements.

While spatial distribution maps are quite good at showing the element concentrations in relation to environmental features, graphical displays of element concentrations along stream profiles are useful in comparing element distributions and their concentrations. The concentration curves along stream profiles also give indications of correlating elements. The similarities and differences observed in the stream profile graphs are confirmed in the correlation coefficient analysis results, particularly when the Mn data plotted on the stream profile graph is compared with the other elements graphs. The graphs are observed to be opposite indicating a somewhat inverse relationship, which is observed between Mn and the other elements on the correlation matrix.

Principal components analysis methods become useful in revealing element relationships indicated in the other methods used in analysing the data. Manganese was found to be antipathetic with the other elements, while strong associations were observed between Fe and the other elements. The indicated element associations are mainly described by the inherent relationship of those elements in the mineralization of the sulphide ore deposits, which are manifested in the floatation tailings in the area. The associations are also described by the leaching and precipitation processes, which take place under different pH conditions.

Stream sediments data was also analysed for inter-element associations using Factor analysis by the Varimax rotation method. The results of the FA method are the same as the PCA results given above, which indicate that mineralization and surface geo-fluvial processes are the main factors responsible for the loading of stream sediments with heavy metals.

6. GEOCHEMICAL DATA FROM MINE AREAS AND WATER DRAINING THROUGH THE (OLD) ABANDONED WORKINGS.

Waste materials from mining and mineral beneficiation processes are the main sources of heavy metal contamination in mining environments. The exposure of sulphide mine wastes to the surface makes them vulnerable to oxidation and hydrolysis, which are the surface processes that initiate acid mine drainage. Knowledge of metal concentrations in mine wastes is useful in measuring the magnitude of the potential effects such wastes pose to the environment. Samples collected from the floatation tailings piles were analysed for As, Cd, Cu, Fe, Mn, Ni, Pb, Sb and Zn. The purpose was to determine the concentrations and associations of these elements and evaluate the potential threat posed by these elements to the environment. Waters draining the tailings piles and waters oozing out of the old mine workings were also sampled to determine element concentrations that are being discharged into stream waters.

6.1. Descriptive statistics for tailings data.

The element determinations were analysed for individual element statistics in order to determine the element characteristics. Descriptive element statistics analysis was carried out on the Lahoca east and Lahoca west tailings where large numbers of samples were collected in a grid pattern. Straight averages were determined from the data obtained from the four grab samples collected from exposed parts of the Recsk west tailings piles and 8 grab samples collected from the Recsk east tailings piles. Summary descriptive statistics of the analytical data for Lahoca east and Lahoca west tailings are shown in tables 6.1 and 6.2 respectively.

Table 6.1. Summary of descriptive statistics for Lahoca east geochemical data. Element measurements are given in ppm except for Fe which is in percentage (n = 53).

Element	Min.	Max.	Average	Std Dev	Var.	Skewness
As	49	1568	267	274	75120	2.73
Cd	1.90	5.40	3.23	0.78	0.61	0.26
Cu	86	1484	355	303	92006	2.22
Fe	1.49	3.67	2.76	0.41	0.17	-0.49
Mn	18	766	129	141	19816	3.17
Ni	1	43.40	11.27	9.03	81.62	2.16
Pb	15	252	51	52.00	2704	2.27
Sb	0.01	1.60	0.36	0.32	0.10	1.39
Zn	43	763	125	112	12484	3.97

Table 6.2. Summary of descriptive statistics for Lahoca west geochemical data. Element measurements are given in ppm except for Fe which is in percentage (n = 44).

Element	Min.	Max.	Average	Std. Dev.	Var.	Skewness
As	196	2789.	622	448	200501	3.13
Cd	1.40	7.20	2.80	1.24	1.54	2.26
Cu	303	2065	875	458	209758	1.19
Fe	1.42	3.15	2.26	0.40	0.16	0.40
Mn	15	207	53	35	1202	2.43
Ni	0.60	13.70	3.73	2.83	8.01	2.13
Pb	40	807	191	170	28821	2.27
Sb	0.01	4.20	0.84	0.76	0.58	2.78
Zn	69	777	275	182	32945	1.16

Iron is the most abundant element in the two Lahoca tailings showing that iron bearing sulphides like pyrite are the main mineral constituents of the tailings. Fe is evenly distributed in the two tailings and Cd is evenly distributed in the Lahoca east tailings. The strong skewness in the other elements indicates that their distributions are concentrated in some parts of the tailings. Mixing of soil cover with tailings wastes in some parts of the tailings piles could have resulted in skewness of the element data. The tailings are also mixed with coarse pebbles showing that they are composed of mixtures of waste materials from mineral processing, like mill tailings, and tailings wastes from metallurgical beneficiation. The different sources of the tailings obviously give rise to different mineral compositions, which result in varied element concentrations from one place of the tailings to the other. Table 6.3 summarises the averages of base metal concentrations in the four tailings

Table 6.3. Average element concentrations in the four sampled tailings piles. Element measurements are given in ppm except for Fe which is in percentage. LE. Lahoca East; LW. Lahoca West; RE. Recsk East; RW. Recsk West.

Element	**LE**	**LW**	**RE**	**RW**
As	266.53	621.96	504.88	545.15
Cd	3.23	2.80	9.70	4.18
Cu	354.92	874.77	1818.80	506.28
Fe	2.76	2.26	2.85	3.73
Mn	128.69	52.66	551.80	109.18
Ni	11.27	3.73	37.50	5.43
Pb	51.08	190.68	107.05	96.10
Sb	0.36	0.84	33.28	1.78
Zn	124.57	275.48	280.68	104.23

Average Fe concentrations for the four tailings are used as indicators of the amount of metal in the tailings piles because Fe is the most abundant element and its concentration approximates that of total base metal concentrations. Figure 6.1 shows the Lahoca and Recsk locations that were sampled.

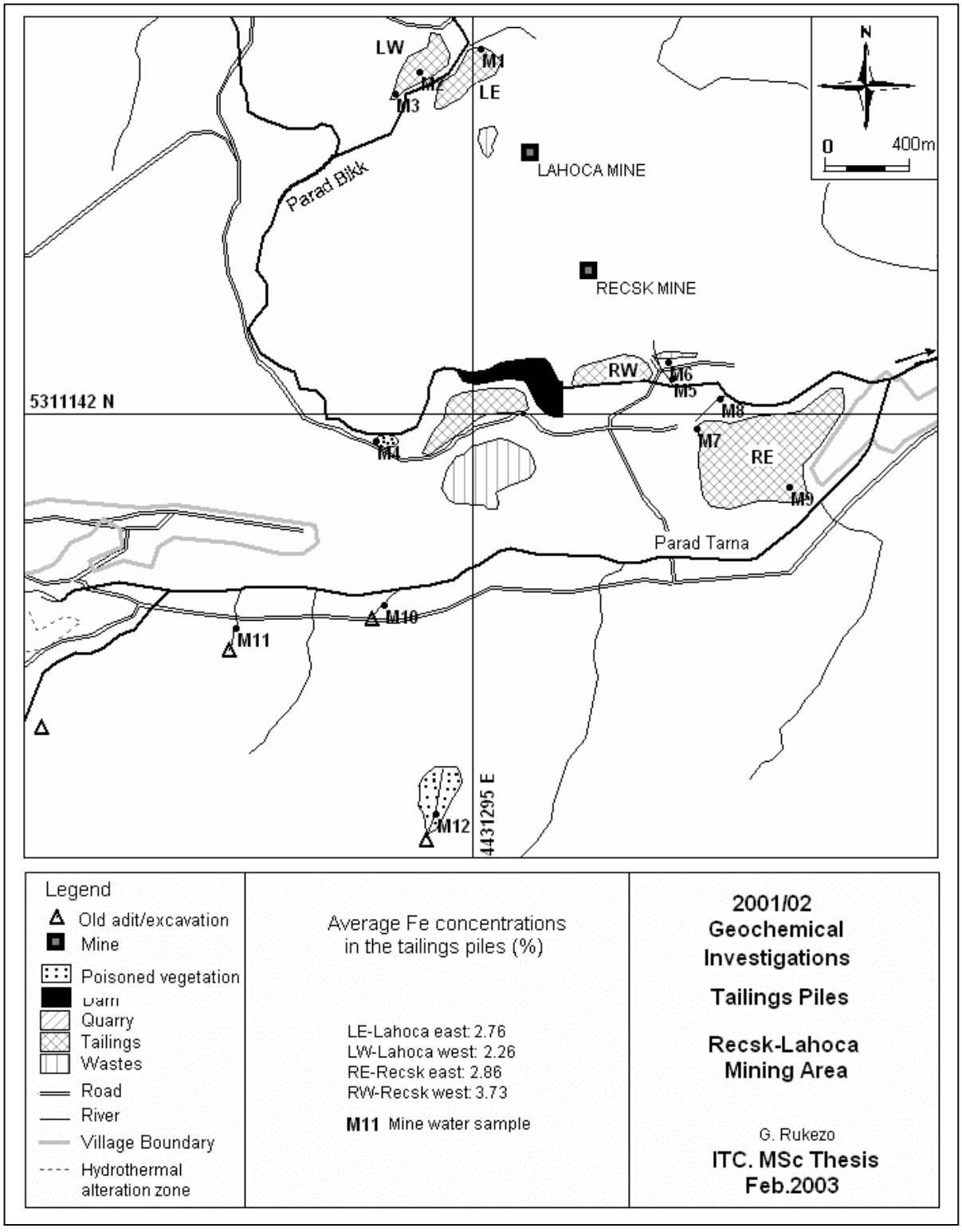

Figure 6.1. Recsk area showing sampled tailings and old adits.

6.2. Mine waters geochemistry

Waters draining tailings piles and waters oozing out of old adits were sampled and analysed for their metal and sulphate content, which can potentially drain into the main stream waters and result in contamination. The locations of the sample sites are displayed in figure 6.1, and their corresponding metal concentrations are shown in table 6.4. The measured EC and pH of the respective sample locations are also included in table 6.4.

The observed pH values are very low indicating that waters draining mine tailings and waters oozing out of old adits are highly acidic. Most of the sampled areas have pH values between 2 and 3 (table 6.4). The high EC values indicate that there is high ion activity in the mine waters. The metal and sulphate concentrations observed in mine waters are generally higher than those observed in stream waters depicting that tailings areas and ancient adits are the major sources of metal contamination in the area. On sample locations M4 and M12 (figure 6.1), pH is so low and heavy metal contamination is so high that vegetation was poisoned by the toxicity of water in these areas.

Table 6.4. pH, EC, SO_4^{2-} and base metal concentrations in waters draining the tailings and waters oozing out of old adits. Sample numbers M10 to M13 are from waters oozing out of old adits while the other samples are from tailings waters.

	M1	M2	M3	M4	M5	M6	M7	M8	M9	M10	M11	M12	M13
pH	3.0	2.0	2.5	2.3	2.0	3.5	2.0	2.5	3.0	5.4	3.3	2.5	3.0
EC	2570	9300	1815	12220	6420	3100	8460	5520	2410	1000	2280	3940	3240
As	0.2	27.5	0.1	1.4	0.6	0.5	0.7	0.3	0.1	0.0	0.1	0.8	0.1
Cd	0.04	0.3	0.02	0.6	0.1	0.0	0.1	0.1	0.01	0.01	0.01	0.1	0.0
Cu	22.49	129.58	10.40	210.55	113.80	33.54	54.06	51.36	11.05	0.03	0.02	10.14	0.19
Fe	389	>1220	82	>1220	993	33	>1220	490	39	0.4	59	534	525
Mn	14.74	18.30	4.14	86.25	5.98	5.00	36.11	31.06	29.24	6.66	24.16	13.58	25.98
Ni	0.35	1.03	0.14	6.14	0.51	0.20	2.23	1.27	0.48	0.02	0.13	0.43	0.11
Pb	0.27	3.78	0.05	3.50	0.05	0.05	0.05	0.05	0.05	0.05	0.05	0.04	1.59
Sb	0.01	0.04	0.02	0.03	0.04	0.02	0.01	0.02	0.00	0.04	0.04	0.02	0.01
Zn	5.32	30.98	2.68	45.42	6.73	3.67	32.80	15.44	1.52	0.36	11.25	8.80	1.29
Al	97.7	620.2	57.2	857.3	319.2	57.5	477.8	324.0	59.4	0.4	0.1	168.4	35.5
K	4.4	0.3	1.8	0.5	3.9	7.6	7.6	8.6	5.7	4.7	0.4	0.5	30.2
Ca	424.0	364.2	100.2	688.1	332.2	337.6	516.8	464.8	200.7	147.2	321.8	180.5	356.3
Mg	92.6	94.3	20.9	974.7	61.2	47.1	530.3	262.4	154.8	27.3	78.0	49.5	50.2
Na	36.5	36.3	7.1	4.6	80.8	78.9	28.9	25.1	22.7	12.7	9.8	32.5	24.7
SO_4^{2-}	1650	8600	1150	24200	6600	1440	11800	4600	1550	500	1380	3750	2150

Graphical displays shown in figure 6.2 show that pH and EC are strongly related with the measured elements and sulphate concentrations in the area.

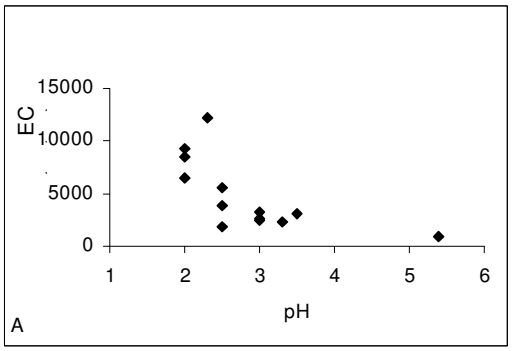

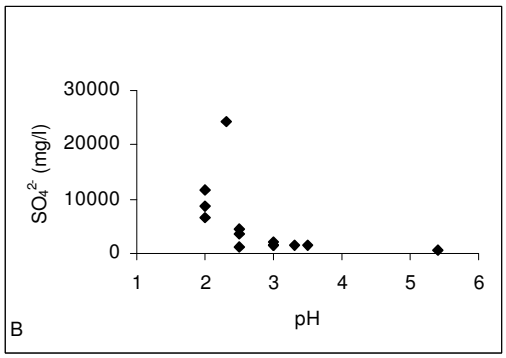

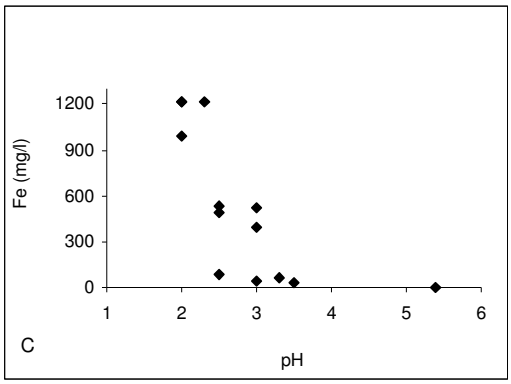

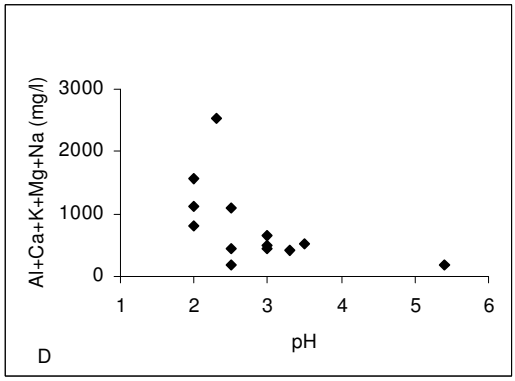

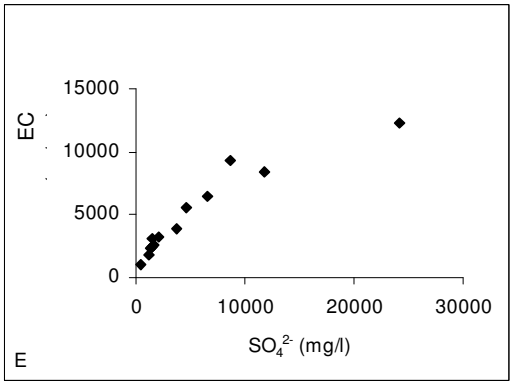

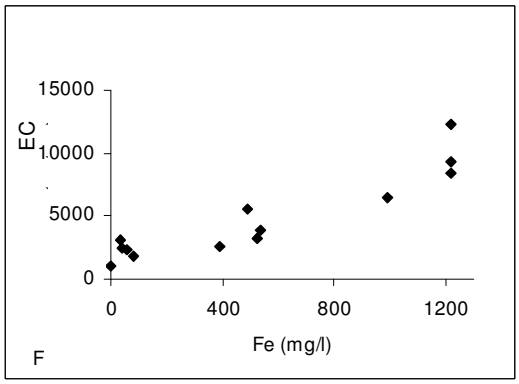

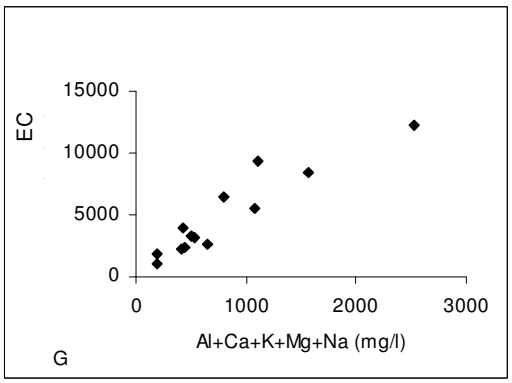

Figure 6.2. Graphs showing the relationships between metal concentrations with pH and EC: A. EC vs pH; B. Sulphate vs pH; C. Fe vs pH; D.Major cations vs pH; E.EC vs Sulphate; F. EC vs Fe.

Metals and sulphate ions are observed to increase with decrease in pH (figure 6.2 B to D) indicating that the dissolution of these elements from their sulphide minerals into water is most favourable in acidic waters. EC is observed to be strongly dependent on metal concentrations in waters. Figures 6.2 E-G show the direct relationships between EC and sulphate (SO_4^{2-}), base metals (Fe) and major cations (Al+Ca+K+Mg+Na). Because EC increases with increase in ion concentrations, it is also observed to increase with decrease in pH (figure 6.2A).

6.3. Conclusions

High element concentrations observed in the water draining tailings piles and old adits shows that the mine tailings piles and underground excavations are strong environmental signatures, which, because of their sulphide mineral association, are causing acid mine drainage in the area. High metal and sulphate contents, extremely low pH and the poisoned vegetation are some of the environmental effects observed in the mine areas. Relationships between element concentrations and physical properties of waters draining mine tailings piles and waters oozing out of ancient adits indicate that acid mine drainage is taking place in these waters. Any waters that drain from mine areas into the main stream drainages are therefore giving rise to metal contamination. The extent of the impact of the pollution to the environment downstream is to be achieved through comparisons with the other water systems in the area.

7. GEOCHEMICAL DATA RELATIONS AND ENVIRONMENTAL IMPLICATIONS.

7.1. Comparison of water, stream sediments and tailings geochemical data

Analysis of geochemical data from tailings samples indicated the presence of high base metal content in the waste materials, and that base metals are being leached into surface waters draining these tailings piles. The highly acidic water from the tailings piles is observed to flow into the nearby streams, which indicates that contamination of the streams by AMD water is definitely taking place in the area. However, the concentrations of metals in the streams are very low, even in the areas where the streams drain the floatation tailings piles. This indicates that there are hydrogeochemical processes responsible for removing metals from stream waters. Metal concentrations of the stream sediments are however quite high in these locations depicting that metals in streams are attenuated into the sediment material. The pH of water is found to be of great influence on metal concentrations in waters, and therefore, analysing pH and metal concentration can interactively indicate the chemical processes taking place in the area.

In order to interpret the variations in drainage water chemistry between the different environments, a classification scheme based on the pH and the sum of the metals is used. Plotting pH against total base metal concentrations and against total major element cations from all the different environments in the area interactively reveals the controlling parameters on element distributions. The element concentrations plotted on a semi-logarithmic scale are compared with the Ficklin classification scheme for acidic and non-acidic distributions of metals in drainage waters. In figure 7.1 the Ficklin classification diagram is shown, which is widely employed to determine different environments of water acidity and metal concentrations.

Base metals

The sum of As, Cd, Cu, Ni, Pb, Sb and Zn is analysed together with pH in order to interpret the variations in drainage water chemistry. Although Fe and Mn are the most abundant metals in the majority of mine and natural drainage waters, differences in the sum of base metals allow differentiation between different environmental controls on water composition, which is difficult to differentiate on the basis of concentrational variations in Fe and Mn. The plots of the sum of the base metals against pH are shown in figure 7.2. The base metals were classified according to their environments, namely, mine waters collected from tailings piles, old adit waters, Parad Bikk waters, Parad Tarna waters and waters after the confluence of these two streams.

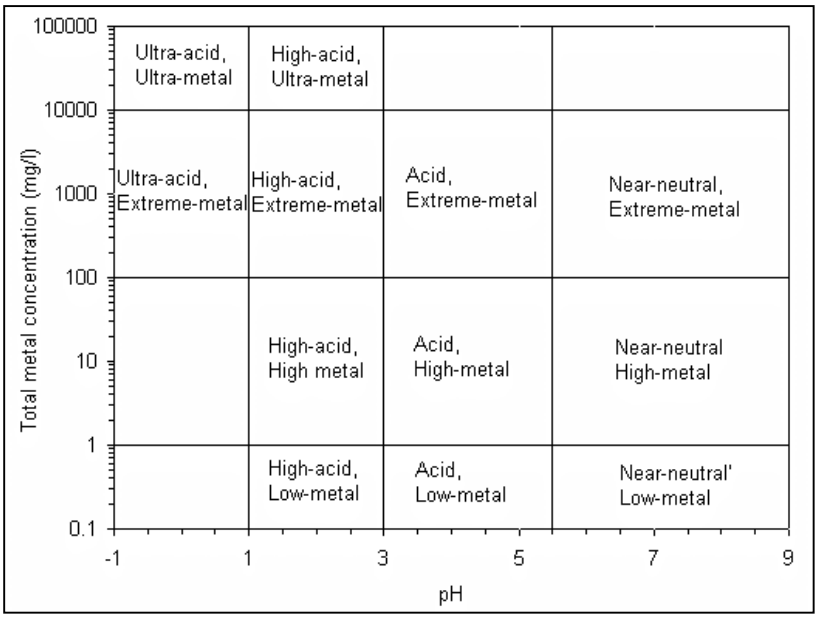

Figure 7.1. Ficklin diagram showing the classification scheme for mine and natural drainage waters (from Plumlee, 1995; named after the late Walter Ficklin, an environmental geochemist).

The sums of the base metals from samples collected from the same environment are seen to form clusters in a certain pH range when plotted on the Ficklin diagram, which shows that the distribution of base metals in drainage waters is controlled by pH characteristic of that environment. Element concentrations from mine tailings plot in the high acid-high metal and the high acid-extreme metal zone, while waters oozing out of the old adits plot in the high acid-high metal and the acid-high metal zone on the Ficklin diagram (figure 7.2). The distribution of these high metal concentrations in highly acidic waters draining mine areas proves, beyond any reasonable doubt, that AMD is taking place in the mine environments. Metal concentrations distributed in Parad Tarna, Parad Bikk and the waters after the confluence of the two streams are clustered mainly in the near-neutral-low metal zone of the Ficklin diagram, except a few measurements from Parad Tarna and Parad Bikk, which are in the low acid-low metal and near neutral-high metal zones respectively. A big gap in both pH and metal concentrations exist between the mine waters and waters from the streams, except for one from an old adit, which plotted in the low acid-low metal zone. Even the stream water measurements from Parad Bikk in the area the stream drains the Recsk and Lahoca tailings, and the stream measurements from Parad Tarna in those areas the old adits drains into the stream, are characterised by near neutral waters and low metal concentrations. A similar relationship is observed when sulphate is plotted against pH on a Ficklin diagram, mainly because both base metals and sulphate are similarly leached from the metal sulphide minerals they form. There are two possible explanations for this situation: 1) The amount of acidic water discharge is extremely low that the effect is hardly noticeable in the main streams and/or 2) there must be some other element/compound ions present in the streams that act as buffers to changes in the pH of water.

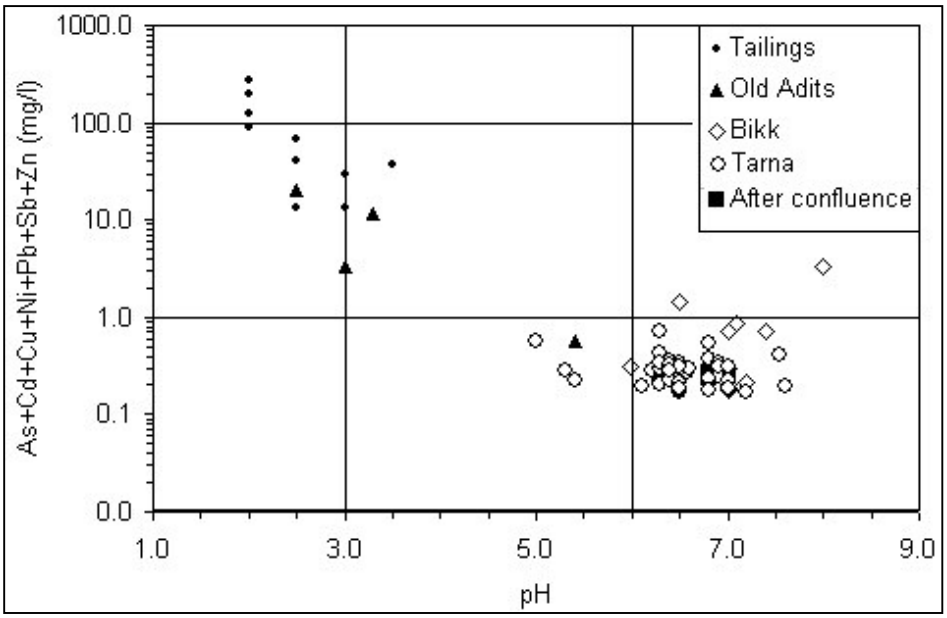

Figure 7.2. Plots of dissolved base metal concentrations as a function of pH of the waters draining the area.

The total concentrations of the major element cations (i.e. Al+Ca+K+Mg+Na) were also plotted as a function of pH in order to determine their relationships. Figure 7.3 shows the plots of the major element cations. Measurements from upstream of the Lahoca tailings were denoted by a different symbol in order to determine the relationship with pH on that part of the stream because higher concentrations were observed for most of the major elements in that environment.

High concentrations of the major elements in the acidic waters of the tailings and old adit environments, shown on the graph, are due to the hydrolysis of the silicate minerals in the tailings. The major element concentrations in the streams are also observed to be quite high, especially those from Parad Bikk on upstream of the Lahoca tailings where the stream drains the Oligocene clay. The concentrations are clustered in the higher pH ranges of 7 to 8 in the near-neutral zone of the diagram. Hydrolysis of the alkali/alkaline earth element minerals may result in the formation of buffering complexes like bicarbonates, which maintain more or less constant pH in the streams.

Stream pH values, which are observed to be in the near neutral zone on the Ficklin diagram, are suitable for the precipitation of base metals. Iron, which precipitates at pH values as low as 3, is easily hydrolysed into solid hydroxides when the acidic mine waters discharge into the higher pH stream waters. This accounts for the sharp contrast in Fe concentrations in the mine waters and in the streams. As the Fe precipitates, other base metals are co-precipitated as shown by the multivariate analysis results in the earlier chapters. Results of the principal components analysis indicated that surface processes, which take place in geo-fluvial environments, explain the largest percentages of the variations in the stream sediments. It therefore follows that whilst base metals are leached from the mine areas into the streams, the high pH in the streams results in the precipitation of most of those base metals, giving rise to low base metal concentrations in the streams and high base metal concentrations in the stream sediments.

A sample location in the profile of Parad Bikk between the Recsk and Lahoca tailings showed extremely high metal concentrations and pH of 2, but these characteristics could not be observed in the part of the stream that is located less than 400m downstream. There may be some pH buffers in the stream, which act as geochemical barriers in this area. Carbonate precipitates observed upstream of the tailings area, and elsewhere in the streams, may be hydrolysed to liberate calcium ions and bicarbonate radicals, which are strong buffers of any pH changes.

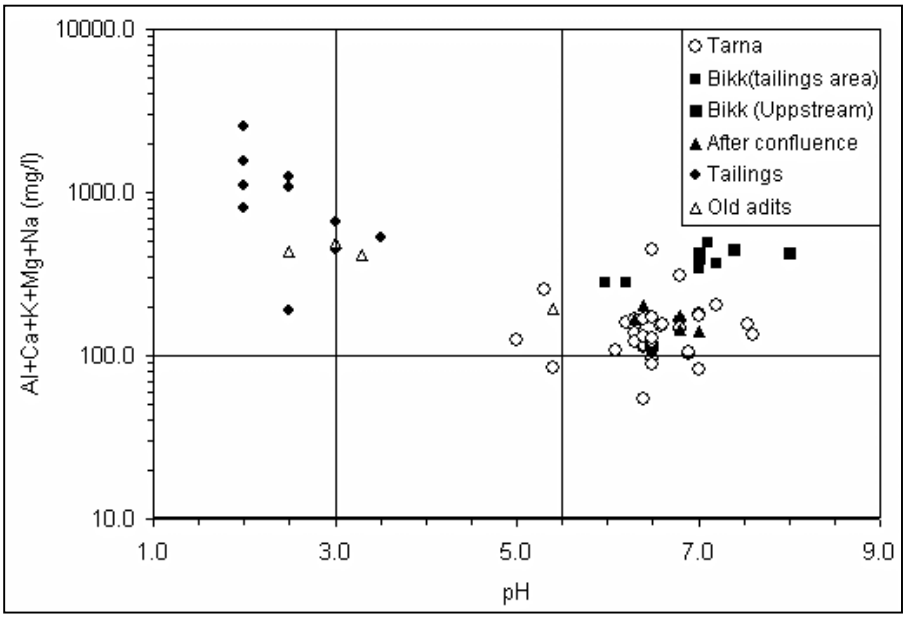

Figure 7.3. Plots of dissolved major element cation concentrations as a function of pH of the waters draining the area.

7.1.1. Summary of geochemical data comparisons

Waters draining the mine areas and old adits are highly acidic and have a high element concentration which shows that AMD processes are taking place in those parts of the drainage system of the area. The effects of the AMD processes are however not easily recognisable in the streams where element concentrations are generally low in the waters and higher in the stream sediments. Conclusive relationships among the analysed parameters of the various investigated environments can only be reached with more geochemical data, and mineralogical data. However, an attempt to relate these drainage characteristics with laid out environmental baselines may be useful in determining the impact the geochemistry of the area has on the environment.

7.2. Environmental implications of the geochemical data

7.2.1. Environmental implications of hydrogeochemical data.

Pollution of surface waters occurs when too much of an undesirable or harmful substance flows into a body of water in concentration levels exceeding the ability of that water body to remove the undesirable material or to convert it to a harmless form (Djuarsa, 1996). Degradation of water is generally judged in terms of the intended use of water, departure from the norm, effects on public health or ecological impacts.

The European Union (EU) standards used as indicators for drinking water were used as thresholds to determine the presence of polluted water bodies in the area. Base metal concentrations were compared with the standards for drinking water because of their high toxicity when their concentration levels rise beyond the standards. Electrical conductivity, pH and sulphate were also analysed because these three parameters are closely related to the base metal distributions. Table 7.1 shows the quality of the waters draining the area in relation to base metal concentrations. The samples analysed for these parameters were grouped according to the environments they were collected as given in the table. The total number of samples collected in each environment is given in parentheses, and in the columns are the numbers of samples with concentrations above the maximum permitted level of concentration for the corresponding measured parameter in column 1.

Metal concentrations in most of the water sample measurements from the tailings and old adits are observed to be extremely higher than the EU parametric standards for drinking water listed in table 7.1, while pH values are far lower than the standard pH range. This clearly shows that waters draining the mine areas are highly polluted by heavy metals from the leaching of sulphide minerals in the tailings piles and mine excavations. The concentrations of the pollutants distributed in the streams are very close to the standard parametric thresholds. Most of the samples showed arsenic levels above the permissible limit in most of the environments in the area while the number of samples with Sb levels above the limit was quite high in Parad Tarna. The pollution levels of the stream water are seen to drop significantly after the confluence of the two streams. Only As is observed to be persistent downstream of the confluence.

Table 7.1. Base metals, sulphate, EC and pH measurements above the European Union standards for drinking water. Base metal and sulphate concentrations are given in mg/l and EC is given in µs/cm.

Parameter	Maximum permitted levels	No. of samples above max. permitted level	Environmental distributions of concentrations above maximum permissible limits for the measured parameters			
			P. Tarna (42)	P. Bikk (15)	Tailings (10)	Old adits (4)
As	0.01	51	34	5	9	3
Cd	0.005	9	0	0	6	3
Cu	2	11	0	0	10	1
Ni	0.02	13	1	2	9	1
Pb	0.01	11	0	4	5	2
Sb	0.005	28	14	1	9	4
Sulphate	250	22	4	4	10	4
EC	2500	13	0	2	9	2
PH	6.5<pH<9.5	34	18	2	10	4

There are more samples with higher than the EU standards in Parad Tarna than Parad Bikk. Besides the little waters from the old adits, there is no other mining area with waters discharging into Parad Tarna. It therefore follows that most of those pollutants are generated by the natural weathering of the rocks drained by the stream, especially hydrothermal alteration zones, where the stream waters are

found to contain elevated metal concentrations. Displayed in figure 7.4 is the map of the area showing parts of the drainage with metal concentrations above the maximum permissible limits for drinking water quality.

7.2.2. Environmental implications of Stream sediments geochemical data.

In some of the stream sediments, pollution is observed to be relatively high when compared with the Dutch norms (NEN) for metal concentrations in soils. Table 7.2 shows the number of samples with metal concentrations above the NEN threshold standards for the four main drainage environments in the research area. The letter A in the thresholds column refers to the reference value corresponding to the maximum metal concentrations required in soils, B is the testing value required for additional investigations and C is the testing value required for cleaning up metal concentrations in water. Metal concentrations in the 4 drainage environments are classified according to the threshold ranges.

Table 7.2. Distributions of trace element concentrations classified according to the NEN standards in the four main drainage environments of the area.

M	**Thresholds**			**P. Tarna**			**P. Bikk**			**AC**		**Old Adits**	
	A	**B**	**C**	**A**	**B**	**C**	**A**	**B**	**C**	**A**	**C**	**A**	**C**
As	29	30	50		5	2		1	7		3		2
Cd	0.8	5	20	41					2	3		1	2
Cu	36	100	500	12	1			1	6	1	2	2	
Pb	85	150	600	2	1								
Zn	140	500	3000										

Arsenic, Cd and Cu are the main elements which are causing polluting in the stream sediments. Most of the As and Cu concentrations above the maximum concentration levels required for cleaning up are distributed in the area between the Recsk and Lahoca tailings piles. Displayed in figure 7.5 are the areas requiring additional investigations and cleaning up according to the NEN standards.

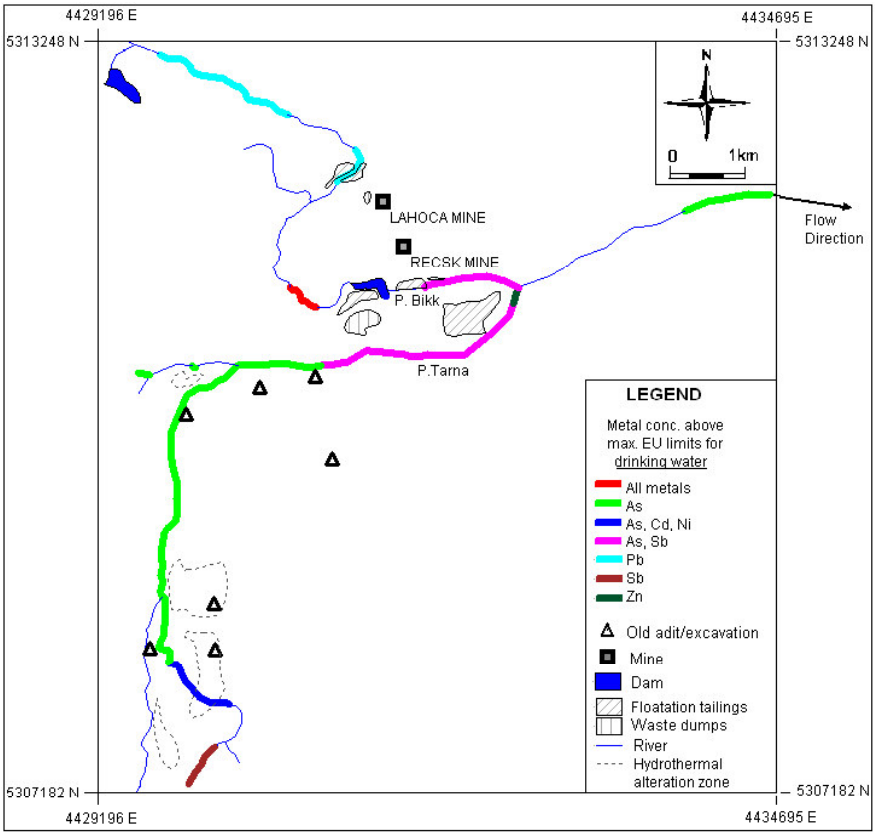

Figure 7.4. Map of the Recsk-Lahoca area showing drainages with base metal concentrations above the maximum permissible limits for EU drinking water standards.

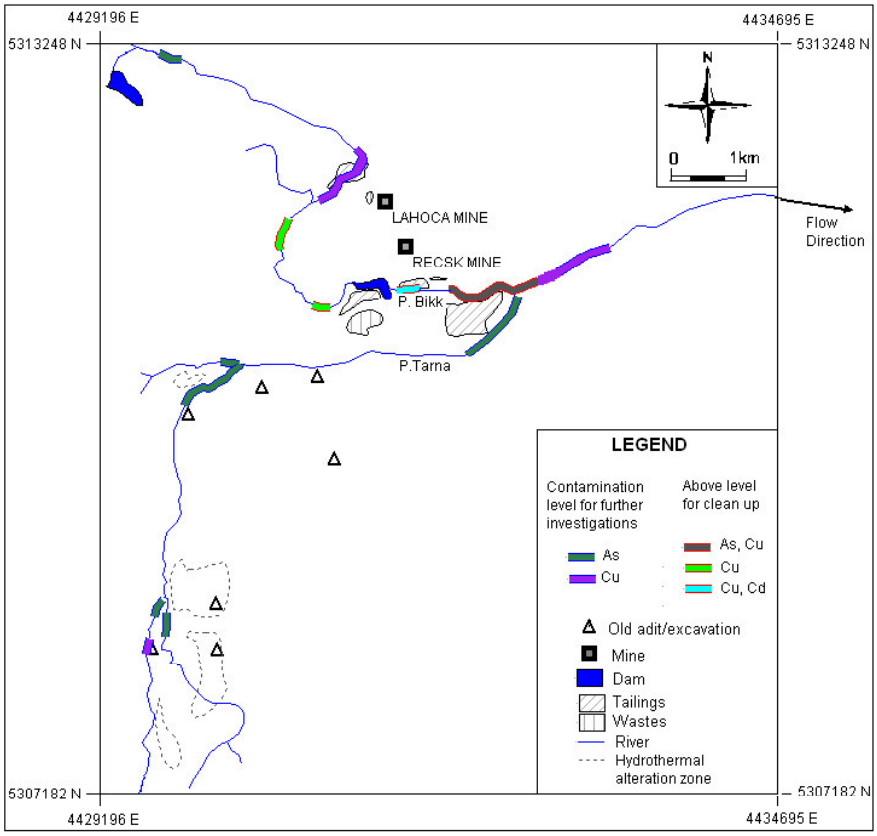

Figure 7.5. Map of the Recsk-Lahoca area showing drainage segments with base metal concentrations in sediments requiring additional investigations and cleaning up according to the NEN standards for soils.

7.3. Conclusions

The distribution of element concentrations in the different environments of the project area is related to the pH of the waters. The high pH in the streams is responsible for the precipitation of most of the metals drained from mine areas, which result in the removal of most of those metals from stream waters. As a result, polluted waters are restricted to water bodies draining mine tailings piles and old adits where AMD processes are actively taking place. However, while precipitation and co-precipitation of metals naturally "clean up" the stream waters, the effects of metal contamination are transferred to the sediments of those streams. As a result of these processes, pollution levels are observed to be very low in the stream waters when the contamination levels are compared with the maximum permissible limits for EU drinking water standards. In the sediments, the precipitating metals result in high pollution levels, particularly in the floatation tailings area where most of the metals leached into the drainages are precipitated into sediments. The sediments of the drainage in the floatation tailings area require cleaning up when the contamination levels are compared with the Dutch norms (NEN) for soils.

8. CONCLUSIONS AND RECOMMENTATIONS

8.1. CONCLUSIONS

1. Reconnaissance mapping of the Recsk-Lahoca mining area revealed distinct natural and mining related environmental signatures some of which are causing heavy metal contamination problems in the drainages of the area, especially in the areas where sulphide minerals were mined but also in the areas of hydrothermal alteration where no mining took place. The Oligocene clayey-marl in the up-stream of the mine areas is observed to load the streams with major element cations like Ca, Na, K and Mg.

2. Oxide precipitates of Fe(III) and higher metal concentrations in the streams and stream sediments in areas where Parad Tarna drains close to sulphide mineralised areas and hydrothermal alteration zones indicate that natural acid rock drainage is taking place in these areas. Field observations indicate that the effects are minimal based on the limited extension of the stream portions covered by the Fe pre-cipitates, the higher metal concentrations in sediments, and the small change noticed in the pH of those stream portions.

3. Any acid generated by the release of H^+ ions in the streams due to the hydrolysis of aqueous Fe(II) to insoluble Fe(III)-hydroxides is buffered by the high major element cation concentrations in the streams, especially in Parad Bikk which has higher major element cations resulting from the weather-ing of both the Oligocene clayey-marl and the sulphide rich tailings piles, which are also rich in some of the major elements due to their andsitic composition.

3. Univariate data analysis methods, coupled with graphs of element concentrations along stream pro-files showed that the distributions of element concentrations are strongly related to the environmental features drained by the streams.

4. Results of principal components analysis revealed the predominance of surface geo-fluvial proc-esses as the main controlling factors of metal attenuation in the stream waters and stream sediments. Element associations showed that high base metal concentrations in the stream sediments are basi-cally due to the scavenging effect of Fe rather than Mn which precipitate at higher pH values. The strong association of Fe and the other metals in the stream sediments explains why there are very low concentrations of base metals in the streams. It therefore follows that whilst alkali metals neutralise any acidic water generated by AMD process, the base metals leached by the same process are quickly removed from the water by the precipitating Fe as soon as they manifest themselves in the streams.

5. Geochemical data can be represented for meaningful interpretation of polluted areas using GIS.
6. Compared with reference literature and standards for water quality, the streams of the Recsk-Lahoca mining area are considered to have a low metal contamination level while the sediments have a relatively high metal contamination.

8.2. Final remarks and Recommendations

1. Pollution of water due to contamination by heavy metals is usually measured, on the maximum level, by maximum permissible standards for drinking water, which allow very low concentrations of base metals in water above the natural range of values. In order to analyse geochemical data for this purpose, analytical techniques with sufficiently low detection limit are required.

2. Whist geochemical analysis methods indicate processes that lead to AMD, they fall short in explaining secondary mineral phases that occur in those processes. It is therefore necessary to augment geochemical methods with mineral analysis methods to fully establish the processes involved in heavy metal contamination. X-ray diffraction, infrared and other multispectral analytical equipment can play significant role in determining the mineral species occurring in the contaminated sediments. Due to the thick vegetation in the area, field or laboratory spectroscopy methods would be more appropriate than airborne or space borne methods in analysing minerals which are indicative of AMD and heavy metal contamination.

3. Geochemical analysis of element data of the area only indicated low metal contaminations in the streams mainly due to precipitation and co-precipitation of base metals. In vegetated areas like the Recsk, vegetation may play significant role in attenuating heavy metals from water and stream sediments through assimilation into the plant system. The use of remotely sensed data like hyperspectral imaging can be very useful in determining the role of vegetation in the attenuation of stream metal loads.

4. In order to fully establish the contamination processes, floodplains further downstream of the mining areas should also be studied because the sediments, which are found to be high in heavy metals, are also deposited with other stream debris during flood erosion.

5. A stricter environmental monitoring program, which among other activities, involves re-vegetating the areas covered by the tailings piles and prohibiting unauthorised and unplanned digging of the tailings by the local people can reduce the processes responsible for the leaching of metals from the tailings piles and their subsequent erosion into the streams.

References

Akos E. V., 1999: Alpine deposit models for the Matra and Borzody Mountains, Northern Hungary. Geologica Hungarica series, Tomus 24: 63-77.

Beckers J., Archambeau C.,1997. The implementation of a nested, coupled hydrodynamical-primary poduction model in the TOROS region. http://www.dstu.univ-montp2.fr/HYDROSCIENCES/toros.html.

Carranza E.J.M.., 1994: A catchment basin approach to the analysis of reconnaissance geochemical-geological data from Albay province, Philippines. MSc. Thesis– ITC, Delft.

Carranza E.J.M., 2002: Geologically-Constrained Mineral Potential Mapping. PhD. Thesis – ITC, Enschede.

Czako T., Zelenka T., 1981: New data about the neotectonics of Matra Mountains, Hungary – Advanced Space Research volume, pp. 289-298.

Cox D.P., Singer D.A., 1986: Mineral Deposit Models–USGS Bulletin 1693. Washington US Department of the Interior.

Djuarsa I., Environmental geology investigation in some mine sites of Cyprus. MSc. Thesis-ITC, Enschede.

Durkin T.V., Hermann T.V., 1994: Focussing on the Problem of Mining Waste: An introduction to Acid mine drainage– http://www.enviromine.com/publicate/amdinto.html.

Davies C.J.,1986: Statistics and Data analysis in Geology(2nd edition). John Willey and Sons, Toronto.

EnvironmentalMining Council., 2001: Acid Mine Drainag: Mining and water pollution issues in Brittish Columbia- British Columbia, Canada

Foldessy J., 1996: Lahoca Epithermal Gold Deposit, Recsk-Hungary – Plate Tectonic Aspects of the Alpine Metallogeny in the Carpatho-Balkan Region UNESCO IGCP Project No.356, Volume 2: 67-74.

Fortescue J.A. C., 1980: Environmental geochemistry. Springer Verlag, New York.

George H. and Bonham-Carter G.F., 1989: Spatial modelling of geological data for gold exploration, Star Lake area, Saskatchewan. In: F.P. Agterberg and G.F. Bonham-Carter (Eds.) Statistical Applications in the Earth Sciences. Geological Survey of Canada, Paper 89-9, pp 157-169.

Hale M., 1990: Multivariate Statistics in Mineral Exploration, ITC.

Howarth J.R. and Sinding-Larsen R., 1983: Multivariate analysis. Publication in Statistics and Data Analysis in Geochemical Exploration. Handbook of Exploration Geochemistry vol. 2 – Elsiever.

Horan J., 1999: Acid producing potential of mine waste, Colorado School of Mines - http://www.mines.edu/fs_home/jhoran/ch126/index.htm.

Jordan G. Szucs A. Qvarfort U. and Szekely B., 1997: Evaluation of Metal retention in a wetland receiving acid mine drainage. Geophysical Research Group, Hungarian Academy of Sciences.

Krauskopf B.K. and Bird K.D., 1995: Introduction to Geochemistry (3rd edition), McGraw-Hill international editions.

Lloyd J.W., Heathcote J.A., 1985: Natural inorganic hydrochemistry in relation to groundwater – Clarendon press, Oxford.

Miller W.R., McHugh J.B.,1999:Calculations of Geochemical baselines of Stream Waters in the Vicinity of Summitville ,Colorado, Before Historic Underground Mining and Prior to recent open Pit Mining. Publication in The Environmental Geochemistry of Mineral Deposits-Reviews in Economic Geology Volume 6B.

Nordstrom D.K and Alpers C.N., 1999: Geochemistry of Acid Mine Waters in The Environmental Geochemistry of mineral deposits Part B, Reviews in Economic geology – Society of economic geologists, Inc.

Odor L., Wanty R.B., Horvath I., Fugedi U., 1999:Deposit Modelling and Mining-induced Environmental Risks. – Geologica Hungarica series, Tomus 24: 107-127.

Odor L., Wanty R.B., Horvath I., Fugedi U., 1998: Mobilisation and attenuation of metals downstream from a base-metal mining site in the Matra Mountains, Northeastern Hungary. – Journal of Geochemical Exploration 65 (1998) 47-60.

Odor L., Csirik G., Akos V.E., Sept. 1998: Geology, mineralisation, and some aspects of environmental impacts (Matra Mountains, Hungary). Field trip guide for the NATO Advanced Study Institute course, September 6-18, 1998, Matrahaza, Hungary.

Plumlee G.S and Nash J.T., 1995: Geoenvironmental Models of Mineral Deposits – Fundamentals and Applications- Publication in USGS preliminary compilation of descriptive geoenvironmental mineral deposit models, Denver Colorado.

Ramsey H.R.,Thompson M., and Hale M., 1992: Objective evaluation of precision requirements for geochemical analysis usind robust analysis of variance. Journal of geochemical exploration , vol. 44.

Reece B., 1995: Perpetual Pollution-Washington DC.

Robbin E.I., Andeson J.E., Cravotta C.A., Nord G.L., Slonecker E.T., 2000 Multispectral signature variations in acidic versus near neutral contaminated coal mine drainage in Pennsylvania: Int. Conf. on acid rock drainage, Littleton Co. Soc. Mining, Metallurgy and Exploration, incl., vol. 2 pp. 1551-1559.

Plumlee et al.,1998:Geologic controls on the composition of natural waters and mine waters draining diverse mineral deposit types in The Environmental Geochemistry of mineral deposits Part B, Reviews in Economic geology – Society of economic geologists, Inc.

Salminen R.. et al., 1998. FOREGS geochemical field manual – Geological Survey of Finland, Guide 47.

Swan R.H., Sandilands M., 1995. Introduction to geological Data Analysis. Blackwell Science.

Williams J.D, Bigham M. J, Cravotta A. C., Traina S.J., Anderson J.E., Lyon J.G., 2001. Assessing mine drainage pH from the colour and Spectral reflectance of chemical precipitates-Journal of Applied Geochemistry 17 (2002) 1273-1286.

Appendices

Appendix A. FOREGS sampling sheet for stream water and stream sediments (from Salminen R.).

FOREGS GEOCHEMICAL BASELINE PROGRAMME **STREAM WATER+STREAM SEDIMENT**

WATER SAMPLE ID _____ Date _____ Sampler _____
STREAM SEDIMENT ID_____ Country _____
Organisation _____
GTN cell coordinator if different from above _____

SAMPLE SITE LOCATION REGION _____ MAP SHEET _____
COORDINATES **(Decimal degrees mandatory)**
National grid Easting _____ Northing _____
Decimal degrees Longitude _____ Latitude _____ Datum _____
Altitude (m) _____
SITE DESCRIPTION
Approximate size of catchment basin _____ km^2
Landscape / topography_____
Land use
□ Agriculture, specify crop _____
□ Pasture, grassland, fallow field
□ Forest: □ Deciduous □ Coniferous □ Mixed
□ Wetland
□ Non-cultivated, moorland etc.
□ Other, specify _____
Bedrock lithology _____ Outcrops □ Yes, specify _____

□ No outcrops
Type of overburden _____
Channel charasteristics □ Natural □ Reinforced □ Man-made (ditch)
Last rainfall before _____ days _____ hours
Water level in stream: □ Low □ Normal □ High
Stream flow: □ Low □ Moderate □ High
Stream bed: Predominant □ Boulders and gravel □ Gravel and sand
□ Sand and silt □ Mud □ Vegetation
Possible sources of contamination, specify _____
NUMBER OF SUBSITES (stream sediment) _____
NUMBER OF SAMPLE BAGS (stream sediment) _____
PHOTOS Film and photo ID
Landscape _____
Site _____
GAMMA-RADIATION Total _____ Th _____ U _____ K _____
Instrument _____
WATER CHEMISTRY Normal sample Duplicate sample Instrument
pH _____ _____ _____
EC mS/m 25°C _____ _____ _____
DRYING (Sediment) □ Freeze drying □ <40°C

Appendix B. FOREGS sampling sheet for soils (from Salminen R.).

FOREGS GEOCHEMICAL BASELINE PROGRAMME **SOIL**

TOP SOIL ID _____ Date _____ Sampler _____

SUBSOIL ID_____ Country _____

Organisation _____

GTN cell coordinator if different from above _____

SAMPLE SITE LOCATION REGION _____ MAP SHEET _____

COORDINATES **(Decimal degrees mandatory)**

National grid Easting _____ Northing _____

Decimal degrees Longitude _____ Latitude _____ Datum _____

Altitude (m) _____

SITE DESCRIPTION

Landscape / topography _____

Land use

- □ Agriculture, specify crop _____
- □ Pasture, grassland, fallow field
- □ Forest: □ Deciduous □ Coniferous □ Mixed
- □ Wetland
- □ Non-cultivated, moorland etc.
- □ Other, specify _____

Bedrock lithology _____ Outcrops □ Yes, specify _____

□ No outcrops

Type of overburden _____

NUMBER OF SUBSITES _____

SOIL TYPE (FAO classification or local name) _____

Ploughing depth (cm) _____

Subsoil, specify soil horizon _____

Sampling interval (cm): Topsoil _____ Subsoil _____

Depth of groundwater table (cm) _____

ABUNDANCE OF SOIL CLASTS %		**TOP**	**SUB**	**TEXTURE**	**TOP**	**SUB**
	0	□	□	sandy	□	□
	0 - 2	□	□	sandy-loam	□	□
	2 - 5	□	□	loamy	□	□
	5 - 15	□	□	clayey-loam	□	□
	15 - 40	□	□	clayey	□	□
	40 - 80	□	□	clay	□	□
	> 80	□	□			
SAMPLE HUMIDITY		**TOP**	**SUB**	**ORGANIC CONTENT**	**TOP**	**SUB**
	wet	□	□	high	□	□
	dry	□	□	low	□	□

Possible sources of contamination, specify _____

PHOTOS Film and photo ID

Landscape _____

Site _____

GAMMA-RADIATION Total _____ Th _____ U _____ K _____

Instrument _____

BALTIC SOIL SURVEY countries only: BSS sample ID _____ is used for this sample.

The BSS sample has already been sent to the NGU □ yes □ no, will be sent by _____

REMARKS

Appendix C. Sample coordinates and field measurements (Coordinates are in Hungarian National Uniform Projection (EOV) system, EC is in µs/cm and temperature is in ^{o}C).

No.	X-coor	Y-coor	Z-coor	H_2O temp	pH	EC	Bedrock geol	Channel characteris-tics	Possible sources of con-tamination
1	4432330.15	5311327.58	165	20.1	7.6	800	oc/a	Natural	Floatation tailings
1D	4432330.15	5311327.58	165	20.1	7.6	800	c/a	Natural	Floatation tailings
2	4432370.04	5311390.48	166	20.9	6.4	1055	c/a	Natural	Floatation tailings
3	4432269.73	5311340.36	165	22.7	6.0	1446	c/a	Natural	Floatation tailings
4	4432067.53	5311231.83	167	23.0	6.2	1414	c/a	Reinforced	Flotation and mine dumps
5	4432173.10	5311043.50	170	19.3	6.2	793	c/a	Natural	Floatation tailings
6	4432000.21	5310862.49	183	19.8	6.6	792	a	Natural	Floatation tailings
7	4431751.96	5310813.85	184	19.9	6.6	800	c/a	Natural	Residential area
8	4431492.11	5310769.30	202	20.0	6.8	814	c/a	Natural	Mine dump
9	4431253.01	5310686.25	203	20.4	6.3	830	a	Natural	ARD from andesite
10	4431009.63	5310585.60	202	17.5	5.4	1000	a	Man-made	AMD from adit
11	4430996.66	5310623.32	197	21.5	6.8	843	a	Natural	Mine dump from adit
12	4430514.19	5310506.83	228	19.3	3.3	2280	a	Man-made	AMD from adit
13	4430565.57	5310658.58	201	22.3	6.3	834	a	Natural	Ancient mines upstream
14	4430251.31	5310683.22	199	20.2	6.3	799	a	Natural	Residential area
14D	4430251.31	5310683.22	199	20.2	4.8	808	a	Natural	Residential area
15	4430011.95	5310617.77	206	20.6	7.6	841	a	Reinforced	
16	4430176.71	5310568.90	206	17.9	6.9	607	a	Natural	
17	4429958.49	5310409.03	213	18.3	6.9	584	a	Natural	Gas seepage
18	4429826.66	5310309.25	220	19.8	6.9	573	a	Natural	Mine dump from adit
19	4429637.60	5310043.93	235	19.5	6.5	569	a	Natural	
20	4429650.39	5309760.70	241	18.9	6.4	564	a	Natural	
21	4429644.02	5309510.16	242	19.0	6.5	617	a	Natural	
22	4429545.38	5309311.28	257	17.8	6.8	1034	a	Natural	
23	4429592.46	5309290.96	243	19.6	6.4	619	a	Natural	Anth(from road)
24	4429652.78	5308990.41	244	20.3	6.4	608	a	Natural	
24D	4429652.78	5308990.41	244	20.2	6.3	609	a	Natural	
25	4429572.84	5308699.26	249	19.0	6.4	603	a	Natural	
26	4429438.25	5308510.52	257	18.8	6.5	565	a	Natural	
27	4429529.73	5308440.87	257	16.4	6.3	650	a	Natural	Anth(from tourists); mbr
28	4429543.58	5308231.00	263	17.0	6.3	647	a	Natural	Mine workings
29	4429522.75	5308102.32	267	17.5	6.4	666	a	Natural	
30	4429532.41	5307851.22	300	19.0	6.5	604	a	Natural	Tourist area
31	4429503.03	5307506.57	303	17.8	6.5	581	oc	Natural	
32	4429486.21	5307278.57	308	17.5	6.5	558	oc	Natural	
33	4429556.06	5306948.63	328	18.9	6.5	451	ms	Natural	
34	4429561.69	5306620.43	337	18.6	6.4	430	ms	Natural	
34D	4429561.69	5306620.43	337	18.4	6.5	433	ms	Natural	
35	4429496.49	5306592.57	340	19.0	6.8	668	ms	Natural	
36	4429582.20	5306553.04	313	18.3	7.0	408	ms	Natural	
37	4429927.63	5307196.26	335	20.3	6.5	593	ms	Natural	
38	4430138.87	5307498.25	325	19.4	6.5	655	oc/a	Natural	

No.	X-coor	Y-coor	Z-coor	H_2O temp	pH	EC	Bedrock geol	Channel characteris-tics	Possible sources of con-tamination
39	4430261.95	5307819.37	310	18.9	6.1	558	a	Natural	
40	4429775.46	5308161.68	268	19.2	5.4	580	a	Natural	altered min. bedrock
41	4429668.84	5308525.48	255	18.5	5.0	679	a	Natural	altered min. bedrock
42	4429932.01	5310587.64	226	18.5	6.4	836	a	Natural	Gas seepage + residences
43	4429940.40	5310576.72	226	20.3	5.3	1230	a	Natural	Gas seepage + residences
44	4429843.05	5310561.95	227	18.7	6.5	828	a	Natural	Gas seepage + residences
45	4429693.85	5310568.63	230	19.6	7.0	800	ad	Natural	Residential area; mining
45D	4429693.85	5310568.63	230	19.4	7.0	795	ad	Natural	Residential area; mining
46	4429521.26	5310659.05	233	19.8	7.0	780	ad	Natural	Residential area; mining
47	4429391.03	5310466.37	237	21.5	7.2	878	oc	Natural	Residential area; mining
48	4431810.54	5311220.72	190	26.7	7.0	1470	a	Reinforced	Mine dumps + tailings
49	4431647.78	5311179.30	191	25.6	7.0	1440	a	Reinforced	Mine waste
50	4431572.28	5311152.48	193	24.9	7.0	1480	a	Natural	Mine waste
51	4431352.30	5311256.73	195	26.4	7.0	1400	a	Man-made	Mine waste
52	4430972.83	5311110.82	202	24.9	2.0	13180	a	Natural	altered min. bedrock
52D	4430972.83	5311110.82	202	24.3	2.5	11260	a	Natural	altered min. bedrock
53	4430736.31	5311245.02	198	25.3	7.0	1290	a	Man-made	
54	4430663.22	5311781.47	199	20.7	7.0	1470	a	Man-made	Mine dump
55	4431129.56	5312208.46	203	22.4	2.0	9300	oc/a	Man-made (ditch)	Mine dump
56	4431102.39	5312116.17	195	17.7	7.1	1690	oc/a	Natural	Mine dump
57	4430987.39	5312063.46	191	20.5	2.5	1815	oc/a	Natural	Mine dump
58	4431211.76	5312242.78	198	17.7	7.2	1702	oc/a	Natural	Mine dump
59	4431332.43	5312325.51	197	20.3	3.0	2570	a	Natural	Mine dump
60	4431423.89	5312294.35	200	18.8	2.5	9050	a	Man-made	Mine dump
61	4431268.88	5312376.00	202	17.7	7.0	1729	oc	Man-made	Clay mining area
62	4430739.14	5312670.41	206	18.3	7.0	1813	oc	Natural	Clay mining area
63	4429700.21	5313145.85	211	18.0	8.0	1812	oc	Natural	
64	4430259.23	5312922.97	211	18.3	7.4	1887	oc	Natural	Mine dump
65	4430622.11	5312201.39	205	19.3	6.5	516	a	Natural	Mine dump
66	4431260.24	5309845.54	230	17.0	2.5	3940	a	Natural	Mine dump
67	4432128.17	5311036.95	193	23.0	3.0	2410	a	Man-made	Mine dump
68	4432002.91	5311130.46	195	21.3	2.0	8460	a	Man-made	Mine dump
69	4432055.12	5311177.08	191	20.0	2.5	5520	a	Man-made	Mine dump
70	4431913.01	5311257.89	189	22.3	2.0	6420	a	Man-made	Mine dump
71	4431865.10	5311333.19	190	20.8	3.5	3100	a	Man-made	Mine dump
72	4432697.74	5311435.03	181	18.4	6.3	656	oc/a	Natural	Mining
73	4433082.86	5311557.66	181	18.6	6.8	740	oc/a	Natural	Mining
74	4433489.23	5311873.34	180	19.1	6.8	749	oc/a	Natural	Mining
75	4433957.24	5311838.90	175	19.0	6.8	746	oc	Natural	Residential area; mining
76	4434472.82	5311969.02	171	19.4	7.0	749	oc	Natural	Residential area; mining
77	4429609.80	5308299.61	265	23.7	3.0	3240	a	Man-made	Mine dump
78	4429547.24	5307683.76	293	14.4	5.5	700	a	Deep well	
79	4429901.62	5310635.99		22.9	6.1	2530	a	Natural	Gas Seeps

Abbreviations: ca - clay-andesite contact; a – andesite; ocm - oligocene clayey-marl; ms - miocene sediments; ad - alluvial deposits; mbr - mineralized bed rock; Anth – anthropogenic; AMD - acid mine drainage; ARD - acid rock drainage.

Appendix D. Analytical results for water samples (Concentrations given in mg/l). Negative values correspond to noise when element concentrations fall below the lower detection limits.

No.	As	Cd	Cu	Fe	Mn	Ni	Pb	Sb	Zn	Al	K	Ca	Mg	Na
W1	0.02	0.00	0.01	0.07	0.08	0.00	-0.01	0.11	0.17	0.36	8.56	94.69	27.92	25.78
W1D	0.00	0.00	0.01	0.10	0.08	0.00	0.00	0.11	0.16	0.46	8.60	94.70	27.70	25.80
W2	0.03	0.00	0.01	0.07	0.40	0.01	-0.01	0.05	0.12	0.46	10.20	112.48	34.47	45.72
W3	0.03	0.00	0.05	0.32	0.93	0.01	-0.01	0.00	0.12	0.40	12.96	137.78	45.96	81.72
W4	-0.02	0.00	0.04	0.38	0.74	0.02	-0.01	0.03	0.08	0.62	14.02	137.38	44.20	82.52
W5	0.04	0.00	0.01	0.04	0.15	0.00	-0.01	0.04	0.10	0.30	10.58	92.99	27.65	28.06
W6	0.02	0.00	0.01	0.06	0.20	0.00	-0.01	0.04	0.09	0.44	11.58	89.22	26.89	23.13
W7	-0.03	0.00	0.00	0.05	0.22	0.00	0.00	0.04	0.12	0.42	11.12	93.31	27.83	22.83
W8	0.04	0.00	0.00	0.04	0.27	0.00	-0.01	0.04	0.18	0.24	11.76	98.73	28.42	23.93
W9	0.05	0.00	0.01	0.03	0.31	0.00	-0.01	0.03	0.24	0.30	12.18	98.55	28.66	25.62
W10	0.00	0.00	0.03	0.45	6.66	0.02	-0.01	0.04	0.36	0.42	4.74	147.15	27.27	12.72
W11	0.02	0.00	0.02	0.07	0.48	0.01	-0.01	0.04	0.34	-0.22	0.98	94.82	26.59	20.80
W12	0.09	0.01	0.02	58.73	24.16	0.13	0.00	0.04	11.25	-0.12	0.36	321.81	77.98	9.82
W13	0.15	0.00	0.02	0.16	0.76	0.00	-0.01	0.04	0.42	-0.18	0.78	93.57	26.57	27.80
W14	0.03	0.00	0.01	0.17	0.30	0.00	0.00	0.00	0.05	-0.23	0.75	92.45	26.18	19.27
W14D	0.00	0.00	0.02	0.18	0.31	0.00	0.00	0.00	0.05	-0.24	0.70	91.60	25.80	17.00
W15	0.04	0.00	0.01	0.17	0.23	0.00	-0.01	0.01	0.03	-0.22	0.96	90.41	25.91	18.18
W16	0.16	0.00	0.01	0.06	0.06	0.00	-0.01	0.01	0.06	0.34	4.80	69.33	19.84	8.58
W17	0.09	0.00	0.01	0.06	0.01	0.00	0.00	0.00	0.03	0.34	5.22	69.41	19.55	10.55
W18	0.16	0.00	0.01	0.06	0.03	0.00	-0.01	0.01	0.03	0.32	4.10	70.06	20.86	9.78
W19	0.18	0.00	0.02	0.07	0.02	0.00	-0.01	0.00	0.03	0.38	4.28	63.32	18.97	8.88
W20	0.08	0.00	0.00	0.04	0.05	0.00	-0.01	0.00	0.04	0.52	4.36	0.90	0.62	48.33
W21	0.18	0.00	0.02	0.05	0.01	0.00	-0.01	0.00	0.03	0.30	4.76	168.39	118.41	153.58
W22	0.08	0.00	0.01	0.27	0.66	0.00	-0.01	0.00	0.03	0.42	21.90	147.69	86.60	52.13
W23	0.20	0.00	0.02	0.06	0.02	0.00	-0.01	-0.01	0.03	0.40	6.00	76.46	23.15	8.35
W24	0.07	0.00	0.01	0.04	0.10	0.00	-0.01	0.00	0.03	0.54	5.44	75.70	22.70	9.38
W24D	0.10	0.00	0.02	0.05	0.10	0.01	0.00	0.01	0.04	0.60	5.80	77.20	23.20	10.20
W25	0.07	0.00	0.00	0.04	0.02	0.00	-0.01	0.00	0.03	0.34	5.58	76.50	23.73	9.31
W26	0.03	0.00	0.00	0.04	0.02	0.00	-0.01	0.00	0.02	0.32	4.72	73.03	22.07	8.25
W27	0.15	0.00	0.00	0.03	0.03	0.00	-0.01	0.00	0.02	0.38	5.76	79.02	25.99	11.62
W28	0.18	0.00	0.00	0.27	0.09	0.00	-0.01	0.01	0.04	0.48	6.68	79.32	24.26	11.50
W29	0.18	0.00	0.01	0.18	0.05	0.00	-0.01	0.00	0.02	0.34	5.06	83.08	29.96	13.28
W30	0.17	0.00	-0.01	0.02	0.00	0.01	-0.01	0.00	0.02	0.32	4.88	76.65	23.24	13.72
W31	0.17	0.00	0.01	0.04	0.00	0.00	-0.01	0.00	0.02	0.34	4.54	76.47	22.67	13.15
W32	0.04	0.00	0.01	0.09	0.00	0.00	-0.01	0.00	0.00	0.40	4.34	74.19	21.30	13.95
W33	0.00	0.00	-0.01	0.00	0.00	0.00	-0.01	0.00	0.00	0.06	4.64	58.41	16.35	15.13
W34	0.08	0.00	0.00	0.03	0.00	0.00	-0.01	0.00	0.01	0.27	4.84	54.96	15.65	12.78
W34D	0.00	0.00	0.00	0.04	0.01	0.00	0.00	0.01	0.00	0.26	4.80	53.20	15.20	12.80
W35	0.01	0.00	0.00	0.02	0.01	0.00	-0.01	0.00	0.02	0.30	15.12	74.20	33.17	24.63
W36	0.18	0.00	0.00	0.01	0.00	0.00	-0.01	0.01	0.01	0.20	4.56	49.49	13.69	14.20
W37	0.00	0.00	0.00	1.63	1.57	0.00	-0.01	0.01	0.02	0.30	3.08	58.92	15.42	29.63
W38	0.00	0.00	0.00	2.48	1.56	0.01	0.00	0.00	0.03	0.40	3.56	66.57	20.04	38.52
W39	-0.01	0.00	0.00	0.41	0.41	0.00	-0.01	0.00	0.03	0.32	2.34	53.11	17.41	34.80
W40	0.02	0.00	0.01	36.68	4.23	0.02	-0.01	0.01	0.07	1.08	10.46	35.83	11.93	24.66
W41	0.19	0.00	0.00	2.26	2.34	0.04	-0.01	-0.01	0.24	1.20	8.12	80.02	20.52	15.32
W42	-0.03	0.00	0.07	0.30	0.23	0.00	0.00	0.00	0.13	0.34	9.50	102.39	29.50	24.23
W43	0.03	0.00	0.00	28.47	4.75	0.02	-0.01	0.00	0.12	0.84	10.86	169.01	40.76	31.33
W44	0.02	0.00	0.00	0.07	0.09	0.00	-0.01	0.00	0.03	0.40	9.48	106.03	29.29	24.75

W45	0.08	0.00	0.00	0.04	0.06	0.00	0.00	0.00	0.02	0.45	9.74	111.77	29.14	26.84
W45D	0.00	0.0	0.00	0.05	0.05	0.00	0.00	0.00	0.02	0.52	9.60	111.9	29.00	26.80
W46	-0.03	0.00	0.00	0.05	0.16	0.00	0.00	0.00	0.03	0.72	10.06	111.23	27.34	27.51
W47	0.01	0.00	0.00	0.00	0.00	0.00	0.00	0.00	0.01	0.34	5.00	131.62	45.95	21.45
W48	-0.03	0.00	0.01	0.09	0.45	0.00	0.00	0.00	0.02	0.50	13.16	185.58	53.97	133.26
W49	-0.03	0.00	0.02	0.07	0.26	0.00	0.00	0.00	0.02	0.48	13.28	173.20	50.72	132.63
W50	-0.02	0.00	0.00	0.09	0.18	0.00	0.00	0.00	0.02	0.42	13.42	170.77	49.86	131.69
W51	-0.02	0.00	0.02	0.07	0.13	0.00	0.00	0.00	0.03	0.48	13.60	166.70	50.18	136.10
W52	1.43	0.61	210.55	>1220	86.25	6.14	3.50	0.03	45.42	857.29	0.51	688.10	974.66	4.61
W52D	1.50	0.60	191	>1220	87.12	5.66	2.75	0.03	46.51	774.3	0.60	701.00	871.00	4.60
W53	-0.02	0.00	0.07	0.09	0.16	0.01	0.00	0.00	0.08	1.84	13.86	164.68	51.75	120.34
W54	0.01	0.00	0.01	0.06	0.25	0.00	0.00	0.00	0.03	0.48	14.08	174.91	54.48	99.82
W55	27.53	0.29	129.58	>1220	18.30	1.03	3.78	0.04	30.98	620.15	0.34	364.24	94.26	36.29
W56	0.65	0.00	0.06	0.19	0.20	0.01	0.00	0.00	0.04	1.44	12.48	145.57	54.58	275.26
W57	0.08	0.02	10.40	82.36	4.14	0.14	0.05	0.02	2.68	57.18	1.84	100.17	20.89	7.05
W58	0.02	0.00	0.04	0.07	0.13	0.00	0.00	0.00	0.02	0.74	13.04	112.21	45.61	191.08
W59	0.20	0.04	22.49	389.47	14.74	0.35	0.27	0.01	5.32	97.66	4.40	423.95	92.64	36.51
W60	-0.01	0.19	21.32	>1220	23.59	1.09	1.72	0.02	16.92	442.78	51.60	403.45	225.81	121.55
W61	-0.06	0.00	0.02	0.10	0.11	0.01	0.65	0.00	0.02	0.70	13.86	117.68	47.94	216.92
W62	0.01	0.00	0.02	0.07	0.16	0.00	-0.02	0.00	0.03	0.54	13.54	119.26	51.20	234.62
W63	-0.03	0.00	0.02	0.08	0.13	0.00	3.10	0.00	0.02	0.68	14.14	116.16	51.87	236.28
W64	-0.01	0.00	0.00	0.08	0.20	0.00	0.57	0.00	0.02	0.80	14.26	114.02	51.36	262.51
W65	-0.02	0.00	0.02	0.08	0.07	0.00	1.28	0.00	0.02	0.68	6.22	61.98	20.88	15.79
W66	0.77	0.06	10.14	534.19	13.58	0.43	0.04	0.02	8.80	168.44	0.46	180.46	49.46	32.53
W67	0.05	0.01	11.05	38.81	29.24	0.48	0.00	0.00	1.52	59.40	5.68	200.70	154.75	22.69
W68	0.67	0.14	54.06	>1220	36.11	2.23	0.00	0.01	32.80	477.79	7.64	516.76	530.29	28.88
W69	0.30	0.07	51.36	489.56	31.06	1.27	0.00	0.02	15.44	324.01	8.60	464.78	262.38	25.14
W70	0.62	0.09	113.80	993.41	5.98	0.51	0.00	0.04	6.73	319.24	3.92	332.18	61.20	80.83
W71	0.52	0.02	33.54	33.30	5.00	0.20	0.00	0.02	3.67	57.49	7.56	337.60	47.10	78.85
W72	0.00	0.00	0.04	0.24	0.22	0.00	0.00	0.00	0.06	0.88	5.82	74.26	22.73	62.10
W73	-0.05	0.00	0.02	0.16	0.17	0.00	0.00	0.00	0.06	0.66	9.90	84.00	28.26	52.24
W74	-0.04	0.00	0.04	0.20	0.17	0.00	0.00	0.00	0.08	0.76	10.36	83.46	25.66	22.81
W75	-0.02	0.00	0.03	0.14	0.17	0.00	0.00	0.00	0.08	0.76	10.16	83.05	25.00	27.10
W76	0.06	0.00	0.04	0.16	0.16	0.00	0.00	0.00	0.06	0.60	10.30	81.05	24.63	23.70
W77	0.08	0.04	0.19	524.73	25.98	0.11	1.59	0.01	1.29	35.54	30.22	356.30	50.24	24.71
W78	-0.03	0.00	0.01	0.38	0.06	0.00	0.00	0.00	0.08	0.50	3.20	89.60	28.12	19.03
W79	0.02	0.00	0.00	39.44	57.35	0.07	0.10	0.00	0.08	0.66	2.90	491.11	100.74	89.13
W04R	0.02	0.00	0.03	0.60	1.14	0.02	0.00	0.00	0.13	0.72	12.18	150.29	48.12	136.23
W10R	-0.04	0.00	0.01	0.57	9.01	0.02	0.00	0.00	0.49	0.48	3.32	167.05	31.93	27.64
W19R	0.00	0.00	0.00	0.05	0.02	0.00	0.00	0.00	0.03	0.44	5.06	79.05	24.03	22.85
W28R	-0.02	0.00	0.01	0.31	0.11	0.00	0.00	0.00	0.06	0.58	4.26	87.91	26.78	23.46
W37R	0.01	0.00	0.02	1.83	1.82	0.00	0.00	0.00	0.03	0.32	3.12	69.19	16.35	29.73
W46R	-0.02	0.00	0.00	0.08	0.19	0.00	0.00	0.00	0.04	0.66	12.24	100.36	31.40	60.30
W55R	86.77	0.33	168.50	>1220	28.85	1.69	4.04	0.06	62.28	659.45	0.40	281.63	88.20	4.37
W64R	0.49	0.00	0.03	-0.01	0.28	0.00	0.00	0.00	0.04	3.82	13.54	119.66	56.07	353.52
W73R	-0.04	0.00	0.06	0.20	0.19	0.01	0.00	0.00	0.07	0.80	13.62	94.91	30.65	66.60

Appendix E. Analytical results for stream sediment samples (Concentrations given in ppm except for Fe which is given in %). Negative values correspond to noise when element concentrations fall below detection limits.

No.	As	Cd	Cu	Fe	Mn	Ni	Pb	Sb	Zn
1	68.50	1.70	152.20	2.18	951.30	12.10	36.20	0.60	112.00
1D	20.30	1.20	38.40	1.49	1200.90	10.40	35.40	0.40	137.80
2	331.70	1.60	708.70	2.19	288.50	9.40	45.00	0.20	83.20
3	1964.70	3.70	1978.60	3.50	216.40	22.60	120.10	19.20	112.20
4	558.20	2.80	1985.50	3.12	131.70	10.90	97.80	0.50	139.70
5	31.50	1.50	31.40	1.93	524.80	9.80	29.90	0.80	87.50
6	28.10	1.70	33.50	2.12	697.30	10.40	36.80	0.20	118.40
7	22.20	1.40	25.90	1.81	542.80	9.60	37.10	0.20	90.60
8	18.40	1.20	30.70	1.52	624.20	9.40	46.40	0.30	89.40
9	23.20	1.30	75.20	1.66	572.00	9.00	39.40	0.20	103.90
10	51.10	7.60	59.80	3.84	276.10	7.60	68.30	1.00	310.00
11	17.10	1.20	39.20	1.50	1145.90	12.20	37.00	0.30	121.90
12	17.80	6.60	35.20	3.93	182.70	3.80	33.50	1.90	110.20
13	25.50	1.50	42.10	1.88	833.50	10.10	40.60	0.50	109.70
14	41.40	2.60	35.00	2.35	707.20	11.50	108.20	0.20	127.00
14D	30.50	2.10	40.60	1.98	600.50	10.80	71.70	0.10	117.20
15	21.80	2.00	31.10	1.90	707.90	10.00	157.30	0.20	102.60
16	34.90	1.90	35.40	1.79	859.40	10.90	23.40	0.10	100.90
17	29.60	1.90	34.00	1.76	706.80	10.40	29.40	0.60	74.90
18	24.60	1.60	24.70	1.66	289.30	7.80	17.10	0.00	92.90
19	26.50	1.80	31.80	1.64	593.20	9.30	25.50	0.10	54.60
20	19.40	2.10	48.80	1.92	809.20	16.30	53.60	0.00	66.20
21	12.00	1.70	17.50	1.65	643.80	14.60	17.10	0.10	43.90
22	18.90	1.90	44.30	1.76	746.60	14.40	17.70	0.20	47.40
23	17.20	1.70	46.80	1.60	572.10	10.40	23.20	0.30	91.10
24	16.40	1.80	33.20	1.65	662.30	10.20	127.80	0.00	85.00
24D	21.80	2.20	54.90	1.92	852.50	11.00	25.30	0.80	92.60
25	37.70	3.10	55.20	2.57	525.50	8.30	22.20	0.70	101.70
26	15.30	1.60	10.30	1.47	482.90	11.10	11.00	-0.10	35.40
27	12.40	2.10	34.20	1.90	692.50	14.40	46.50	0.00	87.10
28	151.10	3.80	108.30	2.91	450.30	8.50	43.10	0.50	76.80
29	7.90	0.80	7.20	0.77	234.80	6.40	5.80	-0.10	30.30
30	4.30	1.50	12.00	1.31	549.90	10.40	10.20	0.10	35.50
31	7.60	1.60	20.60	1.42	339.00	9.60	9.60	0.20	38.40
32	10.80	1.90	21.50	1.64	753.50	11.80	11.30	0.80	42.20
33	6.70	1.30	11.80	1.20	316.80	6.90	8.10	0.30	31.60
34	4.30	1.40	11.20	1.24	391.50	9.40	9.30	0.20	31.70
34D	6.30	1.50	10.90	1.34	493.20	9.20	40.10	0.40	42.20
35	6.70	1.70	14.20	1.54	779.80	12.80	13.90	0.00	38.70
36	10.10	1.40	12.70	1.24	303.40	8.40	9.50	-0.10	33.30
37	11.50	2.50	27.20	2.08	925.00	31.70	14.50	0.10	59.70
38	10.40	1.80	17.60	1.74	819.60	16.70	22.10	0.40	48.00
39	3.80	1.20	12.20	1.20	546.30	9.90	17.40	0.10	28.80
40	13.30	1.00	19.10	1.01	115.60	5.60	15.80	0.10	64.10
41	69.30	3.20	51.40	2.59	1015.60	11.60	27.30	0.30	98.80
42	12.30	1.60	31.40	1.50	403.00	9.50	35.70	0.00	78.90

43	0.80	1.50	23.20	1.48	231.60	7.90	49.50	0.10	71.60
44	7.80	1.20	19.50	1.16	342.40	7.40	27.00	0.50	61.40
45	-2.40	1.90	28.80	1.77	622.20	10.40	59.20	0.60	92.20
45D	12.60	1.90	24.80	1.76	659.80	10.30	42.10	0.30	83.40
46	18.30	1.60	18.80	1.53	450.70	9.10	42.50	-0.10	78.90
47	-3.70	1.30	23.40	1.20	311.80	9.50	15.20	0.10	45.10
48									
49	809.70	8.10	1994.60	3.65	147.50	6.50	36.10	1.60	80.20
50									
51									
52	132.00	6.70	488.60	3.57	193.60	13.00	20.70	0.10	212.10
52D	239.50	10.30	692.90	3.63	252.20	15.50	15.50	0.50	270.60
53									
54	65.90	4.90	1359.20	3.02	1739.20	49.60	49.80	1.50	235.40
55									
56	313.60	2.30	238.40	2.15	103.00	8.20	32.20	0.40	71.10
57									
58									
59	431.50	2.80	324.60	2.57	124.00	10.40	31.20	0.50	186.70
60									
61									
62									
63	36.00	1.20	12.10	0.96	3303.40	0.30	4.10	0.00	15.00
64									
65									
66	204.10	2.00	64.20	2.04	95.80	3.00	38.90	0.30	18.00
67									
68									
69	295.80	1.90	158.90	1.98	33.00	0.20	34.10	1.70	14.70
70	658.80	4.40	518.50	3.31	562.60	15.20	219.70	0.80	711.10
71	1021.10	3.30	1191.80	2.77	209.10	27.10	113.40	1.40	111.50
72	252.70	1.60	593.10	1.51	299.80	8.10	49.30	-0.10	62.80
73	122.60	1.20	258.40	1.15	222.30	6.40	24.80	0.00	50.80
02R	281.40	2.20	796.10	2.17	279.80	9.20	49.70	0.20	86.40
15R	12.60	2.00	37.90	1.91	720.20	10.10	116.20	-0.10	97.00
18R	21.80	1.60	28.80	1.72	304.80	8.00	30.90	0.10	100.10
29R	3.20	0.90	5.80	0.90	250.10	7.10	5.90	0.10	23.10
34R	5.20	1.40	11.40	1.32	417.20	9.80	9.60	-0.10	31.40
41R	52.10		49.90	2.68	1062.10	11.90	27.50	-0.30	99.20
42R	13.10	1.60	27.10	1.57	423.20	8.80	35.90	-0.10	73.50
44R	11.80	1.20	16.90	1.18	334.70	7.30	28.00	-0.20	52.60
47R	22.90	1.40	24.00	1.27	332.80	10.20	15.90	0.20	47.10

Appendix F. Analytical results for tailings samples (Concentrations given in ppm). Negative values correspond to noise when element concentrations fall below detection limits.

No.	As	Cd	Cu	Fe	Mn	Ni	Pb	Sb	Zn
Lahoca Tailings									
T01	1026.7	3.1	1028.7	2.91	44.4	3.7	705.6	3.1	381.5
T02	196.3	1.9	603.6	1.97	125	13.7	48.6	0.6	76.2
T03	303.2	2.1	607.9	2.13	207.6	13.2	81.7	0.5	114.6
T04	2789.3	4.3	2056.8	2.85	35.7	1.8	359.3	4.2	522.5
T05	488.3	3.6	593	3.09	75.9	3.2	148.7	0.6	137
T06	1595.6	7.2	2062.8	2.60	94.3	4.9	639.4	1.8	776.7
T07	1284.1	7.2	2064.7	1.94	89.2	4.8	429.5	2.1	673.3
T08	1500.9	3	1815.6	2.93	50.5	2.4	343.7	1.5	413.6
T08D	1387.3	6.3	1400.4	3.02	53.9	2.7	332.3	1	557.9
T09	484.9	3.7	303	3.15	71.4	7	313.5	0.4	132.3
T10	334.2	4.6	684.3	1.92	57.9	3.8	162.4	0.5	617.2
T11	321.5	4.2	597.1	1.85	44.4	3.4	191.5	0.6	704.9
T12	220.9	1.7	317.7	1.92	22.1	1.5	63.9	0.3	193.5
T13	244.6	2.2	373.6	2.24	57.6	5.2	66	0.4	134.3
T14	537.9	2.8	675.9	2.57	36.3	2.8	92.3	0.8	163.4
T15	408.5	2	618.5	2.21	35.1	2.6	111.9	0.9	245.6
T16	296.4	2.3	492.7	2.26	104.4	7.4	128.4	0.7	153.8
T17	299.4	2.8	444.4	2.59	92.8	7.3	57.7	0.5	164.8
T18	397.8	1.8	627.5	2.10	33.9	3.1	126.6	0.7	262
T19	347.1	2.3	380	2.20	36.5	4	77.9	0.5	68.7
T20	519.7	2.3	748.5	2.31	33	2.4	65.6	0.7	144.6
T21	285.3	2.4	313.3	2.35	53.6	5.3	207.3	0.5	205.5
T21D	326	2.4	329.3	2.35	48.1	4.4	130.8	0.5	205.1
T22	455.3	2.3	419.6	2.23	45.8	4.5	113.1	0.2	156.1
T23	770.7	3.3	1327.4	2.89	40.4	2.9	61.6	0.6	169.5
T24	659.5	2.6	476.8	2.43	42.3	1.7	67.1	0.4	93.2
T25	554.5	3	800	2.53	62.4	2.5	61.5	0.6	74.6
T25D	606.4	2.9	687	2.50	61.6	2.6	58.8	0.4	75
T26	539.7	2.2	689.3	2.17	37.4	2.3	110.5	0.5	123.2
T27	336.4	3.2	570.6	2.72	39.1	3.6	64.5	0.3	79.6
T28	631.3	2.8	1519.6	1.83	33	2	215.4	1	453.7
T29	680.3	2.4	1155.2	2.36	42	2.5	110.4	0.7	259.3
T30	561.9	2.3	1125.6	1.96	37.5	2.4	174.9	1.1	378.2
T31	636.5	2.7	983.5	2.21	57.3	2.8	150.7	0.9	460.3
T32	564.3	2.7	965.6	1.57	16.1	0.6	140	1.1	449.5
T33	818.4	1.9	1028.7	2.01	72.1	3.3	806.9	1.7	252.9
T34	683.6	2.5	723.1	1.98	67.6	4.2	105.7	0.2	432.5
T35	530.2	2.1	1050.8	2.10	32.2	1.9	256.9	0.5	256.2
T36	860.9	1.7	1561.1	1.89	17.7	0.7	172.3	0.6	272.9
T36D	527.6	2.4	736	2.30	27.2	2.4	146.7	1	149.7
T37	611	1.9	1419.4	2.05	32.2	2.3	158.5	1.5	274.6
T38	595.1	1.9	996.2	2.02	25	1.7	267	0.8	276.1
T39	293.6	1.4	455.7	1.62	15.1	0.9	176.1	0	136.3
T40	598.4	1.9	890.5	1.42	22.2	0.8	172	0.3	314.6

T41	770.3	2.2	818.3	2.14	44.3	3.8	209.1	0.3	362.3
T42	393.4	2.7	945.8	2.60	84.5	9.3	40.4	0.5	161.6
T43	599.8	1.7	919.3	1.88	22.5	1.8	161.3	0.6	200.1
T44	515.5	2.4	907	2.39	23.4	1.3	230.6	0.8	187.3
T46	681.2	4.6	270	3.32	73.5	8.5	22.8	0.8	67.8
T47	573	2.6	789.4	2.58	43.9	3.1	221	0.6	346.2
T48	795.6	1.9	1483.7	1.49	17.7	1	251.8	1.6	308.1
T49	348.4	4.2	171.1	3.18	44.9	5.7	16.2	0.1	75.8
T50	718.7	2.9	267.2	2.74	35.5	4.6	127.1	0.6	194.3
T51	747	2.4	1198.9	2.36	33.2	2.7	84.2	0.9	167.7
T52	48.6	2.1	222.9	2.06	243	11.9	26.8	0.2	116.7
T53	161.5	3.7	221.4	3.15	167.5	12.1	18.3	0.3	88.9
T54	417	1.9	970.8	2.12	30.5	2.1	163	1	259.9
T55	214.2	3.3	259.6	2.86	71.3	8.6	53.4	0	106.7
T56	70.2	3.3	128.3	3.00	76.9	7.5	18	0.2	60.9
T57	85.7	2.8	525.2	2.46	766.4	39	20.3	0.1	161.1
T58	274.5	3.7	280.9	3.10	66	7.7	23	-0.1	70.5
T59	197.2	3.6	263.4	3.00	126.6	15.2	28.2	0.3	104.2
T60	67.1	2.7	206.6	2.54	111.2	13.1	26.9	0.1	117.3
T61	100.5	2.3	124.8	2.36	29.7	4.1	20.2	0.3	42.6
T62	186.5	3.8	136	3.22	54.9	9.1	16	0.5	56.1
T63	218.7	4.4	198.3	3.34	131.8	13.8	27.7	0.5	65.9
T64	222	3.9	191.8	3.12	146.8	12.1	18.3	0	81.4
T65	153.5	4.4	199	3.25	107.5	13.1	18.9	0.2	79.2
T66	95.7	2.9	236	2.66	104.1	13.6	30.2	0.3	136.1
T67	112.5	3.7	127.4	2.98	150.4	13.5	14.8	0.3	91.7
T68	229.4	4.1	206	3.24	54.5	8.2	37.3	0.3	65.9
T69	132.5	3	165.8	2.68	47.1	9.5	20.9	0	60.5
T70	107.8	4	201.7	3.12	105.1	16.6	18.6	0	75.2
T71	150	3.4	146.6	2.93	103.8	11.6	22.6	0.1	103.3
T72	187.2	3.3	367.3	2.87	118.1	12.4	51.3	0.5	131.8
T73	121.4	2.1	201.8	2.23	20.6	2.1	154.8	0.1	218.4
T74	73.3	3.5	622.6	2.16	673.1	42.1	46	0.6	762.8
T75	124.3	3.3	365.4	2.78	395.7	23	49.6	0.3	172.2
T76	371.1	3.7	140.9	3.09	72.9	6.9	70.3	0.2	125.1
T77	900.9	4.2	931.8	3.30	66.2	7.3	106.2	1	141.6
T78	220.7	2.9	489.7	2.64	114.7	10.5	57	0.7	200.4
T79	155.7	1.9	262.6	2.12	27.6	4.5	120.7	0.2	245
T80	291.2	3.4	278	2.95	67.2	10.3	53.9	0.3	93.4
T81	210.3	2.9	331.5	2.61	26.8	2.2	58.4	0.6	103.7
T82	1568	5.4	230.7	3.67	258.1	11.8	22.9	0.4	63.2
T83	67.8	4.4	85.5	2.94	344.1	43.4	14.7	0.1	57.3
T84	88.9	3.8	207.5	3.02	170.6	17.2	41.2	0.6	96.8
T85	174.6	2.6	458.6	2.43	100.8	9	44	-0.1	106.6
T86	110.5	3.8	168.2	3.01	97.8	14.1	21.1	0.3	58.2
T87	72.1	3.2	201.2	2.72	76	12.4	16.9	0.1	62.8
T88	150.7	2.4	330.1	2.43	93.6	5	24	0.2	82.4
T89	95	3.5	281.3	2.88	74.9	11.7	19	0.6	56.2
T90	73.8	3.6	255.5	2.98	120	18.1	14	0.1	75.9
T90D	61.6	3.7	256.1	2.97	136.6	17.1	15.4	0.6	70.2

T92	277.3	2.8	363.2	2.56	64.2	7.1	119	0.8	174
T93	159.8	2.5	162.4	2.49	122.3	4.6	32.4	0.7	71.9
T94	514.8	3.5	641.1	2.96	92.3	13.3	24.6	0.1	57
T95	193.9	2.8	131.2	2.66	118.2	3.4	77.3	0.3	59.6
T96	147.8	2.9	1232	2.53	256.8	23	42.1	0.3	111.8
T97	134.9	2.2	308.9	2.26	128.9	4.9	27.5	0.3	61.1
T99	328	2.8	303.1	2.66	58.9	6.1	19.6	0.4	53.3
T99D	367.2	2.9	311	2.66	69.6	4.9	27.9	0.2	75.7
Recsk Tailings									
RT01	97.5	4.5	1995.1	3.08	849.1	35.7	157.4	0.7	387.4
RT02	59.2	3.3	1667.8	2.38	451.9	25	45.4	0.4	161.9
RT03	54.7	5.2	1969.5	3.14	797.1	49.8	110.3	0.7	138.2
RT04	1808.1	25.8	1642.8	2.81	109.1	39.5	115.1	131.3	435.2
RT05	634.6	1.2	220.5	1.28	26.3	0	69	2.8	12
RT06	81.1	4.6	303.5	3.16	113.6	6.8	27.7	1.1	40.5
RT07	237.9	0.4	141.3	0.43	7.7	0.2	22.3	1.3	3
RT08	775	1.4	604.9	1.57	27.1	4.1	28	0.8	229.6
RT09	187.6	1.2	297.3	1.35	96.4	5.6	23.4	0.4	38.7
RT10	123.9	3.8	359.8	2.87	121.1	3.9	58.2	0.3	64.5
RT11	70.5	2.2	65.4	2.27	27.4	0.8	114.7	0.2	19.1
RT12	70	1.9	32.4	1.97	17.1	0.3	41.1	0.2	9.5

Abbreviations:

ca = clay-andesite contact
a = andesite rock
ocm = oligocene clayey-marl
ms = miocene sediments
ad = alluvial deposits
mbr = mineralized bed rock
Anth= anthropogenic